N65 28354
(ACCESSION NUMBER) (THRU)
139 1
(PAGES) (CODE)
CR-54345 12
(NASA CR OR TMX OR AD NUMBER) (CATEGORY)
FACILITY FORM 602

NASA-CR-54345

GPO PRICE $ _____

OTS PRICE(S) $ _____

Hard copy (HC) 4.00

Microfiche (MF) 1.00

MATERIALS FOR POTASSIUM LUBRICATED JOURNAL BEARINGS

Quarterly Progress Report No. 7
Quarter Ending January 22, 1965

EDITED BY R. G. FRANK

prepared for
NATIONAL AERONAUTICS AND SPACE ADMINISTRATION
CONTRACT NAS 3-2534

SPACE POWER AND PROPULSION SECTION
MISSILE AND SPACE DIVISION
GENERAL ELECTRIC
CINCINNATI, OHIO 45215

NOTICE

This report was prepared as an account of Government sponsored work. Neither the United States, nor the National Aeronautics and Space Administration (NASA), nor any person acting on behalf of NASA:

A.) Makes any warranty or representation, expressed or implied, with respect to the accuracy, completeness, or usefulness of the information contained in this report, or that the use of any information, apparatus, method, or process disclosed in this report may not infringe privately owned rights; or

B.) Assumes any liabilities with respect to the use of, or for damages resulting from the use of any information, apparatus, method or process disclosed in this report.

As used above, "person acting on behalf of NASA" includes any employee or contractor of NASA, or employee of such contractor, to the extent that such employee or contractor of NASA, or employee of such contractor prepares, disseminates, or provides access to, any information pursuant to his employment or contract with NASA, or his employment with such contractor.

CASE FILE COPY

Requests for copies of this report should be referred to:

National Aeronautics and Space Administration
Office of Scientific and Technical Information
Washington 25, D.C.
Attention: AFSS-A

NASA-CR-54345

MATERIALS FOR POTASSIUM LUBRICATED JOURNAL BEARINGS

QUARTERLY PROGRESS REPORT NO. 7

Covering the Period
October 22, 1964 to January 22, 1965

edited by

R. G. Frank
Program Manager

approved by

J. W. Semmel, Jr.
Manager, Materials and Processes

prepared for

NATIONAL AERONAUTICS AND SPACE ADMINISTRATION

Contract NAS 3-2534

Technical Management
NASA - Lewis Research Center
Space Power Systems Division
R. L. Davies

SPACE POWER AND PROPULSION SECTION
MISSILE AND SPACE DIVISION
GENERAL ELECTRIC COMPANY
CINCINNATI, OHIO, 45215

FOREWORD

The work described herein is being performed by the General Electric Company under the sponsorship of the National Aeronautics and Space Administration under Contract NAS 3-2534. Its purpose, as outlined in the contract, is to evaluate materials suitable for potassium lubricated journal bearing and shaft combinations for use in space system turbogenerators and, ultimately, to recommend those materials most appropriate for such employment.

R. G. Frank, Manager, Physical Metallurgy, Materials and Processes, is administering the program for the General Electric Company. L. B. Engel, Jr., D. N. Miketta, T. F. Lyon, W. H. Hendrixson and B. L. Moor are directing the program investigations. The design for the friction and wear testers was executed by H. H. Ernst and B. L. Moor.

R. L. Davies of the National Aeronautics and Space Administration is the technical manager for this study.

CONTENTS

Section		Page
I	INTRODUCTION	1
II	SUMMARY	5
III	MATERIALS PROCUREMENT	7
IV	TEST FACILITIES	9
	Compression	9
	Friction and Wear	11
	Friction and Wear in High Vacuum	11
	Helium Leak Test	21
	Diaphragm Pressure Test	21
	Diaphragm Temperature Distribution Test	26
	Tare-Weight Tests	26
	Friction and Wear in Liquid Potassium	26
	Instrumentation	31
	Test Facility	32
	Wetting	32
V	TEST PROGRAM	37
	Potassium Purification	37
	Corrosion	37
	Dimensional Stability	43
	Test Run No. 2	43
	Test Run No. 3	51
	Specimen Evaluation, Test Runs No. 2 and No. 3	51
	Thermal Expansion	60
	Hot Hardness	61
VI	FUTURE PLANS	119
	REFERENCES	121
	DISTRIBUTION LIST	123

ILLUSTRATIONS

Figure		Page
1	Room Temperature Load-Strain Curve for Mo-TZM Alloy in Compression.	12
2	High Vacuum Friction and Wear Tester	13
3	High Vacuum Friction and Wear Tester Installed on a General Electric Vacuum System Incorporating a 1,000 ℓ/Sec Getter-Ion Pump	14
4	Major Components for High Vacuum Friction and Wear Tester. . .	15
5	Upper Drive Shaft, Nonmagnetic Diaphragm, Main Shaft with Specimen Holders and Loading Arm Assemblies for High Vacuum Friction and Wear Tester	16
6	Main Shaft Assembly for High Vacuum Friction and Wear Tester .	17
7	Loading Arm Assembly for High Vacuum Friction and Wear Tester	18
8	Upper Drive Shaft Assembly for High Vacuum Friction and Wear Tester	19
9	Nonmagnetic Diaphragm (Inconel 718) for Magnetic Coupling Used in High Vacuum Friction and Wear Tester	20
10	Location of Strain Gauges Applied to High Vacuum Friction and Wear Tester Diaphragm No. 1; Gauge Symbols Indicate Direction of Grids	22
11	Stress in Inconel 718 Diaphragm as a Function of Internal Chamber Pressure	25
12	Location of Thermocouples and Test Setup for Temperature Distribution Test of Inconel 718 Diaphragm	27
13	Temperature of Diaphragm Membrane at T_1, T_2, T_3 and T_4 as a Function of the Temperature of the Inconel Support Ring at T_5 .	29
14	Tare-Weight Flange Assembly for the Calibration of the Loading Arms for the Friction and Wear Testers as a Function of Internal Pressure.	30
15	Partially Completed Cb-1Zr Alloy Sump for Liquid Potassium Friction and Wear Tester	33

ILLUSTRATIONS (Cont'd)

Figure		Page
16	Columbium-1% Zirconium Alloy Pump Impellers for Potassium Friction and Wear Tester	34
17	Components for Specimen Holder Assembly Used in Liquid Potassium Friction and Wear Tester	35
18	Internal View of Vacuum Distillation Cleaning Facility	40
19	Pressure Curve for Dimensional Stability Test No. 2	50
20	Average Temperature for Dimensional Stability Test No. 2	52
21	Pressure Curve for Dimensional Stability Test No. 3	55
22	Average Temperature for Dimensional Stability Test No. 3, 1200°F Test	56
23	Average Temperature for Dimensional Stability Test No. 3, 1600°F Test	57
24	Mean Coefficient of Thermal Expansion of Pyros 56 as a Function of Temperature	71
25	Mean Coefficient of Thermal Expansion of K601 as a Function of Temperature	71
26	Mean Coefficient of Thermal Expansion of TiC as a Function of Temperature	72
27	Mean Coefficient of Thermal Expansion of TiC+5%W as a Function of Temperature	72
28	Mean Coefficient of Thermal Expansion of TiC+10%Mo as a Function of Temperature	73
29	Mean Coefficient of Thermal Expansion of TiC+10%Cb as a Function of Temperature	73
30	Mean Coefficient of Thermal Expansion of Star J as a Function of Temperature	74
31	Mean Coefficient of Thermal Expansion of TiB_2 as a Function of Temperature	74
32	Hot Hardness of Unalloyed Arc Cast Tungsten as a Function of Temperature	78

ILLUSTRATIONS (Cont'd)

Figure		Page
33	Hot Hardness of Unalloyed Arc Cast Tungsten as a Function of Temperature.	81
34	Hot Hardness of Unalloyed Arc Cast Tungsten as a Function of Temperature.	84
35	Hot Hardness of Mo-TZM Alloy as a Function of Temperature.	108
36	Hot Hardness of TiC as a Function of Temperature	109
37	Hot Hardness of Carboloy 999 as a Function of Temperature.	110
38	Hot Hardness of Carboloy 907 as a Function of Temperature.	111
39	Hot Hardness of Grade 7178 as a Function of Temperature. .	112
40	Hot Hardness of Zircoa 1027 as a Function of Temperature .	113
41	Hot Hardness of Star J as a Function Temperature	114
42	Hot Hardness of K601 as a Function of Temperature.	115
43	Hot Hardness of TiC+5%W as a Function of Temperature . . .	116
44	Hot Hardness of TiC+10%Cb as a Function of Temperature . .	117

TABLES

Table		Page
I	Candidate Bearing Materials	3
II	Room Temperature Compressive Properties of Mo-TZM Alloy	10
III	Effect of Internal Chamber Pressure on the Stress and Strain Exerted by the Diaphragm on the High Vacuum Friction and Wear Tester	24
IV	Temperature Distribution of Diaphragm on High Vacuum Friction and Wear Tester	28
V	Chemical Analyses of Potassium	38
VI	Oxygen Analyses of Potassium	39
VII	Dimensional and Weight Changes of Specimens Exposed in Potassium for 1,000 Hours at 1600°F	42
VIII	Chemical Analyses of Potassium Transferred from the Cb-1Zr Alloy Corrosion Capsules After a 1,000-Hour Exposure at 1600°F	44
IX	Visual Examination of Corrosion Test Specimens After a 1,000-Hour Exposure to Potassium at 1600°F	45
X	Location of Specimens for Dimensional Stability Test No. 3, 1200°F	53
XI	Location of Specimens for Dimensional Stability Test No. 3, 1600°F	54
XII	Dimensional and Weight Changes of Specimens Exposed to Vacuum for 1,000 Hours at 800°F	58
XIII	Dimensional and Weight Changes of Specimens Exposed to Vacuum for 1,000 Hours at 1200° and 1600°F	59
XIV	Calibration Tests of the Chevenard Dilatometer Using a Pyros 56 Standard	62
XV	Thermal Expansion Data for K601	64
XVI	Thermal Expansion Data for TiC	65
XVII	Thermal Expansion Data for TiC+5%W	66

TABLES (Cont'd)

Table		Page
XVIII	Thermal Expansion Data for TiC+10%Mo.	67
XIX	Thermal Expansion Data for TiC+10%Cb.	68
XX	Thermal Expansion Data for Star J	69
XXI	Thermal Expansion Data for TiB_2	70
XXII	Summary of Thermal Expansion Data for the Candidate Bearing Materials	75
XXIII	Hot Hardness Data for Unalloyed Arc Cast Tungsten	76
XXIV	Hot Hardness Data for Unalloyed Arc Cast Tungsten	79
XXV	Hot Hardness Data for Unalloyed Arc Cast Tungsten	82
XXVI	Hot Hardness Data for Mo-TZM Alloy.	87
XXVII	Hot Hardness Data for TiC	89
XXVIII	Hot Hardness Data for Carboloy 999.	91
XXIX	Hot Hardness Data for Carboloy 907.	93
XXX	Hot Hardness Data for Grade 7178.	95
XXXI	Hot Hardness Data for Zircoa 1027	97
XXXII	Hot Hardness Data for Star J.	99
XXXIII	Hot Hardness Data for K601.	102
XXXIV	Hot Hardness Data for TiC+5%W	104
XXXV	Hot Hardness Data for TiC+10%Cb	106
XXXVI	Comparison of Hot Hardness Data for TiC	118

I. INTRODUCTION

The program reviewed in this seventh quarterly report, covering activities from October 22, 1964 to January 22, 1965, is performed under the sponsorship of the National Aeronautics and Space Administration. Its purpose is to evaluate materials suitable for potassium lubricated journal bearing and shaft applications in space system turbogenerators operating over a 400° to 1600°F temperature range. The critical role of bearings in such systems demands the maximum reliability attainable within today's state-of-the-art. Achieving this reliability requires an interdisciplinary approach employing the best mechanical designs of journal bearings combined with the selection of the optimum materials to serve as the structural members. Satisfying this latter requirement constitutes the aim of this program.

A number of investigators have conducted studies in this field and their contributions have advanced the state-of-the-art considerably (Section VIII, Ref. 1). Although their work is significant, there are no common criteria for a comparison of the existing data. Therefore, establishing a unified approach to the development and evaluation of materials for potassium lubricated bearing application is deemed essential. The program involves a comprehensive investigation of material properties adjudged requisite to reliable journal bearing operation in the proposed environment. This includes: 1) corrosion testing of individual materials and potential bearing couples in potassium liquid and vapor, 2) determination of hot hardness, hot compressive strength, modulus of elasticity, thermal expansion and dimensional stability characteristics, 3) wetting tests by potassium and 4) friction and wear measurements of selected bearing couples in high vacuum and in liquid potassium.

In cooperation with the cognizant NASA Technical Manager, 14 candidate materials were selected (Table I) from a compilation of existing data on available materials. The materials reviewed fall into four broad categories:

- Superalloys and refractory alloys with and without surface treatment
- Commercial metal bonded carbides.
- Refractory compounds such as stable oxides, carbides, borides and nitrides
- Cermets based on the refractory metals and stable carbides

Each material is procured from appropriate suppliers to mutually acceptable specifications and subsequently is subjected to chemical, physical and metallurgical analyses to document its characteristics before utilization in the program. After the documentation of processes and properties, the candidate materials undergo corrosion, dimensional stability, thermal expansion, compression and hot hardness testing. Considering the bearing material requirements and the preliminary

information obtained on materials subjected to both potassium and non-potassium testing, a number of materials combinations will be selected in cooperation with and subject to the approval of the NASA Technical Manager. Potassium corrosion and wetting tests and friction and wear measurements in high vacuum and liquid potassium will then proceed with these combinations.

The ultimate product of this program will be a recommendation, substantiated with complete documentation, of the material or materials which have the greatest potential for use in alkali metal journal bearings in high speed, high temperature, rotating machinery for space applications. Hopefully, the results will indicate the future course of alloy or material development specifically designed for alkali metal lubricated journal bearing and shaft combinations.

TABLE I. CANDIDATE BEARING MATERIALS

Material Class	Candidate Material
A. Nonrefractory Metals and Alloys	Star J (17%W-32%Cr-2.5%Ni-3%Fe-2.5%C-Bal. Co)
B. Refractory Metals and Alloys	Mo-TZM (0.5%Ti-0.08%Zr-Bal. Mo) Tungsten
C. Fe-Ni-Co Bonded Carbides	Carboloy 907 (74%WC-20%TaC-6%Co) Carboloy 999 (97%WC-3%Co) K601 (84.5%W-10%Ta-5.5%C)
D. Carbides	TiC (94%)
E. Oxides	Lucalox (99.8% Al_2O_3) Zircoa 1027 (95.5% ZrO_2)
F. Borides	TiB_2 (98%)
G. Refractory Metal Bonded Carbides	TiC+5%W TiC+10%Mo TiC+10%Cb Grade 7178

II. SUMMARY

During the seventh quarter of this program, the topics abstracted below were covered and the results are interpretatively presented in this report.

Essentially all of the test specimens have been received and the overall procurement status is 96% complete. The status of individual test specimen configurations is: corrosion, 100% complete; dimensional stability, 100% complete; thermal expansion, 100% complete; hot hardness, 100% complete; compression, 85% complete.

Approximately 25 pounds of potassium were purified by hot trapping for 24 hours at 1200° to 1350°F in a titanium-lined, zirconium-gettered hot trap after being purified by vacuum distillation at 500° to 550°F and a receiver pressure of 2×10^{-5} torr. The potassium will be used for the initial checkout tests of the friction and wear tester facility.

The construction of the vacuum distillation facility for the cleaning of the tested corrosion specimens has been completed and checked out. Subsequently, the 14 Cb-1Zr alloy corrosion capsules exposed for 1,000 hours at 1600°F were opened under argon, the potassium drained and the 28 test specimens cleaned by vacuum distillation. All the specimens were measured dimensionally and weighed; the potassium was spectrographically analyzed for metallic impurities. The two oxides, Lucalox and Zircoa 1027, exhibited the largest change in dimensions.

To evaluate dimensional stability, duplicate specimens of 13 of the 14 candidate materials were tested for 1,000 hours at 800°F and four materials were tested for 1,000 hours at 1200° and 1600°F in vacuum. The chamber pressures at the conclusion of the tests were 1.0×10^{-9} torr and 2.4×10^{-9} torr, respectively. Of the 13 materials evaluated at 800°F, the Zircoa 1027 was the only material to show a change in dimensions of any significance and this was quite small, i.e., approximately +0.03%. No detectable changes were observed for any of the other materials. Of the four materials evaluated at 1200° and 1600°F (TiC+10%Mo, TiC+5%W, TiB_2 and Star J), the Star J alloy was the only material to exhibit a significant change in dimensions, i.e., +0.06%, and this occurred in the 1600°F test. Previous tests at 1200° and 1600°F showed Zircoa 1027 to be the only other material to have exhibited a dimensional change, i.e., on the order of +0.4% after a 1,000-hour exposure at 1600°F.

The mean coefficient of thermal expansion was determined as a function of temperature from room temperature to 1600°F for seven candidate materials, i.e., K601, TiC, TiC+10%Cb, TiC+10%Mo, TiC+5%W, TiB_2 and Star J. Excellent agreement of the data was observed between duplicate specimens and between heating and cooling cycles of the same material. Hot hardness data were obtained on one specimen for all 14 candidate materials and data are reported for 11. Considerable scatter was observed in the data for a number of materials and will require further investigation. The compression load train was checked out successfully at room temperature with Mo-TZM Alloy specimens and the compressive 0.2% yield strength of the Mo-TZM alloy was found to be 113,300 psi. The elastic modulus, as calculated

from the stress-strain curve developed from extensometers attached to the specimen and using an estimated gauge length for the specimen, is 42×10^6 psi.

The high vacuum friction and wear tester was received from the vendor and preliminary checkout tests were initiated. The tester was helium leak tested and found to be leak tight at a sensitivity of 5×10^{-10} std cc air/sec. The non-magnetic diaphragm, which is part of the magnetic drive, was pressure tested and found to have a safety factor of 4.66 at room temperature for an internal pressure of 50 psi. The temperature distribution also was determined for the diaphragm with an internal heat source. The liquid potassium friction and wear tester essentially is completed and final assembly should begin the week of February 22, 1965. Build-up of the supporting facilities for the liquid potassium friction and wear tester has been initiated.

III. MATERIALS PROCUREMENT

During the report interim, the following candidate bearing material test specimens were received:

Material	Specimen Configuration	Number Received
Star J	Compression	10
Star J	Thermal Expansion	1
TiB_2	Compression	1
TiC	Compression	2
TiC+10%Mo	Compression	2

The receipt of these test specimens brings the over-all procurement status of all the specimens ordered to approximately 96%; the compression specimen configuration being the only group of specimens lacking 100% completion.

Four of the Star J compression specimens were returned to the vendor for a more complete evaluation of their soundness. Examination of radiographic films, which were submitted to General Electric for approval, had revealed minor indications. The specimens were returned to the vendor under an agreement that the specimen containing the largest apparent defect would be sectioned through the questionable area and evaluated. The vendor's examination revealed no defect to be present and that the indications were the result of x-ray reflections on the radiographic film. The three remaining specimens were returned to General Electric for inclusion in the compression testing program and completes the procurement of Star J specimens.

Although the vendor of the TiC and TiC+10%Mo materials, through a determined effort, was able to deliver 2 compression specimens of the TiC composition (9 total) and 2 specimens of the TiC+10%Mo (10 total), continued problems were experienced in attempts to produce sound compression specimens from the K601 material. Repeated attempts to produce the configuration resulted in rejection, usually in the final grinding operations, of entire lots of 12 to 15 specimens each. However, porosity also has been a problem. Various modifications to the processing sequence were tried without success. At the end of the report period, the vendor could offer no firm delivery date for the K601 compression specimens.

Delivery of the unalloyed tungsten bar that is required for the fabrication of compression specimens was realized during the reporting period. Surface defects reduced the yield so that only 29.5 inches of sound material were delivered instead of the 36 inches originally ordered. However, this is sufficient material to produce the required number of compression specimens. The stock was shipped to the machining vendor and delivery of the completed specimens is expected in February.

Based on the receipt of the tungsten compression specimens and the probable inability to obtain the K601 specimens, the over-all procurement of all the specimens ordered for the program to-date will be 98%.

IV. TEST FACILITIES

Compression

Checkout tests were carried out on the compression testing facility using Mo-TZM alloy specimens procured specifically for this purpose. The Mo-TZM material was produced by Climax Molybdenum Company in the form of 1.56-inch diameter rod from heat TZM-7496 and was supplied in the stress-relieved condition, i.e., one hour at 2350°F. The compression specimen configuration was machined from the 1.56-inch diameter raw stock by Dawson Carbide Industries, Incorporated, of Detroit, Michigan.

In order that an autographic readout of the stress-strain curve would be realized, the signals from the load cell and the LVDT extensometer system were fed into a Leeds and Northrup "Azore" millivolt X-Y recorder. Strain in the specimen was transmitted from the extensometer collars, which were spring loaded onto the radii of the reduced section, through rods to the LVDT located inside the load cell. The signal from the LVDT was rectified by an ATC demodulator and subsequently activated the X axis of the recorder. By varying the magnification factor of the recorder, full range for strain on the X axis could be set for 0.010 inch, 0.020 inch or 0.050 inch with a corresponding loss in sensitivity as the range is increased.

Load was sensed by four Type C6121 strain gauges mounted on 90° intervals on the load cell. Power was supplied by a constant voltage DC power source. The output of the strain gauges was plotted on the Y axis of the recorder. The LVDT was calibrated against a drum micrometer capable of being read to the fourth decimal place. The output of the load cell strain gauges was plotted against increments of load imparted by the Baldwin testing machine which recently was calibrated with Morehouse proving rings and certified to be within an accuracy of ± 0.5%.

The first test was performed using an initial strain rate of 0.005 inch/inch/minute and the 0.020 inch (2% strain) full scale range on the X axis of the recorder. A coarse range was selected for the first test to ensure sufficient capacity on the recorder for evaluation of the full stress-strain diagram. Full scale on the Y-axis represented a 100,000-pound load. Although an attempt was made to maintain the starting strain rate of 0.005 inch/inch/minute beyond the 0.2% yield point, it was not possible to apply the load at a uniform rate as the specimen deformed plastically. The load was released at a total strain of 1.82%. The 0.02% and 0.2% yield stress values are presented in Table II.

A second test was performed using the more sensitive 0.010 inch (1% strain) full scale range for the initial segment of the stress-strain diagram. A strain rate of 0.005 inch/inch/minute was employed through the 0.2% yield point. The valve setting on the testing machine to achieve the 0.005 inch/inch/minute rate was left unchanged for the duration of the test so that the resultant strain rate for the latter portion of the test is not known. The specimen was strained to 0.8% on the 0.010 inch full range on the recorder and an additional 0.72% on the 0.020 inch full scale range for a total strain of 1.52% before the load was released. Yield strength calculations from this test, shown in Table II, are in good agreement with the initial test. Data for a third specimen, tested under the same

TABLE II. ROOM TEMPERATURE COMPRESSIVE PROPERTIES OF Mo-TZM ALLOY

Identity - MCN-1037-G

Heat No. - TZM-7496

Condition - Stress-Relieved 2350°F/1 Hour

Strain Rate - 0.005 Inch/Inch/Minute Through 0.2% Yield

Specimen Identity	0.02% Yield Strength, psi	0.2% Yield Strength, psi	Strength at 1.0% Total Strain	Modulus of Elasticity psi x 10^6
MCN-1037-G-21	106,200	120,200(1)	--	38.3(4) 43.1(5)
MCN-1037-G-22	99,000	115,000(2)	117,200	34.2(4) 38.6(5)
MCN-1037-G-23	93,100	104,800(3)	104,800	39.3(4) 44.2(5)

---

(1) Test Terminated at 1.82% Total Strain.

(2) Test Terminated at 1.52% Total Strain.

(3) Test Terminated at 1.0% Total Strain.

(4) 1.0-Inch Measured Gauge Length.

(5) 1.125-Inch Estimated Effective Gauge Length.

conditions as used for the second test, also are presented in Table II. The resultant load-strain diagram developed with the third specimen is shown in Figure 1.

The modulus of elasticity was calculated from the stress-strain diagram using the measured gauge length of one inch and an estimated effective gauge length of 1.125 inch. It has been shown[2] that the effective gauge length of specimens with a reduced gauge section tested in compression extends beyond the shoulder of the specimen by a distance approximately equivalent to one half the wall thickness. From the data in Table II, it is quite apparent that the estimated effective gauge length used in the calculations for the modulus of elasticity of Mo-TZM alloy specimens is close to the true gauge length. The accepted value for the modulus of elasticity of unalloyed molybdenum is 46×10^6 psi.

To verify the assumption that the effective gauge length does extend into the shoulder of the compression specimen configuration and to accurately establish the additional length to be added to the measured gauge length, strain will be measured in a fourth Mo-TZM alloy specimen (MCN-1037-G-11) by means of strain gauges. Four strain gauges, type C6121, will be attached to the specimen in the center of the reduced section at 90° intervals, two parallel and two perpendicular to the long axis of the specimen. The data evolved in stressing this specimen, within the elastic limit, should provide a correction factor to be used in calculating the modulus of elasticity for the remaining candidate materials.

Friction and Wear

Friction and Wear in High Vacuum

Assembly of the major components of the vacuum friction and wear tester was started on December 18, 1964, and final assembly of the tester was started on December 28, 1964. The General Electric project engineer was on-site during the entire final assembly and vendor checkout. Only a few minor adjustments were required and only a few machining discrepancies were found. All parts were assembled and the necessary assembly inspections were made to properly position the diaphragm and magnetic clutch. The rotating parts were assembled on the two shafts and balanced; subsequently, they were marked so that they could be reassembled in the same position at General Electric. Friction appeared to be quite acceptable on both sets of shaft bearings and the magnetic clutch appeared to work properly.

The tester was received at General Electric on January 6, 1965, after which it was completely disassembled for dimensional and penetrant inspection of all rotating parts, i.e., shaft and specimen holders. The components that were inspected were found to be free of defects and dimensionally acceptable. The vendor's inspection reports for the remainder of the parts were accepted without verification as the General Electric project engineer was present during the final assembly and it was established that all components fit without impairment of their functions.

The general appearance of the vacuum friction and wear tester as it was received from the vendor is shown in Figure 2 and after it was installed on the vacuum system in Figure 3. An exploded view of the components of the tester and photographs of the major components are shown in Figures 4 to 9.

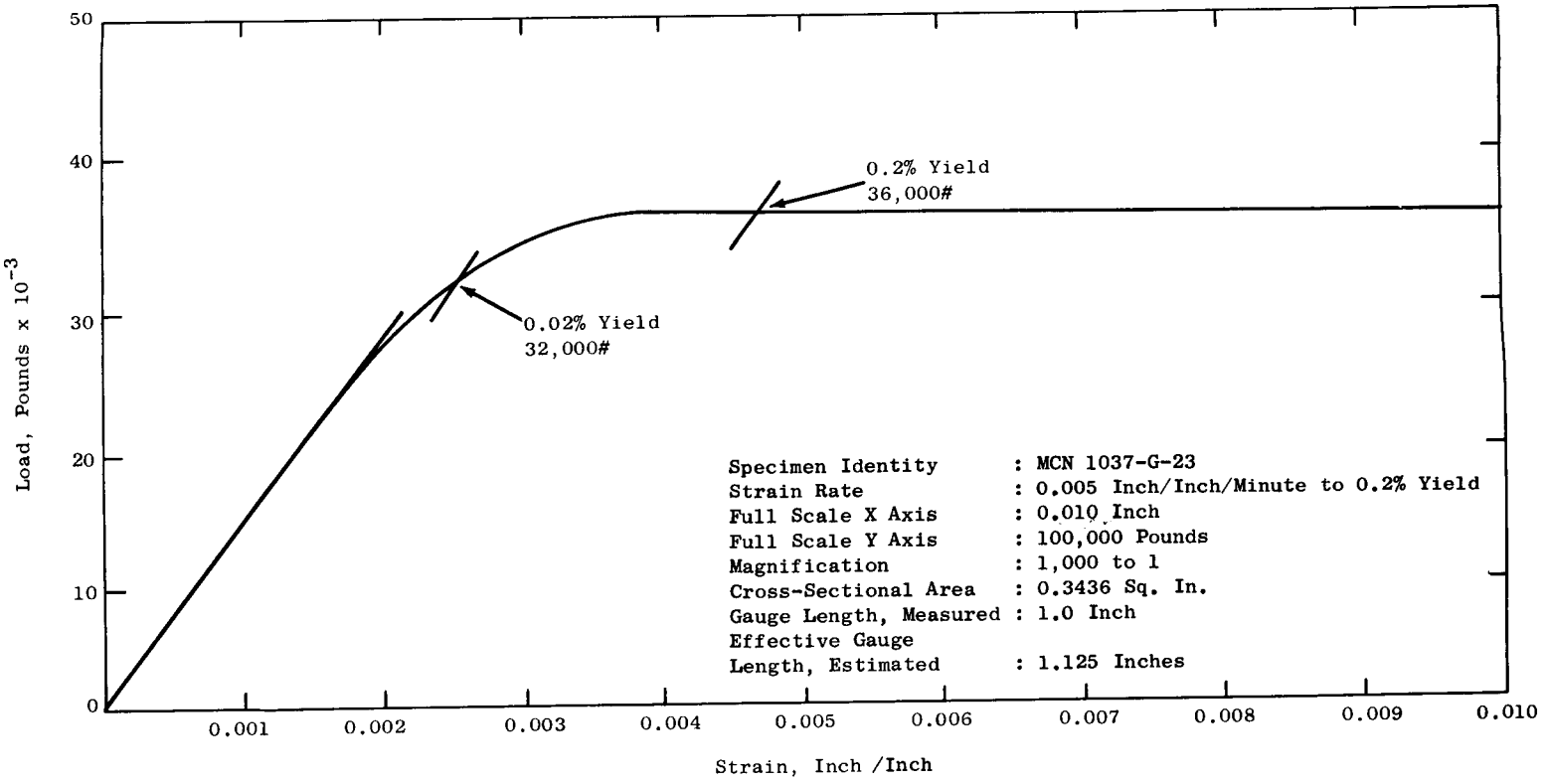

Figure 1. Room Temperature Load-Strain Curve for Mo-TZM Alloy in Compression.

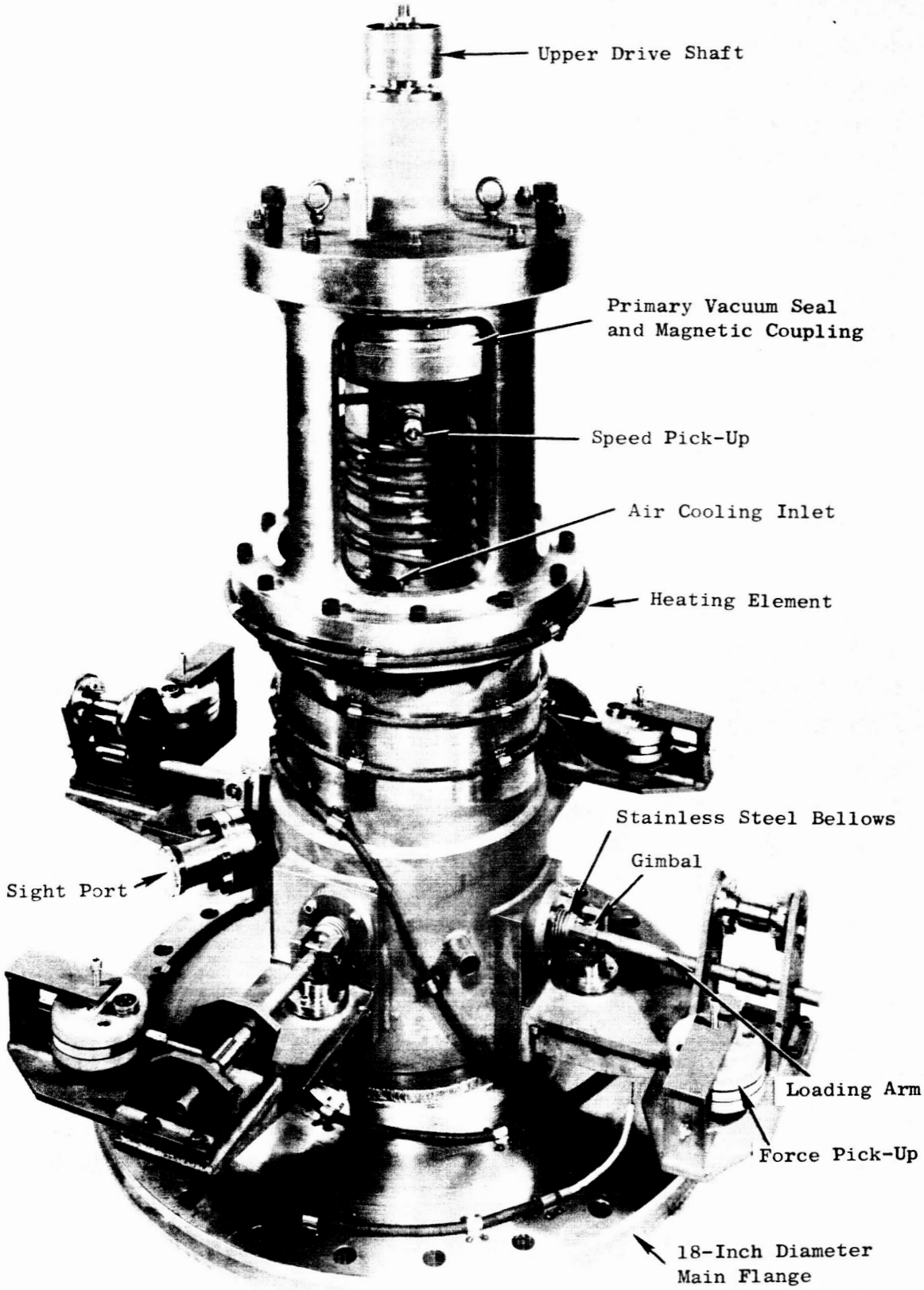

Figure 2. High Vacuum Friction and Wear Tester. (C65010860)

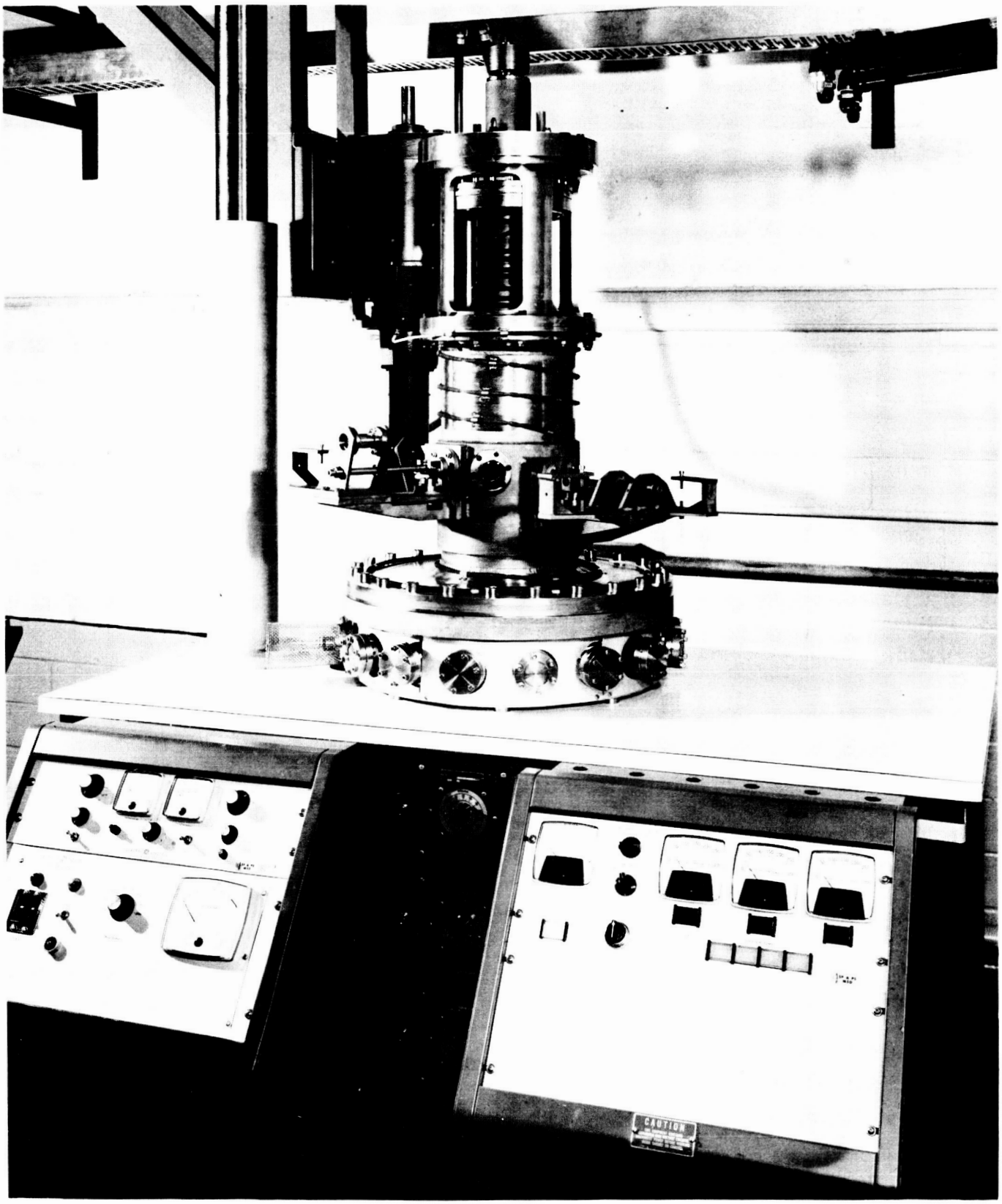

Figure 3. High Vacuum Friction and Wear Tester Installed on a General Electric Vacuum System Incorporating a 1,000 ℓ/Sec Getter-Ion Pump. (C65011121)

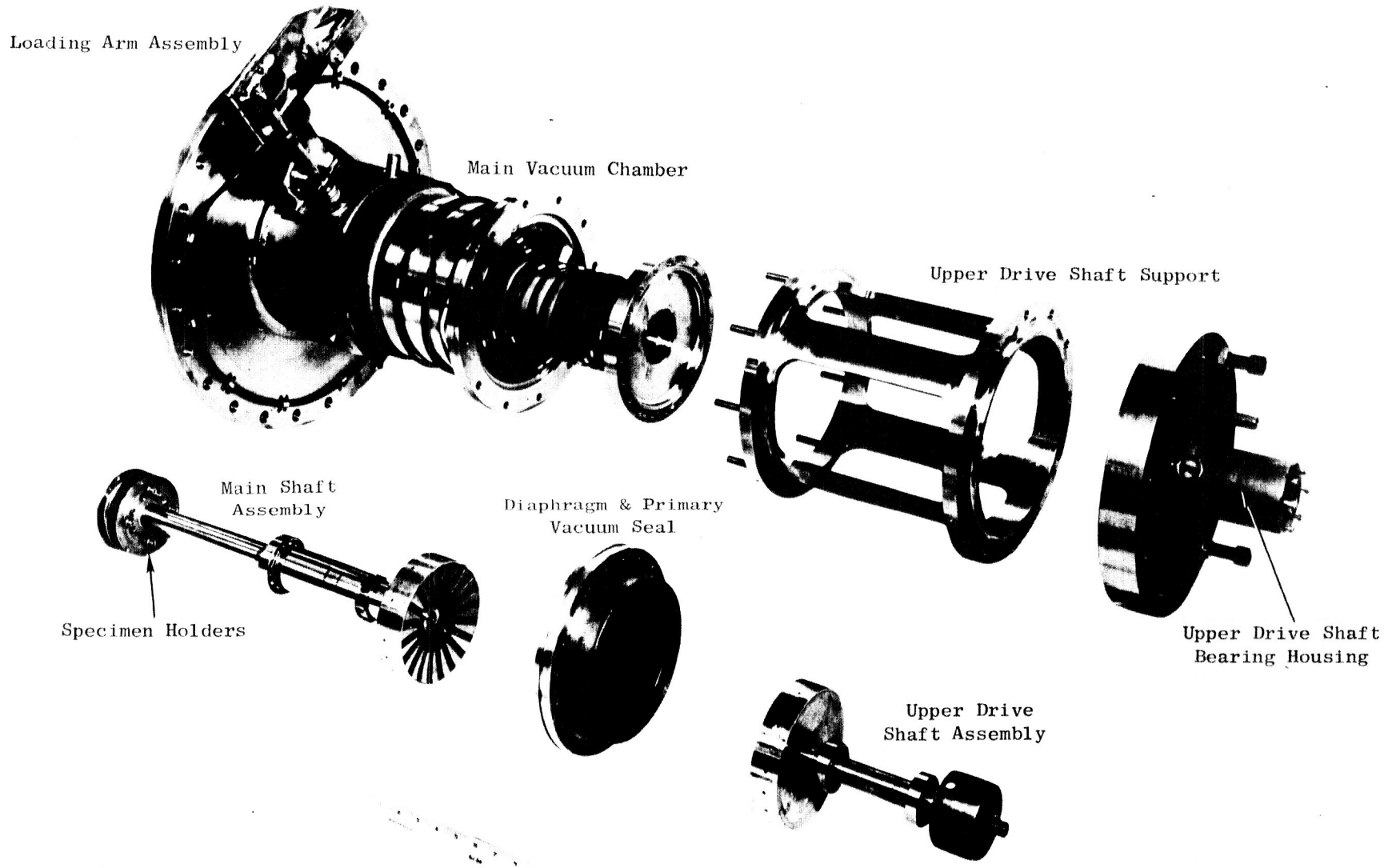

Figure 4. Major Components for High Vacuum Friction and Wear Tester.
(C65012240)

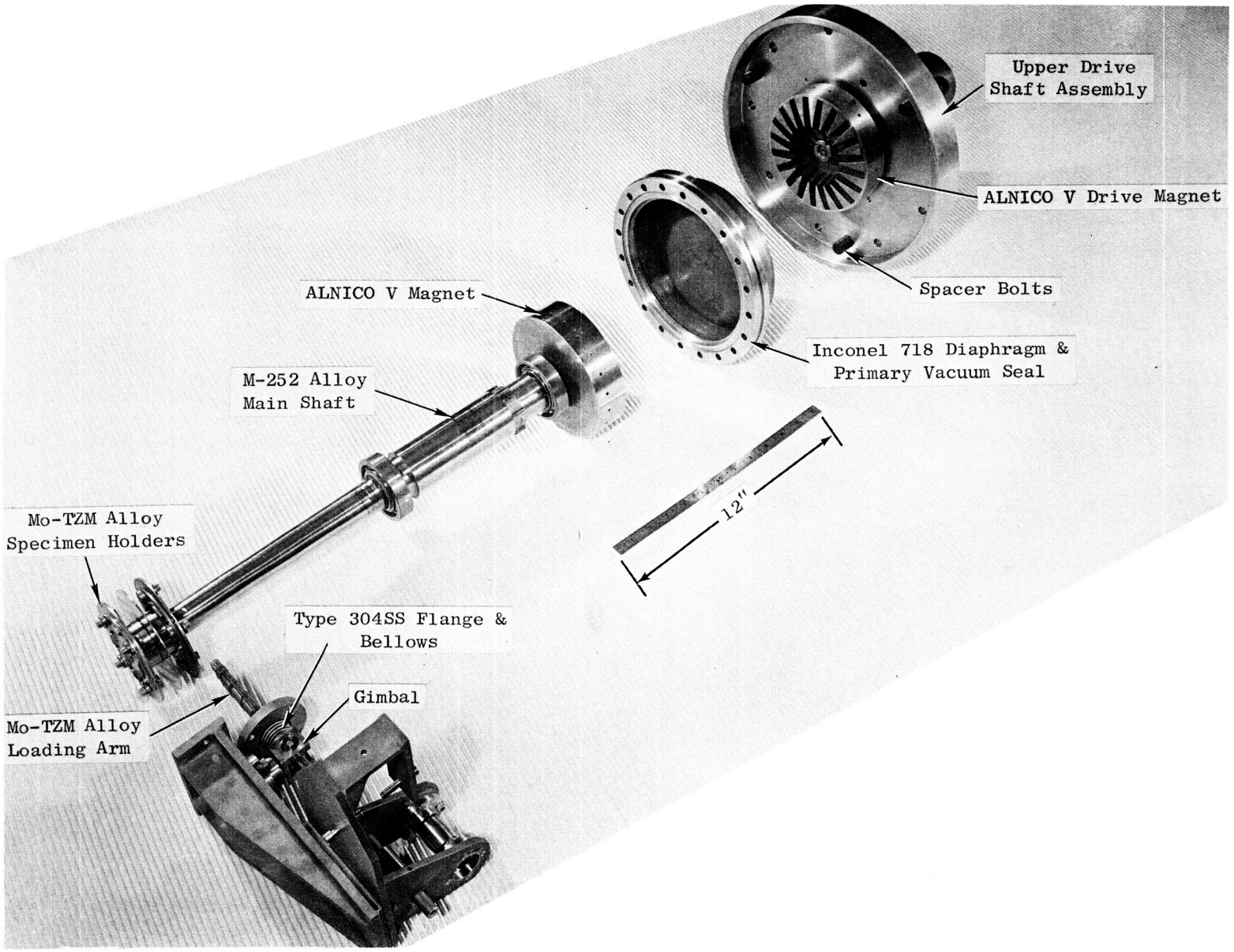

Figure 5. Upper Drive Shaft, Nonmagnetic Diaphragm, Main Shaft with Specimen Holders and Loading Arm Assemblies for High Vacuum Friction and Wear Tester. (C65011119)

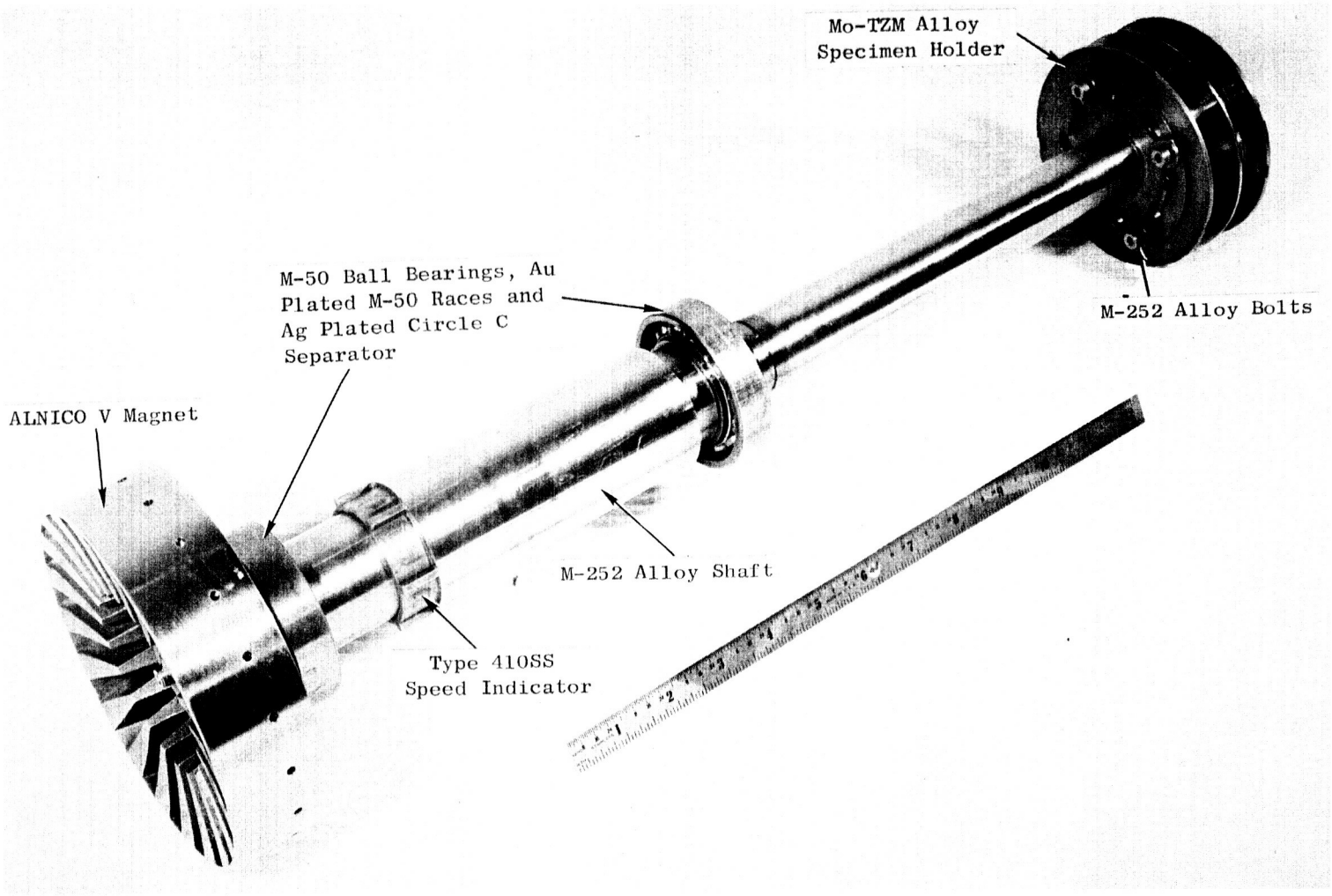

Figure 6. Main Shaft Assembly for High Vacuum Friction and Wear Tester. (C65011118)

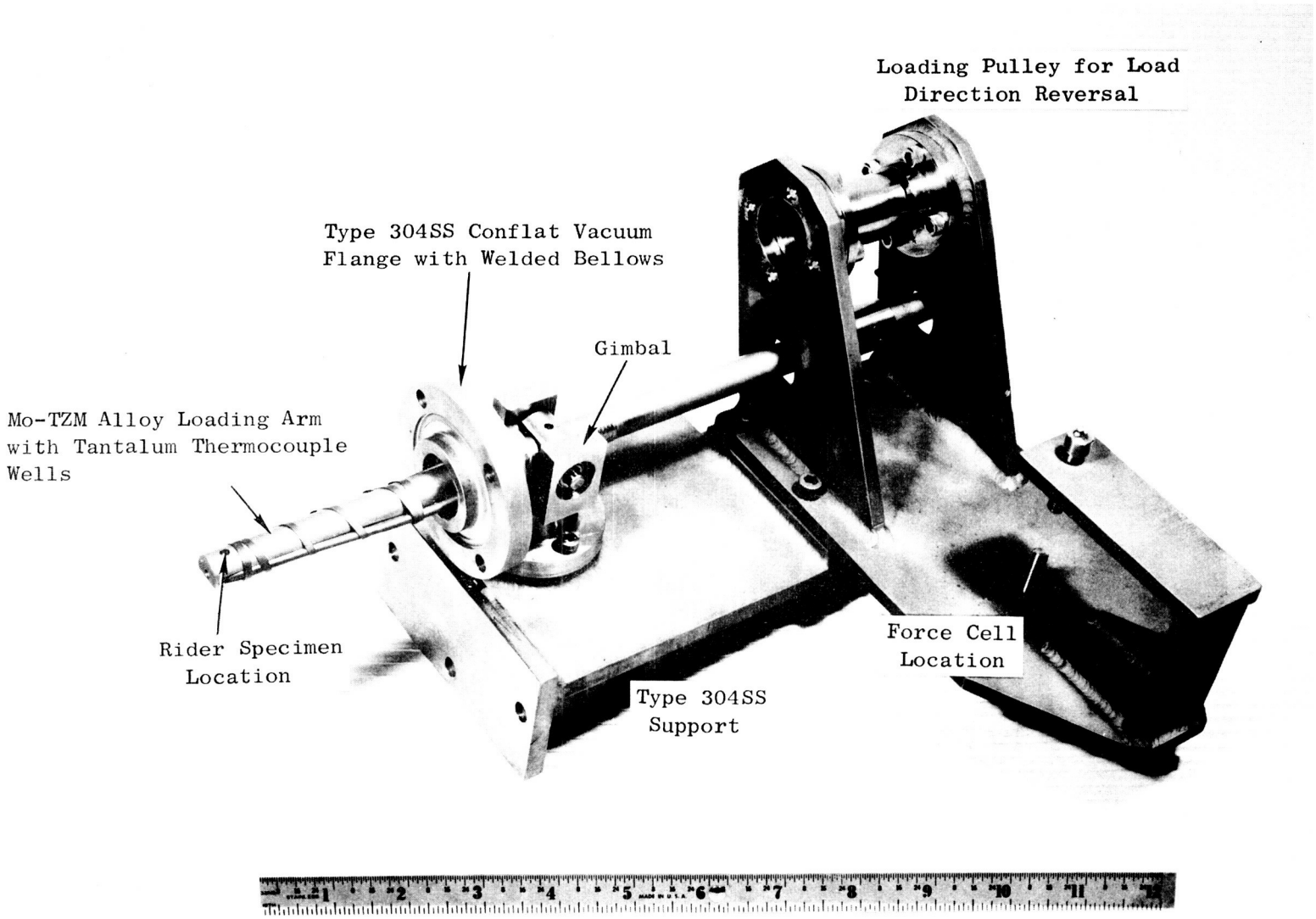

Figure 7. Loading Arm Assembly for High Vacuum Friction and Wear Tester. (C6501113)

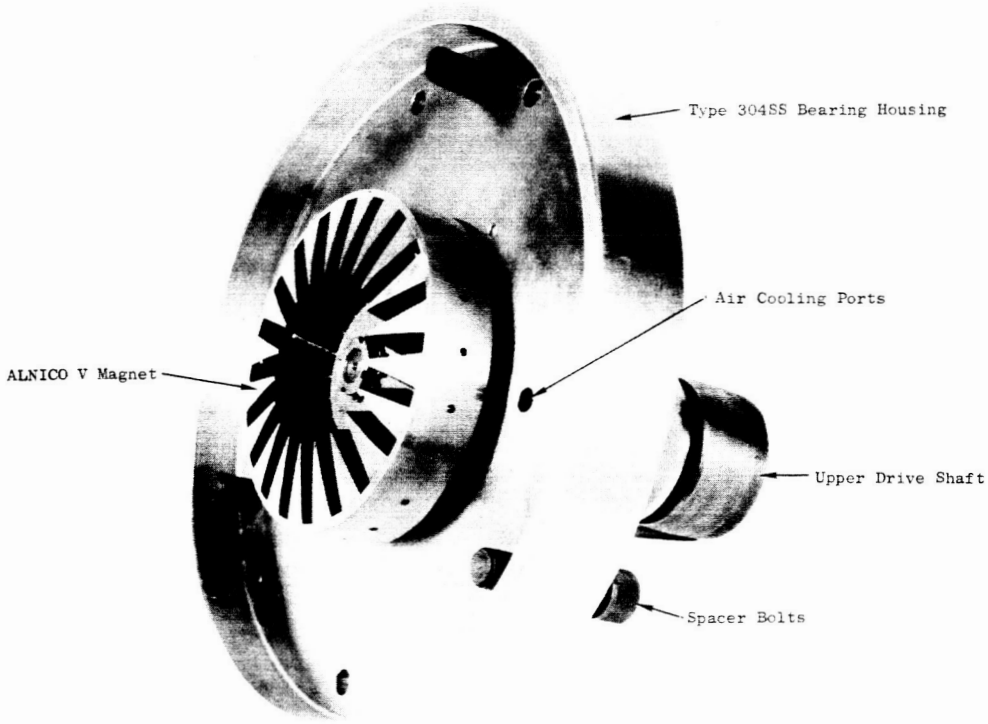

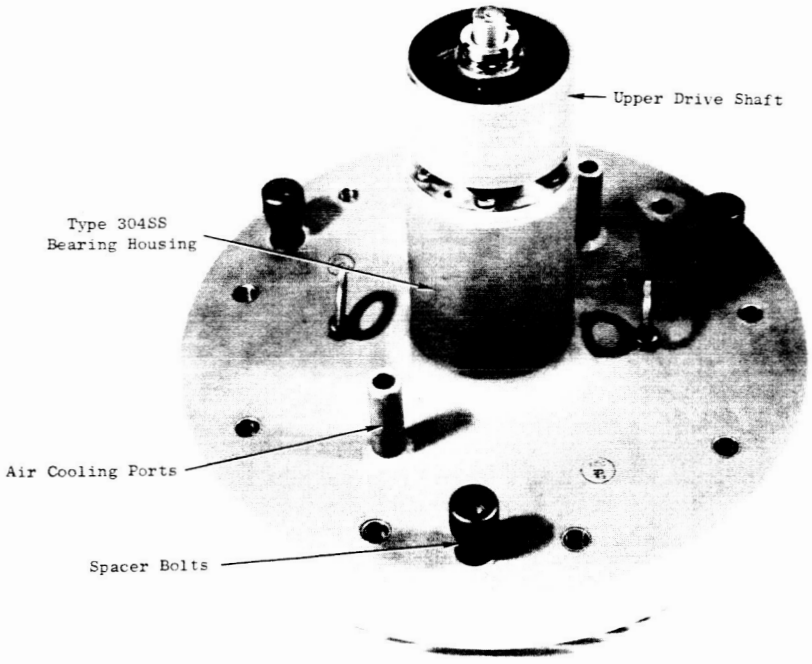

Figure 8. Upper Drive Shaft Assembly for High Vacuum Friction and Wear Tester. (Top: C65011124)(Bottom: C65011120)

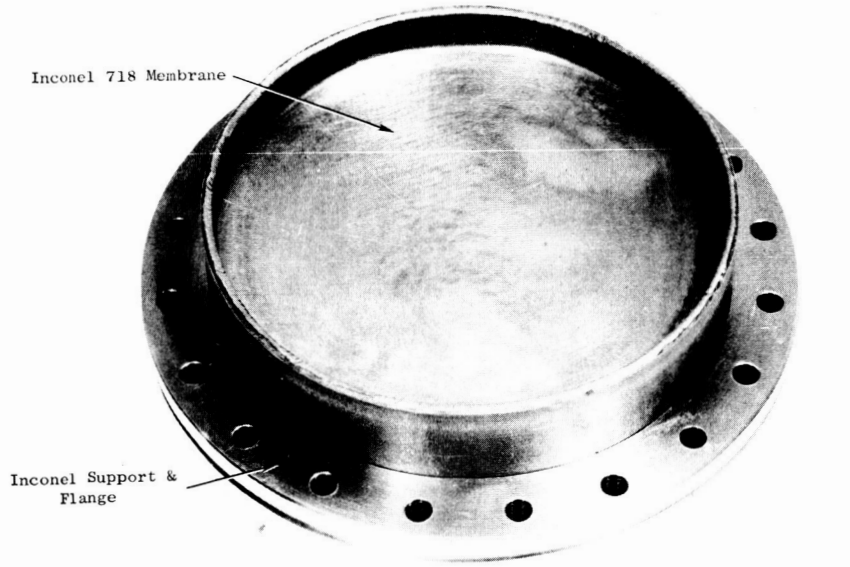

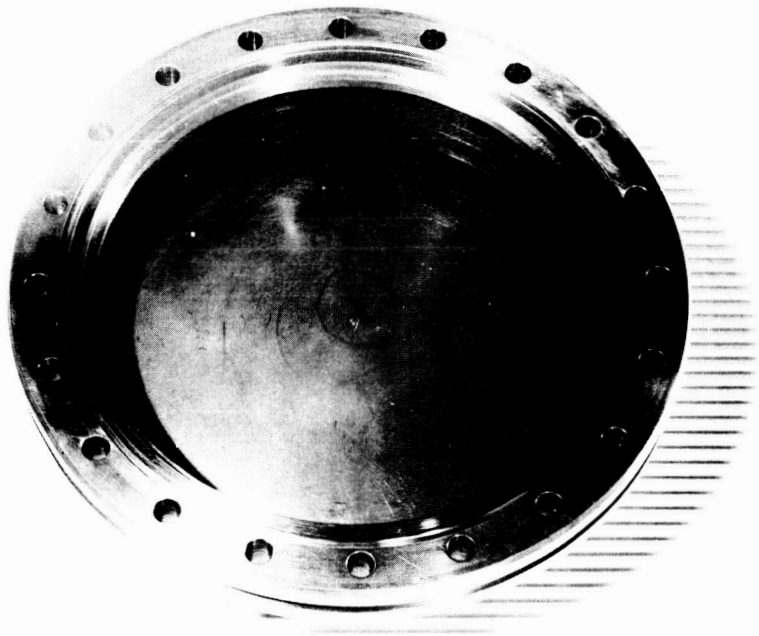

Figure 9. Nonmagnetic Diaphragm (Inconel 718) for Magnetic Coupling Used in High Vacuum Friction and Wear Tester. (Top: C65011117) (Bottom: C65011116)

The following tasks must be completed before the first tests can be run:

1. Assembly dimensional checks on components fabricated at General Electric which could not be simulated at the machining vendor's shop, i.e., heating elements, heat shield support, cover and bus bar.

2. Tare-weight tests on loading arms and load cells.

3. Diaphragm pressure test.

4. Vacuum capability test.

5. Heat distribution tests.

Of these preliminary tests, the following were accomplished:

Helium Leak Test. Excluding the main drive shaft and rotating parts and with the loading arms, viewing port and diaphragm No. 2 installed, a helium mass spectrometer leak test was made on the vacuum chamber installed on the base assembly as shown by Figure 3. The only leak that was detected was a minor one of 8×10^{-10} std cc air/sec at the bellows weld of loading arm No. 1. The leak was repaired by furnace brazing.

Diaphragm Pressure Test. This test was conducted to prove the acceptability of diaphragm No. 1 because of its deviations from the originally designed contour. In addition, the test was intended to prove the capability of the design to withstand an internal pressure of 60 psig, which could occur if that pressure were being used as the cover gas pressure in the potassium friction and wear tester with no external backup pressure on the diaphragm, or the equivalent of which could occur if a lower pressure in the chamber were used and the backup pressure were lost suddenly.

Again, the basic equipment setup was as shown in Figure 3 except that the upper bearing housing assembly was removed, a system of supplying nitrogen (regulated by a 0-60 psi gauge at 1/4 psi intervals) was added and strain gauges were applied to the diaphragm as shown in Figure 10. As the pressure was increased in the chamber, the actual strain of the diaphragm was measured by use of the strain gauges. Stress was calculated from the equation:

$$\sigma_\theta = \frac{E(\epsilon_\theta + \epsilon_x)}{1 - \mu^2}$$

where:

σ_θ = Stress, θ direction

ϵ_θ = Strain, θ direction

ϵ_x = Strain, X direction

E = Modulus of elasticity of Inconel 718 = 30×10^6 psi

μ = Poisson's Ratio = 0.3

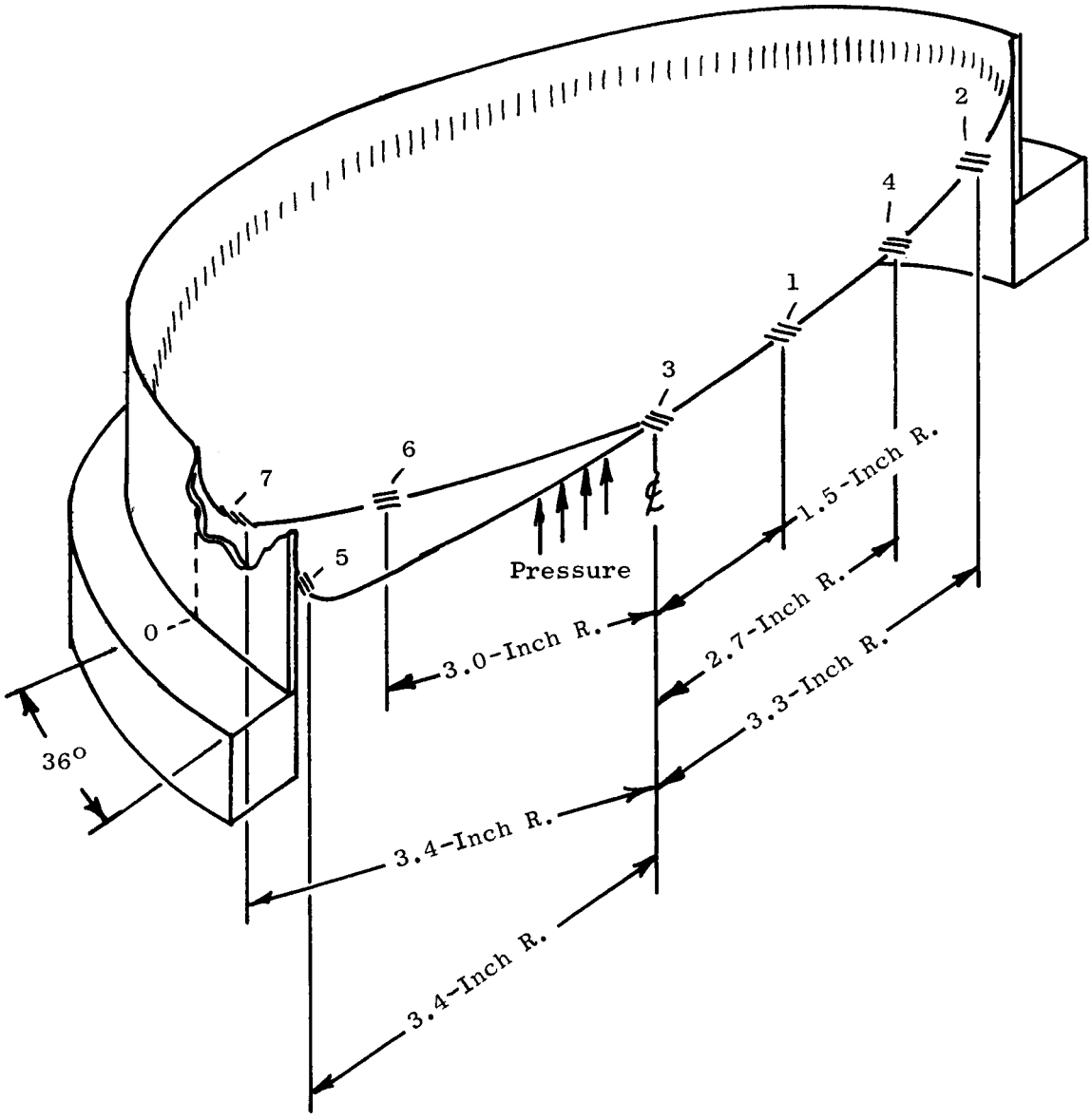

Figure 10. Location of Strain Gauges Applied to High Vacuum Friction and Wear Tester Diaphragm No. 1; Gauge Symbols Indicate Direction of Grids.

then,

$$\sigma_\theta = 30.0 \times 10^6 \left[\frac{(\epsilon_\theta + 0.3\ \epsilon_x)}{0.91}\right]$$

$$\sigma_\theta = 32{,}967 \left[\epsilon_\theta + 0.3\ \epsilon_x\right] \qquad (1)$$

similarily,

$$\sigma_x = 32{,}967 \left[\epsilon_x + 0.3\ \epsilon_\theta\right] \qquad (2)$$

The strain data obtained from the pressure test and the calculated stresses in the diaphragm using equations (1) and (2) are presented in Table III and a plot of the calculated stress vs the internal pressure in the chamber is shown in Figure 11.

The calculations at 1.5-inch and 2.7-inch radius assume the same axial/circumferential stress field ratio as calculated by the computor. A conversion to "effective stress" may be made using VonMises' criteria:

$$\sigma_e = \sqrt{\sigma_x^2 + \sigma_\theta^2 - \sigma_x \sigma_\theta} \qquad (3)$$

Then for 50 psi, the effective stress is:

σ_e = 29,130 psi in compression at the 3.0-inch radius

and

σ_e = 29,590 psi in compression at the 3.4-inch radius.

Using a value of 138,000 psi for the 0.2% yield strength of the Inconel 718 at room temperature, the factor of safety is:

$$\text{F.S.} = \frac{\text{allowable}}{\text{maximum}} = \frac{138{,}000}{29{,}590} = 4.66 \text{ (room temperature)}$$

The computor-calculated stresses for the "inner" surface (on which strain gauges were applied), σ_{ei}, and the "outer" surface, σ_{eo}, at 50 psi were:

σ_{ei} = 34,070 psi in compression at the 3.0-inch radius

σ_{eo} = 26,970 psi in compression at the 3.0-inch radius

σ_{ei} = 79,160 psi* in compression at the 3.4-inch radius

σ_{eo} = 67,703 psi in compression at the 3.4-inch radius

* Highest Calculated Stress

TABLE III. EFFECT OF INTERNAL CHAMBER PRESSURE ON THE STRESS AND STRAIN EXERTED BY THE DIAPHRAGM ON THE HIGH VACUUM FRICTION AND WEAR TESTER

Diaphragm Radius Inches	Gauge No. & Direction	Gauge Pressure (psig) 10		20		30		40		50	
		ϵ In/In x 10^{-6}	σ psi	ϵ In/In x 10^{-6}	σ psi	ϵ In/In x 10^{-6}	σ psi	ϵ In/In x 10^{-6}	σ psi	ϵ In/In x 10^{-6}	σ psi
0	3 (x,θ)	-20	-860	-50	-2,140	-80	-3,430	-105	-4,500	-115	-4,930
1.5	1 (θ)	-40	-1,680	-115	-4,840	-190	-7,990	-285	-11,990	-415	-17,457
2.7	4 (θ)	+60	+2,160	+110	+3,950	+180	+6,470	+240	+8,630	+310	+11,140
3.0	2 (θ)	+150	+4,050	+300	+7,710	+460	+11,600	+610	+15,120	+765	+18,400
	6 (x)	-90	-1,480	-220	-4,290	-360	-7,320	-505	-10,620	-690	-15,180
3.4	5 (θ)	+100	+1,420	+210	+3,070	+350	+5,750	+470	+8,080	+585	+10,730
	7 (x)	-190	-5,270	-390	-10,780	-585	-15,820	-750	-20,080	-865	-22,730

NOTE: - Signifies Compression

+ Signifies Tension

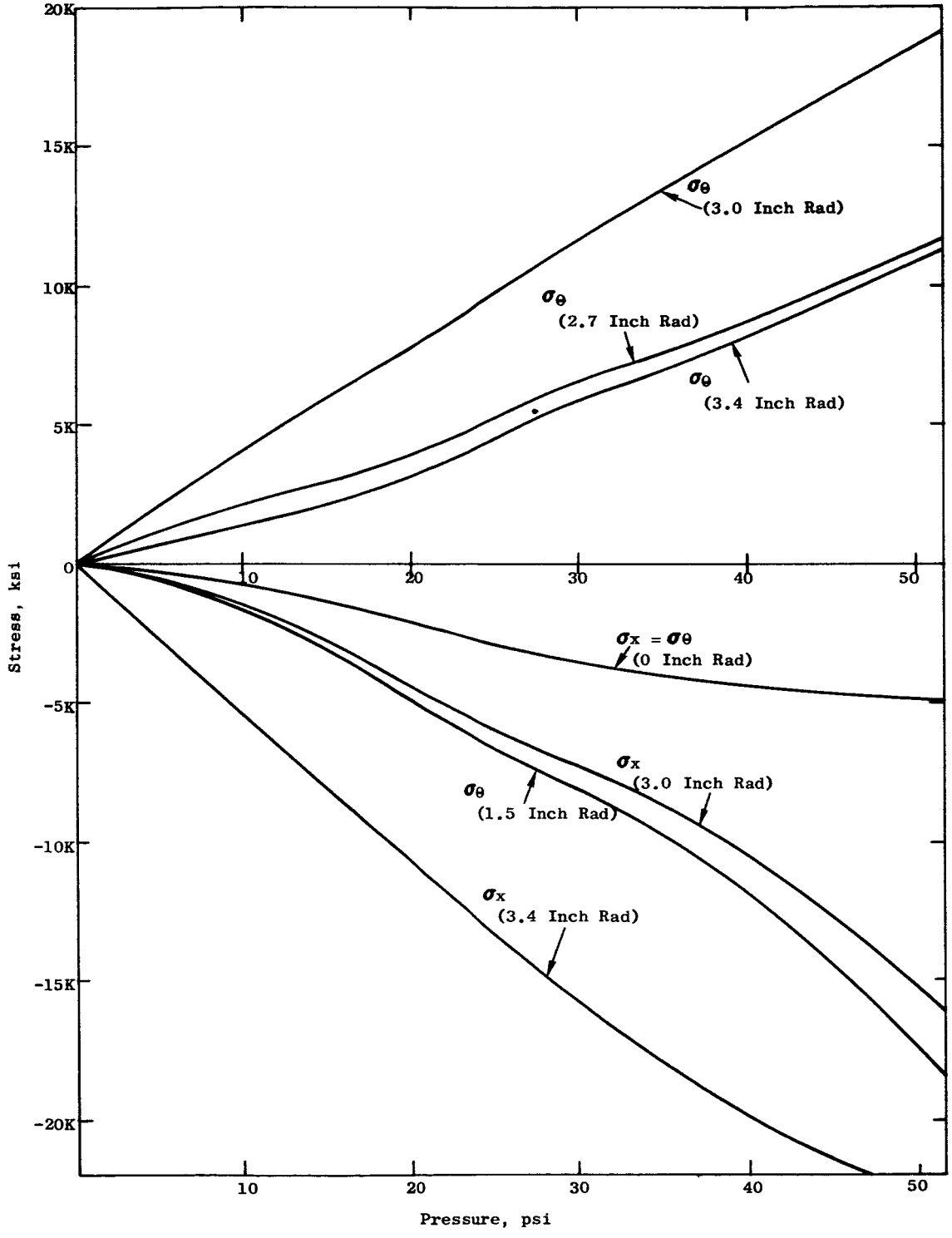

Figure 11. Stress in Inconel 718 Diaphragm as a Function of Internal Chamber Pressure.

Although the computer-calculated stresses are satisfactory, the measured stresses were appreciably lower; this is probably due to an "averaging" of the loads which the computer does not predict.

In raising the pressure from 50 to 60 psig, the membrane buckled inward. The knowledge of the pressure at which this occurs is extremely valuable, insofar as neither the computor program nor the pressure-stress plot gave any indication that this would happen.

Diaphragm Temperature Distribution Test. Because of space limitations between the membrane and the magnet and the possibility of weakening the membrane by tack-welding a thermocouple directly to the membrane, it is impossible to monitor the membrane temperature directly during actual running of the friction tester. Therefore, it is necessary to obtain a correlation between the temperature of the 0.031-inch thick Inconel 718 membrane portion of the diaphragm and the temperature of the 0.032-inch thick Inconel circumferential support ring. It is necessary to know the temperature of the membrane in order that the strength of the membrane can be maintained within safe limits during operation of the tester.

Chromel and alumel thermocouple wires were tack-welded directly to diaphragm No. 1 about 1/8-inch apart, using the membrane to complete the circuit between the two wires. The location of the thermocouples on the diaphragm and the general build-up of the test setup is shown in Figure 12. Temperatures were allowed to stabilize after each change in heater power and recorded on a strip chart by a Bristol recorder. The results of the test are recorded in Table IV and plotted in Figure 13.

Tare-Weight Tests. A tare-weight flange and O-ring plate were designed to allow the use of the vacuum chamber of the friction and wear tester to determine the tare forces associated with the loading arm bellows as a function of internal pressure, Figure 14. The loading arms for both the vacuum and potassium test rigs will be calibrated at station No. 1 for the high vacuum test rig vacuum chamber. The loading arm will be installed at station No. 1 and the O-ring plate and tare-weight flange installed in the lower bearing housing of the vacuum chamber. The stem of the tare-weight flange is located above the specimen hole in the loading arm. A wire tray is attached to the loading arm through the specimen hole with a protrusion above the arm which is set to contact the end of the stem when the arm is exactly horizontal. Calibrated weights are loaded into the tray and the vacuum chamber is bolted to the base assembly. Pressure is applied to the chamber and external weights are added to the loading arm belt until balance is achieved, as noted by looking through the vacuum chamber viewing port and felt by finger pressure on the outside end of the loading arm. Accuracy of about 0.005 pound should be possible. The force pickups will be calibrated in a similar manner.

Friction and Wear in Liquid Potassium

All component parts for the potassium friction and wear tester, excluding the potassium sump heater, essentially are completed and final assembly should begin the week of February 22, 1965. The M-252 alloy main shaft, the Cb-1Zr alloy sump

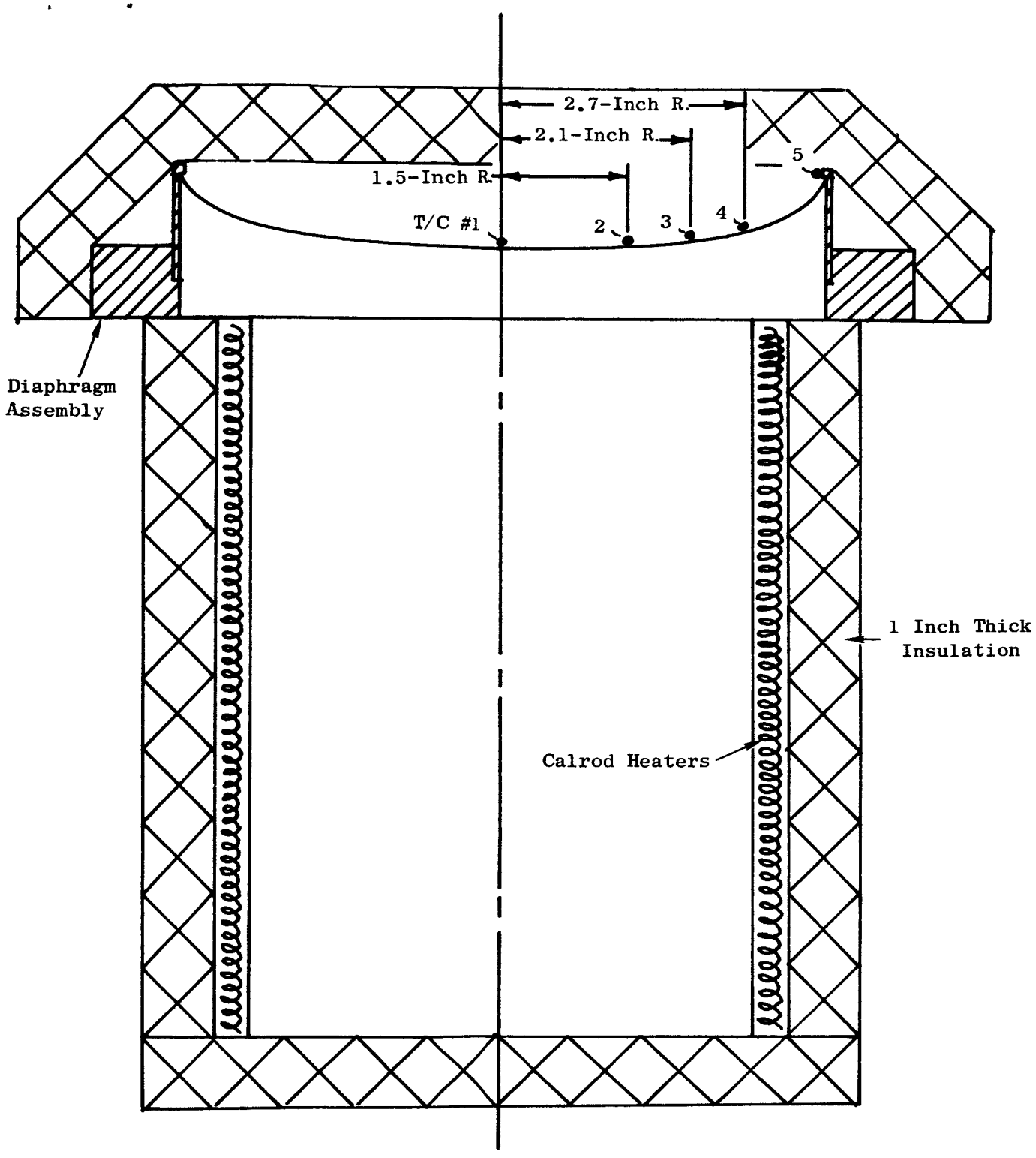

Figure 12. Location of Thermocouple and Test Setup for Temperature Distribution Test of Inconel 718 Diaphragm.

TABLE IV. TEMPERATURE DISTRIBUTION OF DIAPHRAGM ON HIGH VACUUM FRICTION AND WEAR TESTER

Time	Temperature, °F				
	T_1	T_2	T_3	T_4	T_5
0705	213	211	200	--	113
0755	295	293	270	245	152
0807	360	358	338	310	211
0821:30	430	424	402	369	253
0835:30	500	492	468	429	292
0840	560	556	529	488	331
0855	700	692	663	612	422

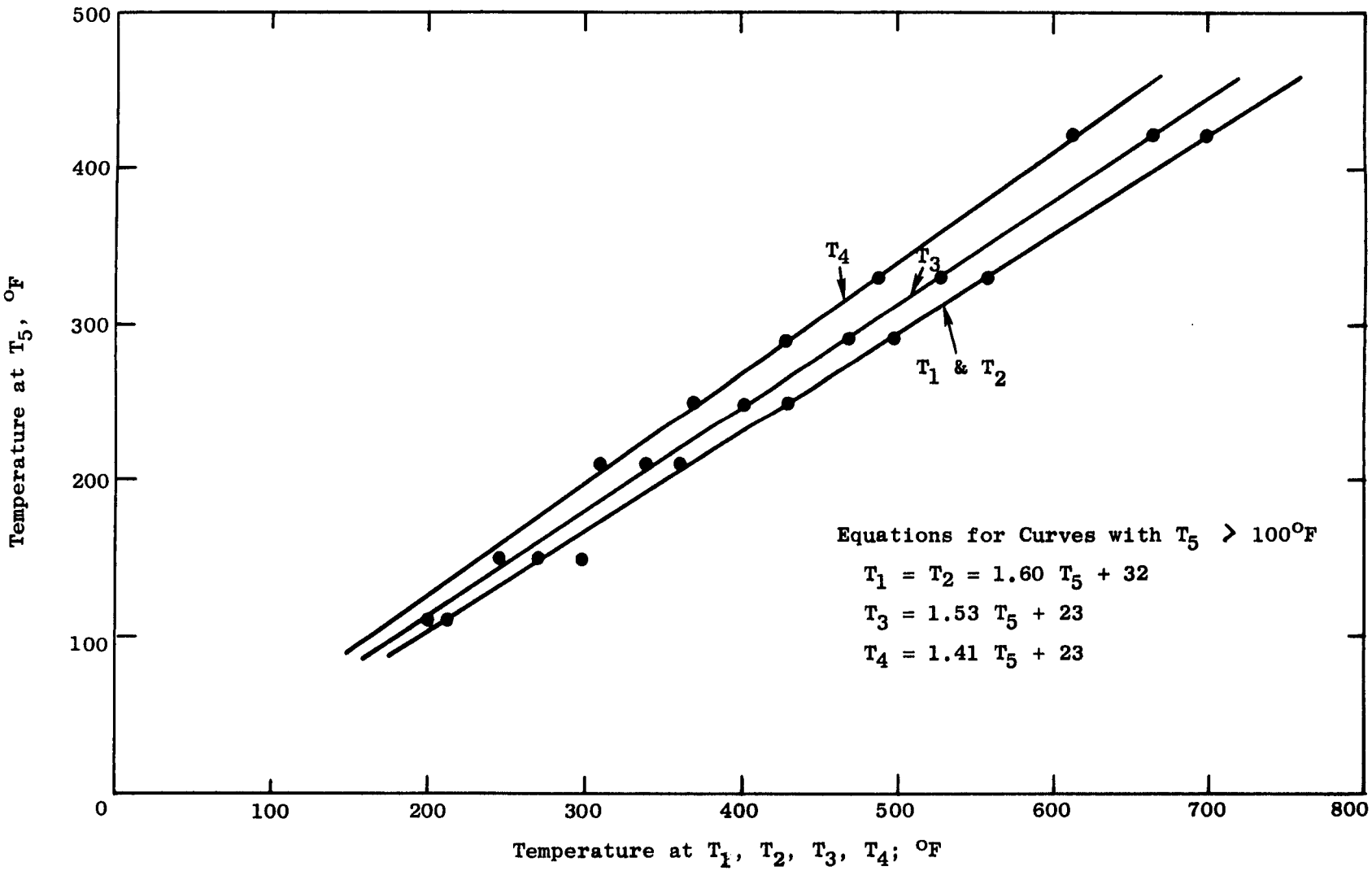

Figure 13. Temperature of Diaphragm Membrane at T_1, T_2, T_3, and T_4 as a Function of the Temperature of the Inconel Support Ring at T_5

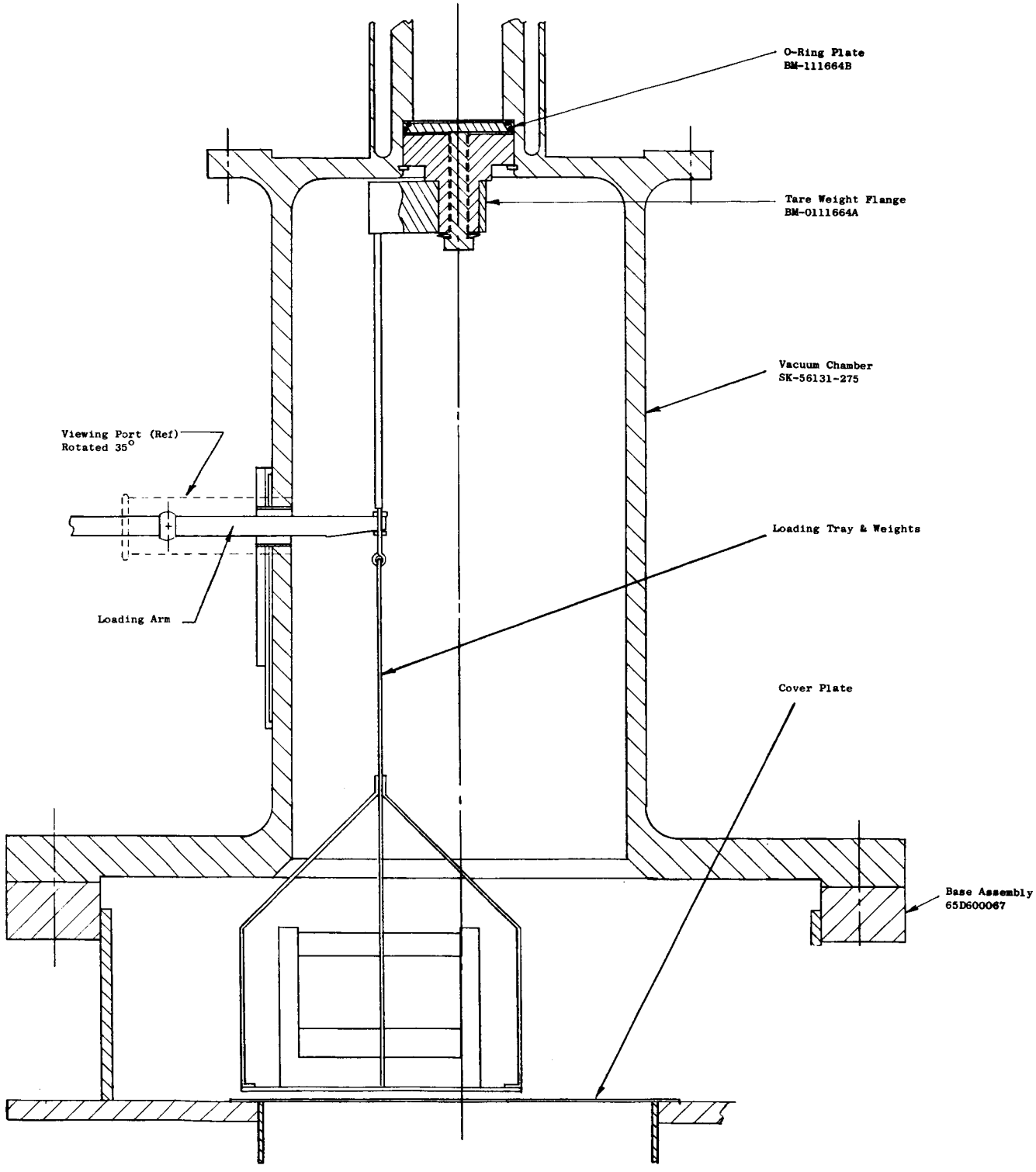

Figure 14. Tare-Weight Flange Assembly for the Calibration of the Loading Arms for the Friction and Wear Testers as a Function of Internal Pressure.

(Figure 15) and the Type 304SS vacuum chamber are the pacing items. Brazing techniques for the joining of the heating elements to the outer wall of the inner liner of the vacuum chamber are being verified before committing the actual components. The pump impellers, which the vendor was unable to machine, have been satisfactorily machined at General Electric and are shown in Figure 16. An exploded view of the specimen holder assembly with the low-speed Cb-1Zr alloy pump impeller is shown in Figure 17.

The conductive immersion heaters are presenting some fabrication difficulties. Because the BN core insulators are close to theoretical density, the BN cores crack during the swaging operation, allowing the heating wires to be imbedded into the cracks and therefore decreasing the uniformity of the distance from the heater wires to the Cb-1Zr alloy sheath. Although disconcerting, it is not known at this time whether the non-uniform spacing of the heating elements will have a serious effect on the efficient functioning of the "fire-rods" or whether the life of the heaters may be reduced by only a few percent. Rather than permit the vendor to substitute a different core material at this time, the following plan of attack is being pursued:

1. General Electric will vacuum degas sufficient cores and powder to make four BN and four Al_2O_3 "fire-rod" type heating elements. Separate lots of boron nitride cores and powder will be vacuum degassed at 2200° and 2800°F; the Al_2O_3 will be vacuum degassed at 2200°F.

2. The vendor will fabricate four "fire-rods" from each type of core material with Cb-1Zr alloy sheaths, maintaining the insulators under inert gas as much as possible in order to minimize the pickup and subsequent entrappment of air and water vapor in the cores of the heaters.

3. General Electric will submit the elements to a life test in hard vacuum at 1600°F to determine whether the production method, or insulator core material, should be changed.

Instrumentation

All instrumentation for both the vacuum and potassium friction and wear testers has been ordered. The instrumentation will provide the following readings:

	Item	Liquid Potassium Tester	High Vacuum Tester
1.	Thermocouples (T/C), 2 per arm	4	8
2.	T/C, potassium sump	1	0
3.	T/C, facility flange	1	0
4.	T/C, 2 per main bearing	4	4
5.	T/C, diaphragm	1	1
6.	T/C, miscellaneous (including dummy arm)	4	2

Item	Liquid Potassium Tester	High Vacuum Tester
7. Speed (rpm), main shaft	1	1
8. Speed (rpm), drive motor	1	1
9. Force pickups, 1 per arm	2	4
10. Vibration pickups, 2 per main bearing	4	4

Test Facility

The area preparation and facility build-up for the liquid potassium friction and wear tester, as described in Quarterly Progress Report No. 43, was initiated during the report period. Electrical services, cooling air facilities, drains and an air purifier and filter to remove oil, water and foreign material from the shop air to be used for cooling were installed. Air lines for both testers were installed and the air heaters for the liquid potassium tester were hooked-up and checked out.

The control consoles were received and installed and all disconnect switches, wireways, drive-motor controls and transformers were positioned and wired. The drive motor and vacuum system for the vacuum friction and wear tester were positioned, final hook-up made and checkout completed.

The Pyr-A-Larm emergency ventilation system and air conditioning system were installed. The checkout of the Pyr-A-Larm will complete this installation. The new air conditioning system supplies one-pass fresh air which is exhausted continuously through a scrubber.

The build-up of the liquid potassium friction tester facility was started with many of the small components that have been completed. The primary cold trap, hot trap and waste tank were received and are being incorporated into the build-up. The inert atmosphere chamber has been completed and has been shipped by the vendor. It is anticipated that the facility will be completed prior to the receipt of the potassium friction and wear tester.

Wetting

Engineering drawings of the wetting test facility were completed and have been submitted to the NASA Technical Manager on November 13, 1964, for review and approval.

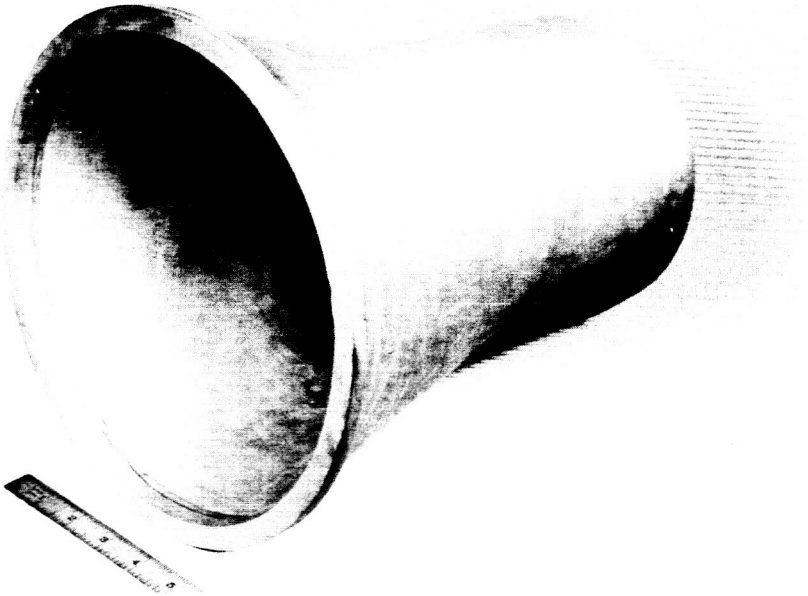

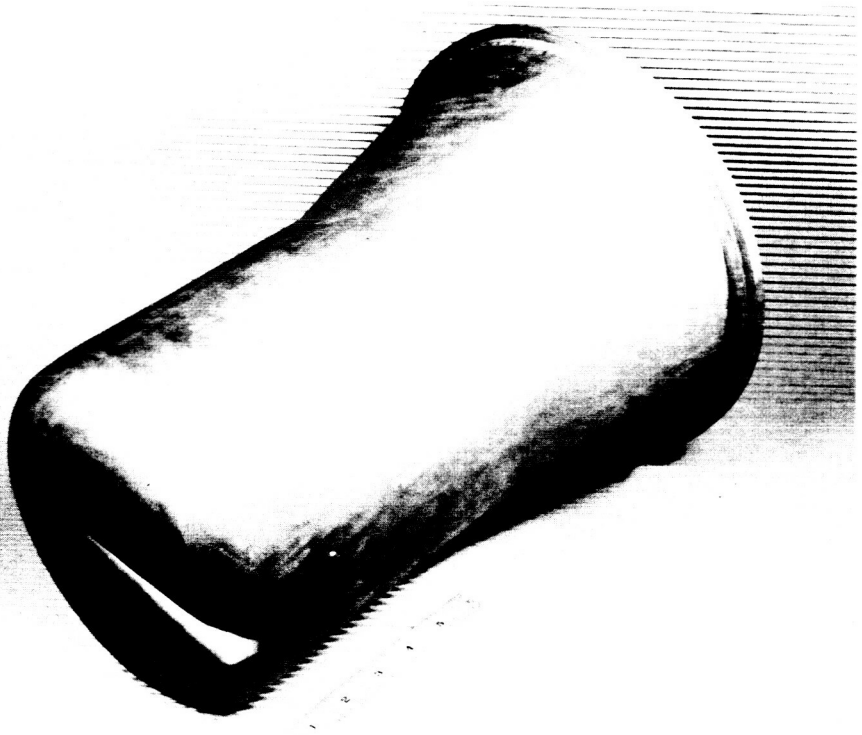

Figure 15. Partially Completed Cb-1Zr Alloy Sump for Liquid Potassium Friction and Wear Tester. (Top: C64121203) (Bottom: C64121204)

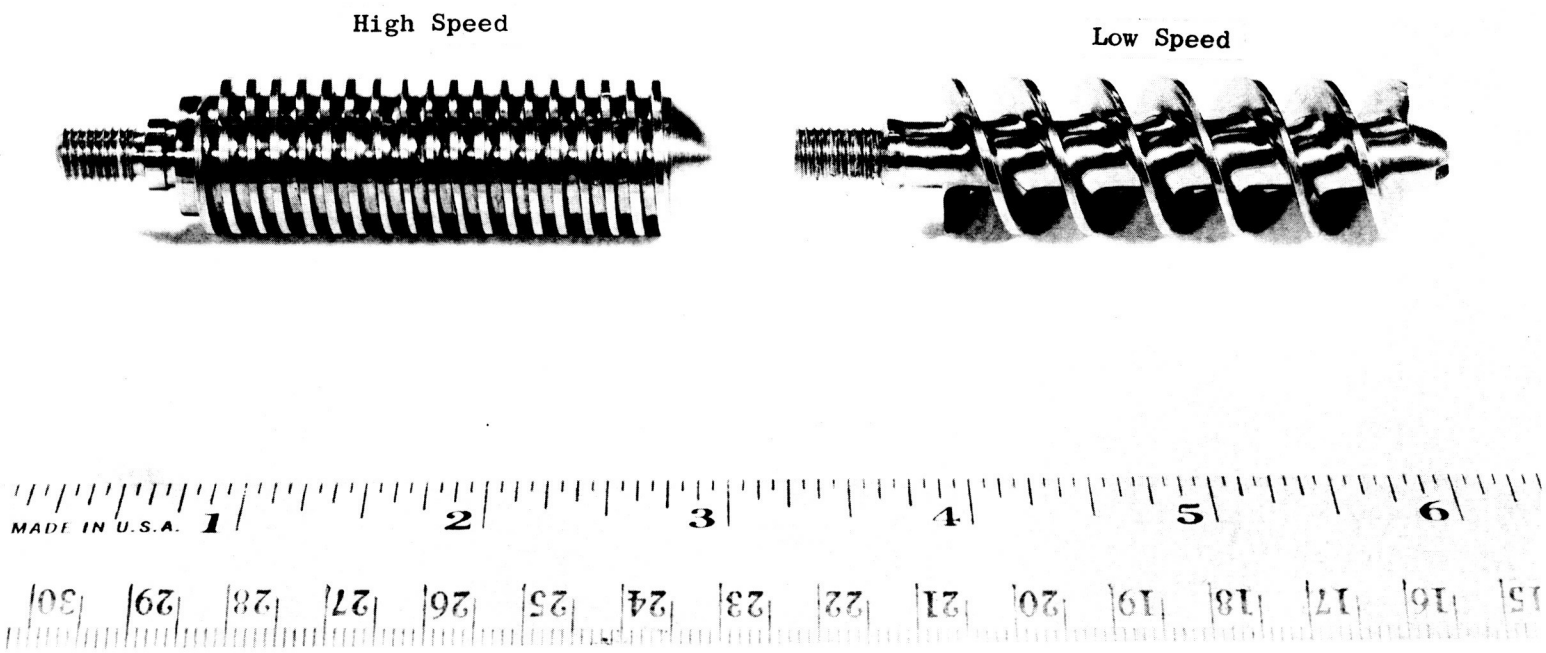

Figure 16. Columbium-1% Zirconium Alloy Pump Impellers for Potassium Friction and Wear Tester. (C65011465)

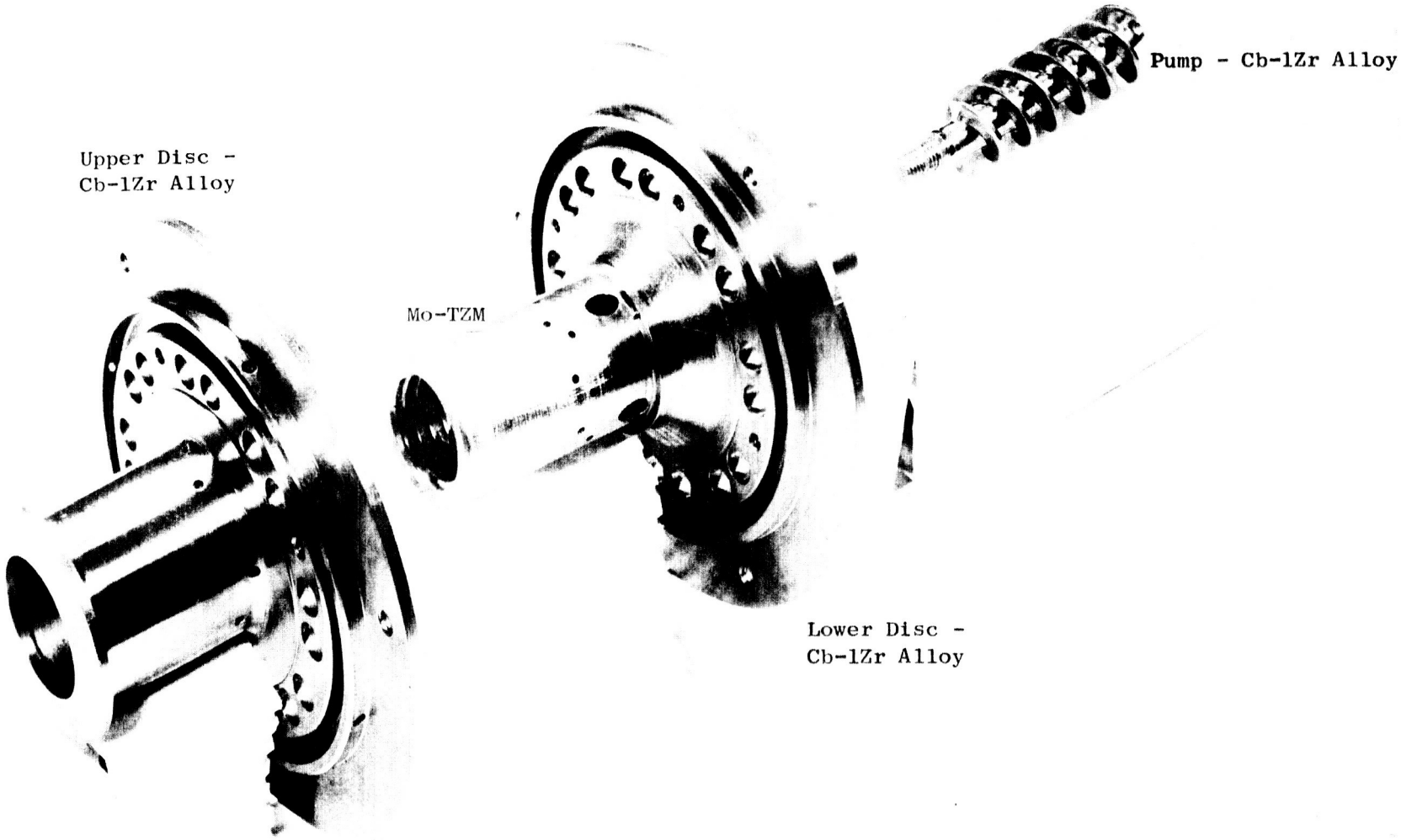

Figure 17. Components for Specimen Holder Assembly Used in Liquid Potassium Friction and Wear Tester.

(C65011404)

V. TEST PROGRAM

Alkali Metal Purification

Approximately 25 pounds of potassium were vacuum distilled and hot trapped in a titanium-lined, zirconium-gettered hot trap. The distillation was carried out at 520° to 540°F and a receiver pressure of about 3×10^{-5} torr, which resulted in a distillation rate of 2.5 pounds per hour. The hot trapping was conducted at 1200° to 1350°F for a period of 24 hours.

Various samples of the purified potassium were analyzed by the mercury amalgamation method for oxygen and the results are shown in Tables V and VI. A sample of the distillate after hot trapping also was analyzed for oxygen by General Atomics using neutron activation techniques and a value of 13.4 ± 17.8 ppm was obtained. This sample corresponds to analytical runs No. 7, 8, and 9 in Table VI. The limits for the average oxygen by the mercury amalgamation method are three times the standard deviation of the oxygen content. The linear correlation between the sample weight and micrographs of oxygen is given by the equation:

$$Y = 1.06 \times +7.4 \pm 7.6 \text{ (i.e. } 3\sigma\text{)} \ \mu\text{gms oxygen,}$$

where:

x = sample weight in grams.

The neutron activation and amalgamation methods appear to agree within 15 ppm oxygen for this potassium.

Due to the indeterminate difference between the oxygen contents of the distilled and the distilled and hot trapped potassium, there appears to be no advantage to hot trap after vacuum distillation using potassium of the starting quality as has been used in this program.

Potassium samples of the distillate from receiver, distillate in hot trap prior to hot trapping, and distillate after hot trapping also were analyzed for metallics and the results are shown in Table V. The one high silicon value is believed to be the result of contamination during the sample preparation.

Corrosion

The vacuum distillation facility to be used in the cleaning of corrosion test specimens, and described schematically in Quarterly Progress Report No. 5[4], has been installed in the electron beam welding chamber similar to the one which was used to fill the test capsules with high-purity potassium, Figure 18. The ultimate pressure reached with the facility clean and empty was 7×10^{-6} torr.

Four trial capsule assemblies were utilized in the determination of optimum time-temperature parameters for distilling off the residual potassium on the surface of the specimens after being removed from the capsules. The prime objective was to keep both the time and temperature at a minimum and after several trials,

TABLE V. CHEMICAL ANALYSES OF POTASSIUM

Sample Identification	O Analysis[1] as K_2O	Chemical Analyses[2], ppm																			
		Al	Ag	B	Be	Ca	Cb	Co	Cr	Cu	Fe	Mg	Mn	Mo	Na	Ni	Si	Sn	Ti	V	Zr
Distillate from receiver	3.6 8.1	<1	<1	<25	<1	<1	<1	<1	<1	<1	<5	<1	<1	<1	<5	<1	<1	<1	<1	<15	<5
Distillate in hot trap before hot trapping	1.7 3.3	<1	<1	<25	<1	<1	<1	<1	<1	<1	<5	<1	<1	<1	<5	<1	1-10	<1	<1	<15	<5
Distillate after hot trapping	3.3 3.7 4.0 10.3 12.2	<1	<1	<25	<1	<1	<1	<1	<1	<1	<5	<1	<1	<1	<5	<1	<1	<1	<1	<15	<5

---

(1) By Mercury Amalgamation Method Using High-Purity Helium Cover Gas.

(2) Metallic Impuritires in KCl Analyzed by Spectrographic Techniques.

TABLE VI. OXYGEN ANALYSES[1] OF POTASSIUM

Sample Identity	Analytical Run No.	Wgt, gms	Oxygen Analyses as K_2O	
			μgms	ppm
Distillate from receiver	1	3.973	14.4	3.6
	2	3.382	27.4	8.1
Distillate in hot trap before hot trapping	3	4.008	6.8	1.7
	4	3.238	10.6	3.3
Distillate after hot trapping	5	3.890	12.8	3.3
	6	3.308	12.4	3.7
	7	1.713	6.8	4.0
	8	1.114	11.5	10.3
	9	0.547	6.7	12.2

---

(1) By Mercury Amalgamation Method Using High-Purity Helium Cover Gas.

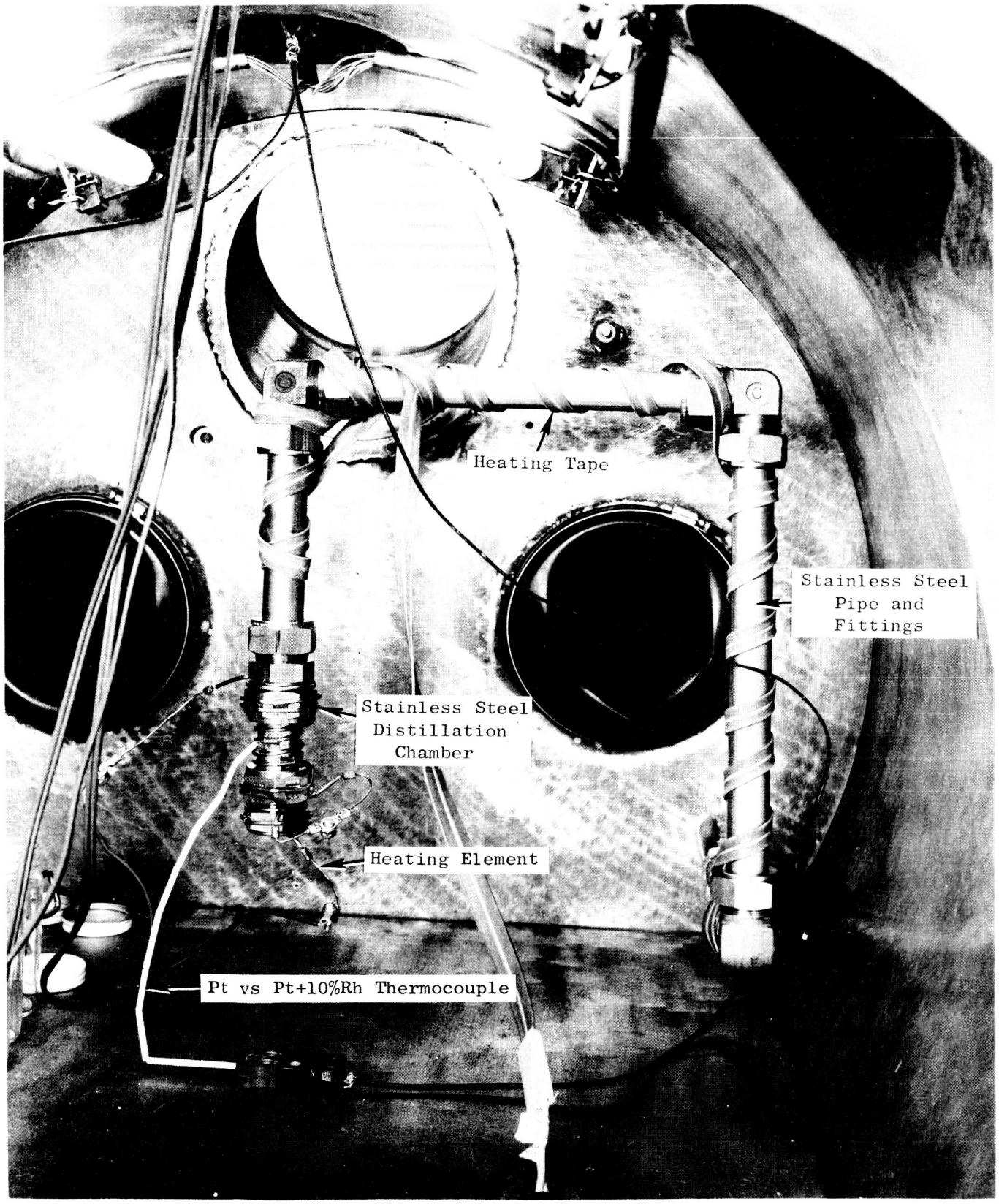

Figure 18. Internal View of Vacuum Distillation Cleaning Facility. (C64111224)

a temperature of 400°F for a period of 1 hour was found to be most suitable. The pressure during distillation is maintained at less than 3 x 10^{-4} torr.

Fourteen corrosion capsules, which were tested for 1,000 hours at 1600°F and which contained the following specimens in the liquid and vapor regions:

Star J	TiC+10%Cb
Unalloyed Tungsten	TiC
Mo-TZM	Carboloy 999
Zircoa 1027	Carboloy 907
Lucalox	Grade 7178
TiC+5%W	K601
TiC+10%Mo	TiB_2

have been opened, drained and their specimens cleaned by vacuum distillation. After being cleaned, the specimens were put in small glass vials, 3/4-inch diameter x 2-1/2-inch high, and covered with ethyl alcohol. Then, the vials were capped and gently agitated to remove any last vestiges of potassium after which the specimens were removed, dried, reweighed and remeasured in the same manner as was done prior to testing. The vials and remaining ethyl alcohol were stored for future evaluation, if necessary.

The potassium that was drained from the capsules in the electron beam weld chamber, containing an argon atmosphere, was collected in properly cleaned platinum dishes so that a chemical analysis of the potassium for metallic impurities, using spectrographic techniques, could be obtained. The potassium is to be drained from the capsules tested at 800° to 1200°F in the same manner and is to be retained in capped glass jars under an argon atmosphere.

The empty Cb-1Zr alloy capsules were cleaned by reacting the slight amount of remaining potassium with water and subsequently rinsing with ethyl alcohol and drying in air.

The weight and dimensional measurements of the specimens of the 14 materials, before and after testing at 1600°F for 1,000 hours, are given in Table VII. By the repeated dimensional measuring of a test specimen, a probable error for this measurement has been calculated. The dimensional measurements can be said with 0.05 probability of error to be within ±0.00029 inch. Therefore, any changes in dimensions which are observed within that range are considered not necessarily significant.

The weight losses observed in the following specimens: Carboloy Grade 999 (MCN-1035-A-2), K601 (MCN-1041-A-5), TiC+5%W (MCN-1042-A-6), TiC+10%Mo (MCN-1044-A-1 and 1044-A-2), TiC+10%Cb (MCN-1045-A-6), and Grade 7178 (MCN-1046-A-5 and 1046-A-6), may be all or partly caused by chipped edges and/or corners observed after testing

TABLE VII. DIMENSIONAL AND WEIGHT CHANGES OF SPECIMENS EXPOSED IN POTASSIUM FOR 1,000 HOURS AT 1600°F

Specimen Identity			Specimen Length, Inches				Specimen Width$_1$, Inches				Specimen Width$_2$, Inches				Specimen Weight in Grams		
Material	MCN No.	Specimen Location	Before Test	After Test	Dimensional Change Inches x 10^{-3}	Dimensional Change Percent	Before Test	After Test	Dimensional Change Inches x 10^{-3}	Dimensional Change Percent	Before Test	After Test	Dimensional Change Inches x 10^{-3}	Dimensional Change Percent	Before Test	After Test	Weight Change Milligrams
Carboloy Grade 999 Capsule # BIC-10	1035-A1	Liquid	2.00254	2.00244	-0.10	-0.005	0.25165	0.25139	-0.26	-0.103	0.25208	0.25170	-0.38	-0.151	31.6219	31.6110	-10.9
	1035-A2	Vapor	2.00254	2.00227	-0.27	-0.014	0.25181	0.25175	-0.06	-0.024	0.25195	0.25185	-0.10	-0.040	31.6249	31.6210	-3.9
Carboloy Grade 907 Capsule # BIC-9	1036-A5	Liquid	2.00268	2.00337	+0.69	+0.034	0.25165	0.25238	+0.73	+0.290	0.25212	0.25269	+0.57	+0.226	30.5284	30.5254	-3.0
	1036-A6	Vapor	2.00270	2.00248	-0.22	-0.011	0.25145	0.25144	-0.01	-0.004	0.25089	0.25087	-0.02	-0.008	30.4320	30.4320	0.0
Mo-TZM Capsule # BIC-14	1037-A3	Liquid	2.00062	2.00057	-0.05	-0.003	0.24949	0.24930	-0.19	-0.077	0.24819	0.24799	-0.20	-0.081	20.5838	20.5831	-0.7
	1037-A4	Vapor	2.00028	2.00024	-0.04	-0.002	0.24809	0.24790	-0.19	-0.076	0.24925	0.24905	-0.20	-0.080	20.5595	20.5590	-0.5
Tungsten Capsule # BIC-27	1038-A9	Liquid	2.00133	2.00131	-0.02	-0.001	0.25010	0.24999	-0.11	-0.044	0.25064	0.25055	-0.09	-0.036	39.5102	39.5101	-0.1
	1038-A10	Vapor	2.00099	2.00107	+0.08	+0.004	0.25007	0.25002	-0.05	-0.020	0.25039	0.25039	0.00	0.000	39.4849	39.4845	-0.4
Lucalox Capsule # BIC-20	1039-A3	Liquid	2.00324	2.00080	-2.44	-0.122	0.24935	0.24981	+0.46	+0.185	0.25014	0.25053	+0.39	+0.156	8.1335	8.1389	+5.4
	1039-A4	Vapor	2.00319	2.00402	+0.83	+0.042	0.25035	0.25115	+0.80	+0.320	0.25003	0.25065	+0.62	+0.248	8.1521	8.1585	+6.4
Zircoa 1027 Capsule # BIC-23	1040-A3	Liquid	1.99882	2.01281	+13.99	+0.698	0.25104	0.25278	+1.74	+0.693	0.25247	0.25448	+2.01	+0.794	11.8911	11.9070	+15.9
	1040-A4	Vapor	1.99834	2.01388	+15.54	+0.776	0.25106	0.25326	+2.20	+0.879	0.25201	0.25428	+2.27	+0.900	11.8528	11.8761	+23.3
K-601 Capsule # BIC-43	1041-A5	Liquid	2.00154	2.00157	+0.03	+0.002	0.25175	0.25193	+0.18	+0.072	0.25258	0.25269	+0.11	+0.044	32.8874	32.8760	-11.4
	1041-A6	Vapor	2.00155	2.00157	+0.02	+0.001	0.25251	0.25269	+0.18	+0.071	0.25204	0.25225	+0.21	+0.083	32.9362	32.9348	-1.4
TiC Capsule # BIC-37	1042-A5	Liquid	2.00038	2.00044	+0.06	+0.003	0.25057	0.25158	+0.01	+0.004	0.25036	0.25045	+0.09	+0.004	10.1682	10.1675	-0.7
	1042-A6	Vapor	2.00056	2.00092	-0.14	-0.007	0.25276	0.25277	+0.01	+0.004	0.25258	0.25258	0.00	0.000	10.3564	10.3559	-0.5
TiC+5%W Capsule # BIC-46	1043-A5	Liquid	2.00110	2.00125	+0.15	+0.008	0.25174	0.25178	+0.04	+0.016	0.25198	0.25204	+0.06	+0.024	10.6786	10.6767	-0.2
	1043-A6	Vapor	2.00089	2.00095	+0.06	+0.003	0.25182	0.25186	+0.04	+0.016	0.25203	0.25207	+0.04	+0.016	10.6739	10.6723	-1.6
TiC+10%Mo Capsule # BIC-47	1044-A1	Liquid	2.00145	2.00143	-0.02	-0.001	0.25153	0.25157	+0.04	+0.016	0.25159	0.25163	+0.04	+0.016	11.2180	11.2170	-1.0
	1044-A2	Vapor	2.00144	2.00148	+0.04	+0.002	0.25201	0.25206	+0.05	+0.020	0.25128	0.25134	+0.06	+0.024	11.2387	11.2374	-1.3
TiC+10%Cb Capsule # BIC-31	1045-A5	Liquid	2.00040	2.00037	-0.03	-0.002	0.25248	0.25251	+0.03	+0.001	0.25212	0.25215	+0.03	+0.001	10.7637	10.7631	-0.6
	1045-A6	Vapor	2.00037	2.00040	+0.03	+0.002	0.25221	0.25224	+0.03	+0.001	0.25207	0.25210	+0.03	+0.001	10.8244	10.8230	-1.4
Grade 7178 Capsule # BIC-34	1046-A5	Liquid	2.00261	2.00249	-0.12	-0.006	0.25106	0.25122	+0.16	+0.064	0.25104	0.25120	+0.16	+0.064	29.6623	29.6577	-4.6
	1046-A6	Vapor	2.00274	2.00253	-0.21	-0.010	0.25114	0.25132	+0.18	+0.072	0.25155	0.25171	+0.16	+0.064	29.6317	29.6303	-1.4
Star J Capsule # BIC-40	1047-A5	Liquid	2.00111	2.00176	+0.65	+0.032	0.25223	0.25244	+0.11	+0.044	0.25220	0.25283	+0.63	+0.250	18.1860	18.1768	-9.2
	1047-A6	Vapor	1.99737	1.99834	+0.97	+0.048	0.25209	0.25241	+0.32	+0.127	0.25226	0.25263	+0.37	+0.147	18.1580	18.1557	-2.3
TiB_2 Capsule # BIC-48	1048-A1	Liquid	2.00348	2.00358	+0.10	+0.005	0.25187	0.25185	-0.02	-0.008	0.24642	0.24640	-0.02	-0.008	8.5260	8.5275	+1.5
	1048-A2	Vapor	2.00212	2.00209	-0.03	-0.002	0.25209	0.25202	-0.07	-0.028	0.24648	0.24644	-0.04	-0.016	8.6676	8.6669	-0.7

and little significance is attached to these changes. The weight loss of Carboloy Grade 907 (MCN-1036-A-5) and Carboloy Grade 999 (MCN-1035-A-1) specimens may be related to a loss of carbon or cobalt. Little significance is attached to changes in weight as indicated by changes in the fourth decimal place.

The positive dimensional change of the Carboloy Grade 907 specimen (MCN-1036-A-5) is thought to be a surface reaction which resulted from an exposure to argon during the vacuum distillation cleaning after testing.

The dimensional growth observed in the Lucalox specimens (MCN-1039-A-4) is attributed to a surface reaction and the possible formation of $KAlO_2$ as was observed in compatibility studies at Battelle Memorial Institute[5]. Corresponding weight increases also were noted with the Lucalox specimens.

The dimensional growth and weight increases observed for the Zircoa 1027 specimens (MCN-1040-A-3 and MCN-1040-A-4) are believed to be the result of phase changes of the monoclinic structure found to exist in the as-received material and chemical reactions during testing. With regard to the latter, a distinct color change from red-brown to blue-black was observed.

The changes observed in the Star J specimens (MCN-1047-A-5 and MCN-1047-A-6) are believed to be the result of both morphological changes due to aging reactions (dimensional growth) and general solutioning of the alloying elements in potassium (weight loss).

All of the previously mentioned changes are under further investigation so that they may be more clearly understood.

The potassium, which was transferred from the capsules to platinum dishes under argon in the electron beam weld chamber, was reacted with HCl to form the KCl salt and subsequently analyzed for metallic impurities using spectrographic techniques. The data are presented in Table VIII. No significant changes in the metallic content of the potassium were observed except for the potassium which was exposed with the Lucalox specimens. In this case, the potassium exhibited an increase in both chromium and iron contents. Both of these elements exist as impurities in the Lucalox.

A visual examination of the test specimens exposed to potassium liquid and vapor for 1,000 hours at 1600°F was made and the results are summarized in Table IX.

Dimensional Stability

Test Run No. 2

The second 1,000-hour dimensional stability test run, which was conducted at 800°F, was completed on November 2, 1964. The chamber pressures that were recorded during the test are shown in Figure 19. During the heatup of the susceptor, the chamber pressure reached a maximum of 1.6×10^{-6} torr as measured by a tubular Bayard-Alpert ionization gauge. The time required to reach 800°F was 77 hours at which time the pressure was 1×10^{-7} torr. The pressure dropped into the 10^{-9} torr range after about 60 hours at the test temperature. At the conclusion of the 1,000 hours, the pressure was 1×10^{-9} torr.

TABLE VIII. CHEMICAL ANALYSES OF POTASSIUM TRANSFERRED FROM Cb-1Zr ALLOY CORROSION CAPSULES AFTER A 1,000-HOUR EXPOSURE AT 1600°F

Capsule No.	Specimen Material	Date Analyzed	Lab. No.	Chemical Analyses(2), ppm																				
				Al	Ag	Be	Ca	Cb	Co	Cr	Cu	Fe	Mg	Mn	Mo	Na	Ni	Si	Sn	Ti	V	Zr	Pb	B
BIC-9 to 12(1)	---	5-27-64	91-139	1	<1	--	1	<1	<1	<1	<1	1	<1	<1	<1	10	<1	5	<1	<1	--	<5	<1	--
BIC-9	Carboloy Grade 907	12-1-64	138	<1	<1	<1	10	<1	<1	<1	<1	<1	<1	<1	<1	25	<1	<1	<1	<1	<10	<1	<1	<25
BIC-10	Carboloy Grade 999	12-1-64	141	<1	<1	<1	10	<1	<1	<1	<1	<1	<1	<1	<1	15	<1	<1	<1	<1	<10	<1	<1	<25
BIC-13 to 18(1)	---	6-10-64	144	<1	<1	--	<1	<1	<1	<1	<1	5	<1	<1	<1	5	<1	1	<1	<1	--	<5	<1	--
BIC-14	Mo-TZM	12-1-64	142	<1	<1	<1	10	<1	<1	<1	<1	<1	<1	<1	<1	<1	<1	<1	<1	<1	<10	<1	<1	<25
BIC-19 to 24(1)	---	6-10-64	145	<1	<1	--	<1	<1	<1	<1	<1	1	<1	<1	<1	>5	<1	1	<1	<1	-	<5	<1	--
BIC-20	Lucalox	12-1-64	143	<1	<1	<1	15	<1	<1	5	<1	15	<1	<1	<1	<1	<1	<1	<1	<1	<10	<1	<1	<25
BIC-23	Zircoa 1027	12-14-64	144	<1	<1	<1	1	<1	<1	<1	<1	<5	<1	<1	<1	100	<1	<1	<15	<1	<25	<5	<1	<25
BIC-25 to 28(1)	---	6-10-64	146	1	<1	--	>25	<1	<1	<1	<1	5	<1	<1	<1	>10	<1	15	<1	<1	--	<5	<1	--
BIC-27	Tungsten	12-14-64	145	<1	<1	<1	1	<1	<1	<1	<1	<5	<1	<1	<1	<25	<1	<1	<15	<1	<25	<5	<1	<25
BIC-44 to 48(3)	---	---	-	--	--	--	--	--	--	--	--	--	--	--	--	--	--	--	--	--	--	--	--	--
BIC-48	TiB_2	12-14-64	146	<1	<1	<1	10	<1	<1	<1	<1	<5	<1	<1	<1	<25	<1	<1	<15	<1	<25	<5	<1	<25
BIC-47	TiC+10%Mo	12-14-64	147	<1	<1	<1	10	<1	<1	<1	<1	<5	<1	<1	<1	<25	<1	<1	<15	<1	<25	<5	<1	<25
BIC-46	TiC+5%W	12-14-64	148	<1	<1	<1	10	<1	<1	<1	<1	<5	<1	<1	<1	<25	<1	<1	<15	<1	<25	<5	<1	<25
BIC-31,33,36, 39,42,43(3)	---	---	-	--	--	--	--	--	--	--	--	--	--	--	--	--	--	--	--	--	--	--	--	--
BIC-31	TiC+10%Cb	12-14-64	154	<1	<1	<1	20	<1	<1	<1	<1	<5	<1	<1	<1	<25	<1	<1	<15	<1	<25	<5	<1	<25
BIC-43	K601	12-14-64	150	<1	<1	<1	10	<1	<1	<1	<1	<5	<1	<1	<1	<25	<1	<1	<15	<1	<25	<5	<1	<25
BIC-34,37,40(3)	---	---	-	--	--	--	--	--	--	--	--	--	--	--	--	--	--	--	--	--	--	--	--	--
BIC-40	Star J	12-14-64	151	<1	<1	<1	10	<1	<1	<1	<1	<5	<1	<1	<1	<25	<1	<1	<15	<1	<25	<5	<1	<25
BIC-37	TiC	12-14-64	152	<1	<1	<1	10	<1	<1	<1	<1	<5	<1	<1	<1	<25	<1	<1	<15	<1	<25	<5	<1	<25
BIC-34	Grade 7178	12-14-64	153	<1	<1	<1	20	<1	<1	<1	<1	<5	<1	<1	<1	<25	<1	<1	<15	<1	<25	<5	<1	<25

---

(1) Pre-test Analyses; Samples Cast Inside EB Tank Under Vacuum at Same Time Indicated Capsules were Filled.

(2) Metallic Impurities in KCl Analyzed by Spectrographic Techniques.

(3) Samples Cast Inside EB Tank Under Vacuum at Same Time Indicated Capsules were Filled; Pre-test Analyses Not Performed.

TABLE IX. VISUAL EXAMINATION OF CORROSION TEST SPECIMENS AFTER A 1,000 HOUR EXPOSURE TO POTASSIUM AT 1600°F

Capsule No.	Specimen Identity: Material	Specimen Identity: MCN No.	Specimen Location	Description
BIC-23	Zircoa 1027	1040-A3	Liquid	The color of the specimen changed from a light yellow to a very uniform dark grey and the surface has a rougher appearance after the test. A white discoloration was noted where the Cb-1Zr alloy wire cage touched the specimen.
		1040-A4	Vapor	The color of the specimen changed from light yellow to a very uniform light grey. As in the liquid region, the surface has a rougher appearance after testing and white discolorations were observed where the Cb-1Zr alloy wire cage touched the specimen.
BIC-20	Lucalox	1039-A3	Liquid	The appearance of the specimen changed from a translucent white to an opaque "dirty" white. Also, the surface has a glassy appearance with a few areas having what appears to be black colored particles imbedded in the surface. No reaction was noted between the Cb-1Zr wire cage and the specimen.
		1039-A4	Vapor	The specimen looked the same as the liquid region specimen except that a grey discoloration was observed where one of the wires from the Cb-1Zr alloy cage touched the specimen.
BIC-14	Mo-TZM	1037-A3	Liquid	No change was observed in the appearance of the specimen after the test exposure except for a few extremely small holes that were observed on the surface of the specimen. No reaction between the Cb-1Zr alloy wire cage and the specimen was observed.

TABLE IX. (Cont'd)

Capsule No.	Specimen Identity: Material	Specimen Identity: MCN No.	Specimen Location	Description
BIC-14	Mo-TZM	1037-A4	Vapor	No change was observed in the appearance of the specimen after the test exposure except for the presence of one gold/or brown discoloration where a wire from the Cb-1Zr alloy cage touched the specimen. No small holes were observed on the surface as was seen with specimens exposed to the liquid.
BIC-10	Carboloy Grade 999	1035-A1	Liquid	The specimen surface has a dull light grey appearance with gold/or brown spots where the Cb-1Zr alloy wires touched the specimen. Dark grey spots also were observed on the surface.
		1035-A2	Vapor	The specimen surface has a smooth dark grey appearance with rough areas appearing as a fine network on the surface of the specimen. Small brown spots were observed on one end of the specimen and light grey discolorations were observed where wires from the Cb-1Zr alloy cage touched the specimen. One corner of the specimen was chipped.
BIC-9	Carboloy Grade 907	1036-A5	Liquid	The specimen has light grey/or white, dark grey and brown discolorations on the surface. The brown and light grey/or white discolored areas look like crystalline deposits that can be removed easily. A white discoloration was observed where a wire from the Cb-1Zr alloy cage touched the specimen and it too is removed easily.

TABLE IX. (Cont'd)

Capsule No.	Specimen Identity: Material	Specimen Identity: MCN No.	Specimen Location	Description
BIC-9	Carboloy Grade 907	1036-A6	Vapor	The surface of the specimen is light and dark grey in appearance. A few small blue spots were observed and light grey discolorations were noted where the wires from the Cb-1Zr alloy cage touched the specimen. The same type of surface roughening as observed in Carboloy Grade 999, vapor region, was noted but to a lesser degree.
BIC-27	Unalloyed Tungsten	1038-A9	Liquid	No change in the appearance of the specimen was observed.
		1038-A10	Vapor	The specimen looked the same as the liquid region specimen except for dark grey discolorations where the wires from the Cb-1Zr alloy cage touched the specimen.
BIC-48	TiB_2	1048-A1	Liquid	The surface of the specimen has a spotted light and dark grey appearance. Very light grey lines were observed where the wires from the Cb-1Zr alloy cage touched the specimen.
		1048-A2	Vapor	The specimen has a uniform grey appearance with dark grey lines where the wires from the Cb-1Zr alloy cage touched the specimen. There appears to be a few small surface cracks on one surface of the specimen.
BIC-47	TiC+10%Mo	1044-A1	Liquid	The specimen is dull light grey in appearance with some dark grey spots. Chipped edges were observed, and dark grey discolorations were noted where the wires from the Cb-1Zr alloy cage touched the specimen.

TABLE IX. (Cont'd)

Capsule No.	Specimen Identity: Material	Specimen Identity: MCN No.	Specimen Location	Description
BIC-47	TiC+10%Mo	1044-A2	Vapor	The specimen has a similar appearance as the liquid region specimen.
BIC-46	TiC+5%W	1043-A5	Liquid	The specimen is light grey in appearance and a very slight discoloration was observed where the wires from the Cb-1Zr alloy cage touched the specimen. The edges are chipped.
		1043-A6	Vapor	The specimen appearance is the same as the liquid region specimen.
BIC-31	TiC+10%Cb	1045-A5	Liquid	The specimen has a spotted light and dark grey appearance with light grey discolorations where the wires from the Cb-1Zr alloy cage touched the specimen. Two chipped edges were observed on the specimen.
		1045-A6	Vapor	The specimen is light grey in appearance with a few small black spots. Light grey discolorations were noted where a Cb-1Zr alloy wire touched the specimen. A few chipped edges were observed.
BIC-34	Grade 7178	1046-A5	Liquid	The specimen has a light grey appearance with slightly darker grey spots. A dark grey discoloration was observed where the wires from the Cb-1Zr alloy cage touched the specimen. A few chipped edges were noted.
		1046-A6	Vapor	The specimen is bright and shiny except for one end which has a rougher surface. A definite boundary exists between these two areas. The same type of rough area was observed where the wires from the Cb-1Zr alloy cage touched the specimen. A few chipped edges were noted.

TABLE IX. (Cont'd)

Capsule No.	Specimen Identity: Material	Specimen Identity: MCN No.	Specimen Location	Description
BIC-37	TiC	1042-A5	Liquid	The specimen is dark grey with intermittent areas of light grey. A light grey discoloration also was observed where the wires from the Cb-1Zr alloy cage touched the specimen. Several chipped edges were observed.
		1042-A6	Vapor	The specimen is light grey with two dark grey streaks. A light grey discoloration also was observed where wires from the Cb-1Zr alloy cage touched the specimen. A few chipped edges were noted.
BIC-40	Star J	1047-A5	Liquid	The specimen has a spotted light and dark grey appearance. Light grey discolorations were observed where the wires from the Cb-1Zr alloy cage touched the specimen.
		1047-A6	Vapor	The specimen is light grey in appearance with light grey discolorations where wires from the Cb-1Zr alloy cage touched the specimen.
BIC-43	K601	1041-A5	Liquid	The specimen is light grey in appearance with chipped edges and corners.
		1041-A6	Vapor	The specimen is dark grey in appearance with small brown spots. A light grey discoloration was observed where the Cb-1Zr alloy wire cage touched the specimen.

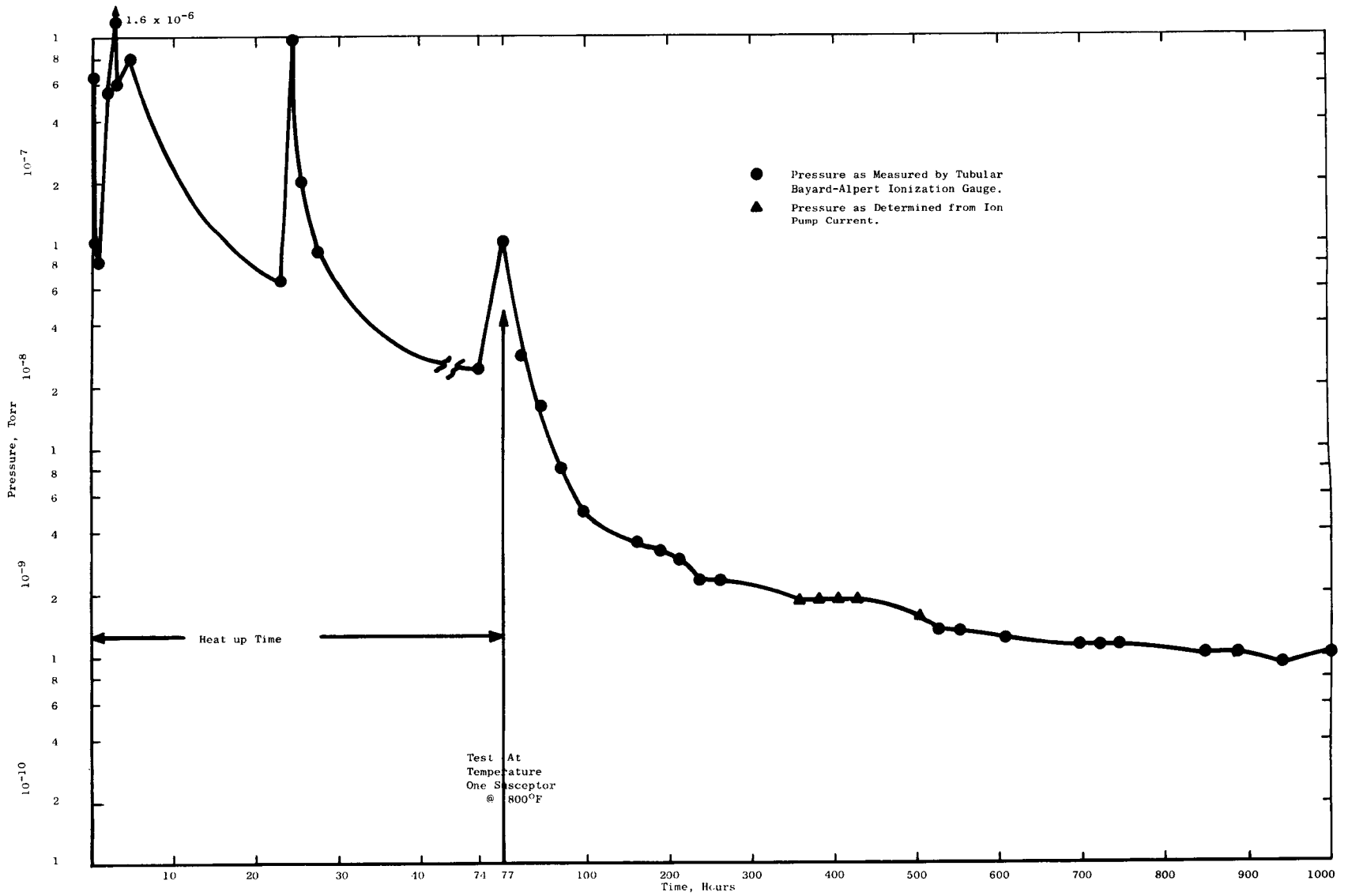

Figure 19. Pressure Curve for Dimensional Stability Test No. 2.

Average temperature readings and mean temperature deviations obtained during the test are shown in Figure 20. These data were obtained with a Leeds and Northrup potentiometer. The thermocouple locations were reported in Quarterly Progress Report No. 6[6].

Test Run No. 3

The third 1,000-hour dimensional stability test, which concluded the testing of all 14 materials at 1200° and 1600°F was started and completed during the report interim. Tables X and XI show the location of the specimens in the two susceptors.

The chamber pressures that were recorded during the test are shown in Figure 21. The time required to reach the test temperatures of 1200° and 1600°F was 52 hours with the maximum pressure reached during that time being 1.0×10^{-6} torr. The pressure dropped into the 10^{-9} torr range after about 85 hours at the test temperature. At the conclusion of the test, the pressure was 2.4×10^{-9} torr.

The average temperature readings of the thermocouples attached to the specimen boxes (see Tables X and XI for location) are shown in Figures 22 and 23.

Specimen Evaluation, Test Runs No. 2 and No. 3

The dimensional/weight measurements of the specimens from dimensional stability tests No's. 2 and 3, after exposure, were completed and are shown in Tables XII and XIII.

All the materials tested at 800°F, except Zircoa 1027, exhibited dimensional changes of no significance. The Zircoa 1027 showed a significantly larger overall change in dimensions relative to the other materials tested, i.e., approximately 0.25×10^{-3} inch. However, this change is still very small and is within the range of dimensional change with which only little significance is attached.

Although the data would indicate that K601, TiB_2, and the three refractory metal bonded TiC compositions (TiC+5%W, TiC+10%Mo, TiC+10%Cb) exhibited anisotropic behavior in that the change in the height dimension measured to be 10-15 times greater than the change in the other two dimensions, the absolute measured change in this direction is small, i.e., 0.15×10^{-3} inch or about 0.02% change. Further, as discussed previously, the confidence in measuring changes of this magnitude is not very great, the 0.05 probability of error being $\pm$ 0.00029 inch. This is born out by the data in Table XIII for duplicate measurements on TiC+10%Mo, TiC+5%W, Star J and TiB_2. For this reason no significance is given to dimensional changes less than 0.2×10^{-3} inch and only minor significance to dimensional changes less than 0.3×10^{-3} inch.

The large dimensional change in length obtained for the tungsten specimen, MCN-1038-B-5, is evidently in error, since the duplicate specimen tested at 800°F and all other tungsten specimens tested at 1200° and 1600°F indicate relatively uniform and neglibible changes in dimensions. A remeasurement of the specimen in question confirmed the post-test length measurement, indicating the pre-test measurement to be incorrect.

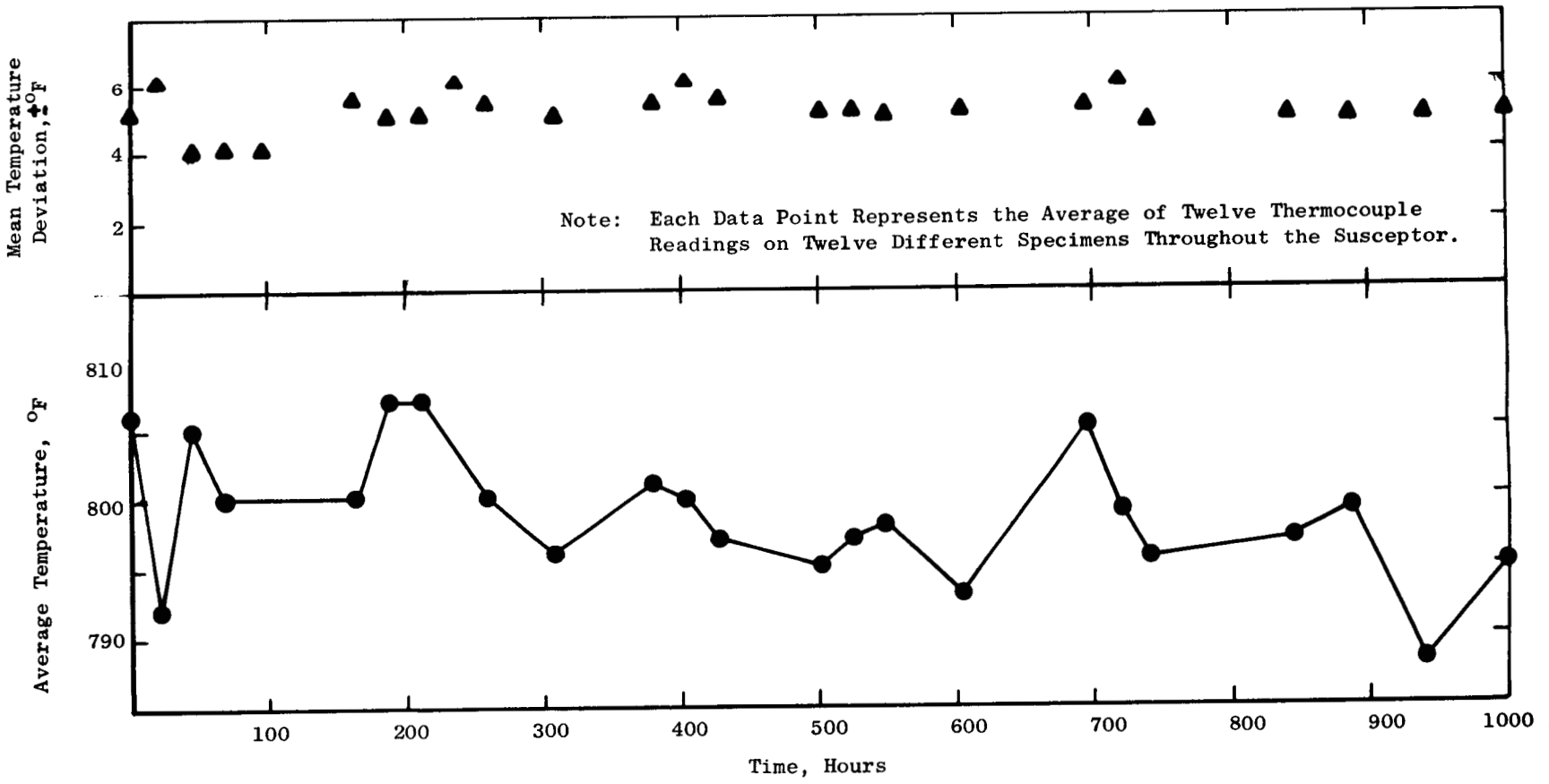

Figure 20. Average Temperature for Dimensional Stability Test No. 2.

TABLE X. LOCATION OF SPECIMENS FOR DIMENSIONAL STABILITY TEST RUN NO. 3

1200°F TEST

Specimen	Column 1	Column 2	Column 3	Column 4	Column 5
1 Top	**	**	**	**	**
2	**	**	**	**	**
3	TiC+10%Mo MCN-1044-B-3*	TiC+5%W MCN-1043-B-4*	TiC+10%Mo MCN-1044-B-4*	**	**
4	TiB_2 MCN-1048-B-3*	Star J MCN-1047-B-3*	TiB_2 MCN-1048-B-4*	TiC+5%W MCN-1043-B-3*	Star J MCN-1047-B-4*
5	Mo	Mo	Mo	Mo	Mo
6 Bottom	Mo	Mo	Mo	Mo	Mo

* Indicates Thermocouples are Attached to These Specimens Boxes.

** Indicates Empty Space.

TABLE XI. LOCATION OF SPECIMENS FOR DIMENSIONAL STABILITY TEST RUN NO. 3

1600°F TEST

Specimen	Column 1	Column 2	Column 3	Column 4	Column 5
1 Top	TiC+5%W MCN-1043-B-6*	TiC+10%Mo MCN-1044-B-5*	TiB_2 MCN-1048-B-1*	Star J MCN-1047-B-2*	Star J MCN-1047-B-1*
2	TiB_2 MCN-1048-B-2*	TiC+5%W MCN-1043-B-5*	Zircoa 1027 MCN-1040-B-7*	TiC+10%Mo MCN-1044-B-6*	Carboloy Grade 907 MCN-1036-B-7*
3	Mo	Mo	Mo	Mo	Mo
4	Mo	Mo	Mo	Mo	Mo
5	Mo	Mo	Mo	Mo	Mo
6 Bottom	Mo	Mo	Mo	Mo	Mo

* Indicates Thermocouples are Attached to These Specimen Boxes.

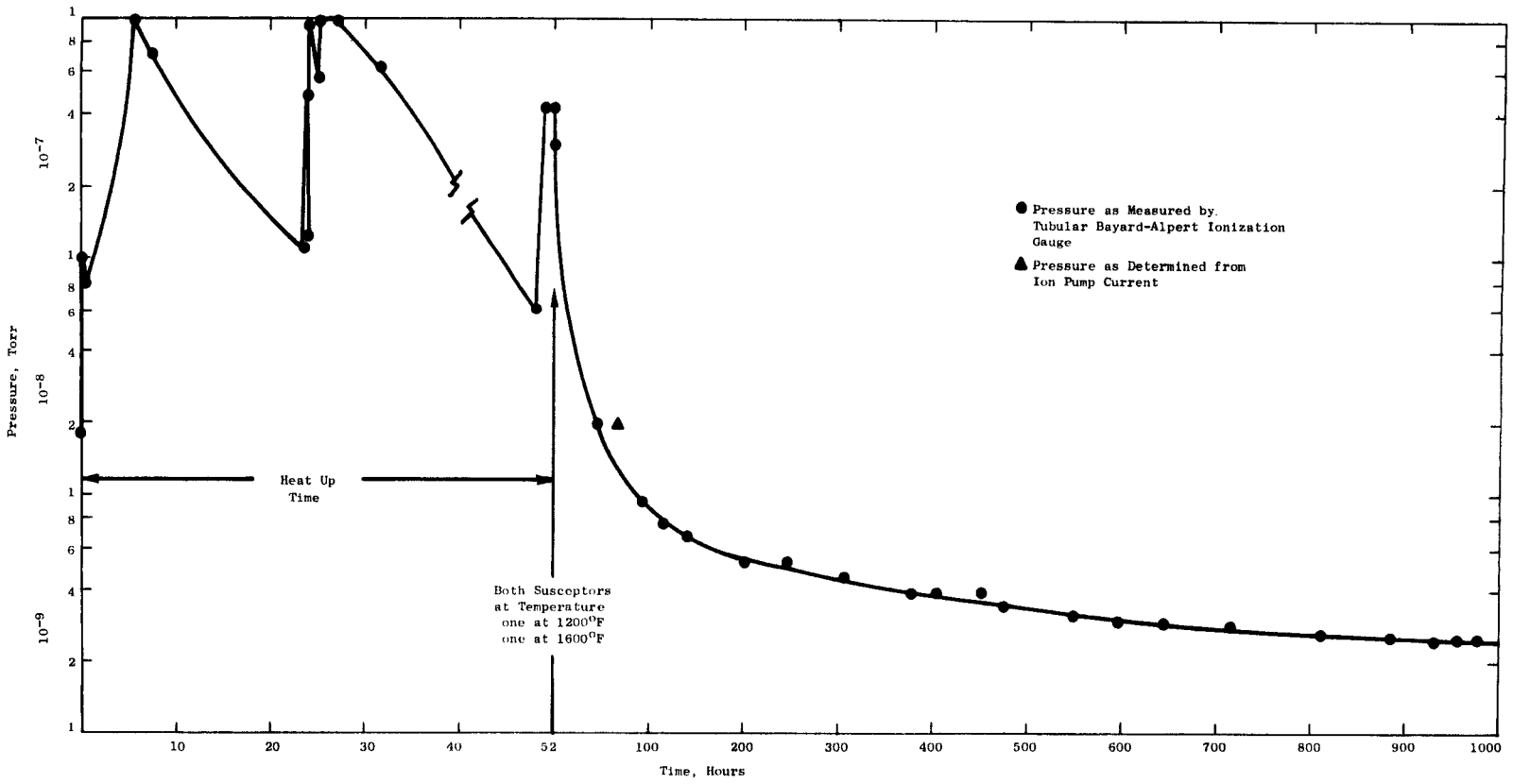

Figure 21. Pressure Curve for Dimensional Stability Test No. 3.

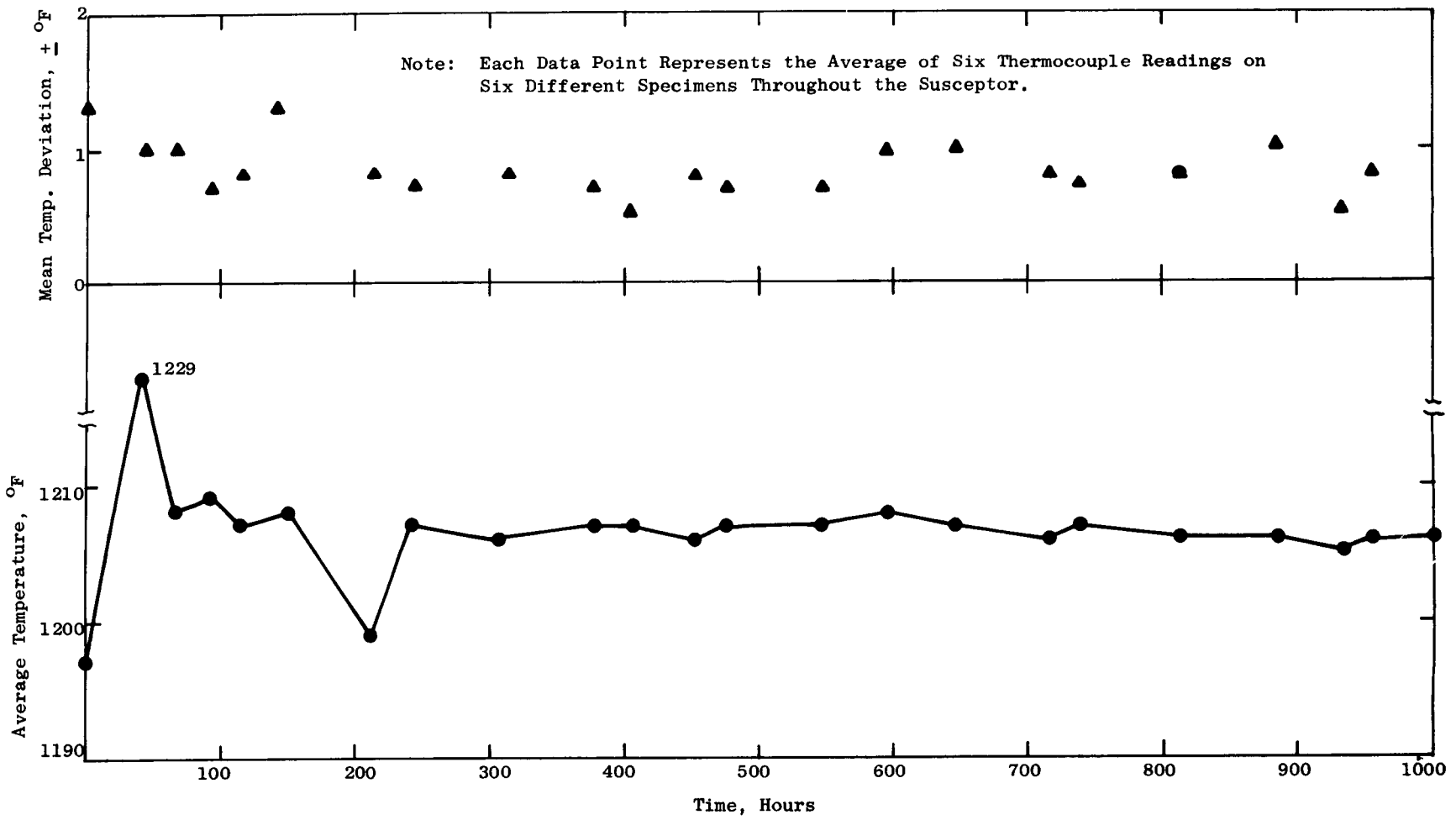

Figure 22. Average Temperature for Dimensional Stability Test No. 3, 1200°F Test.

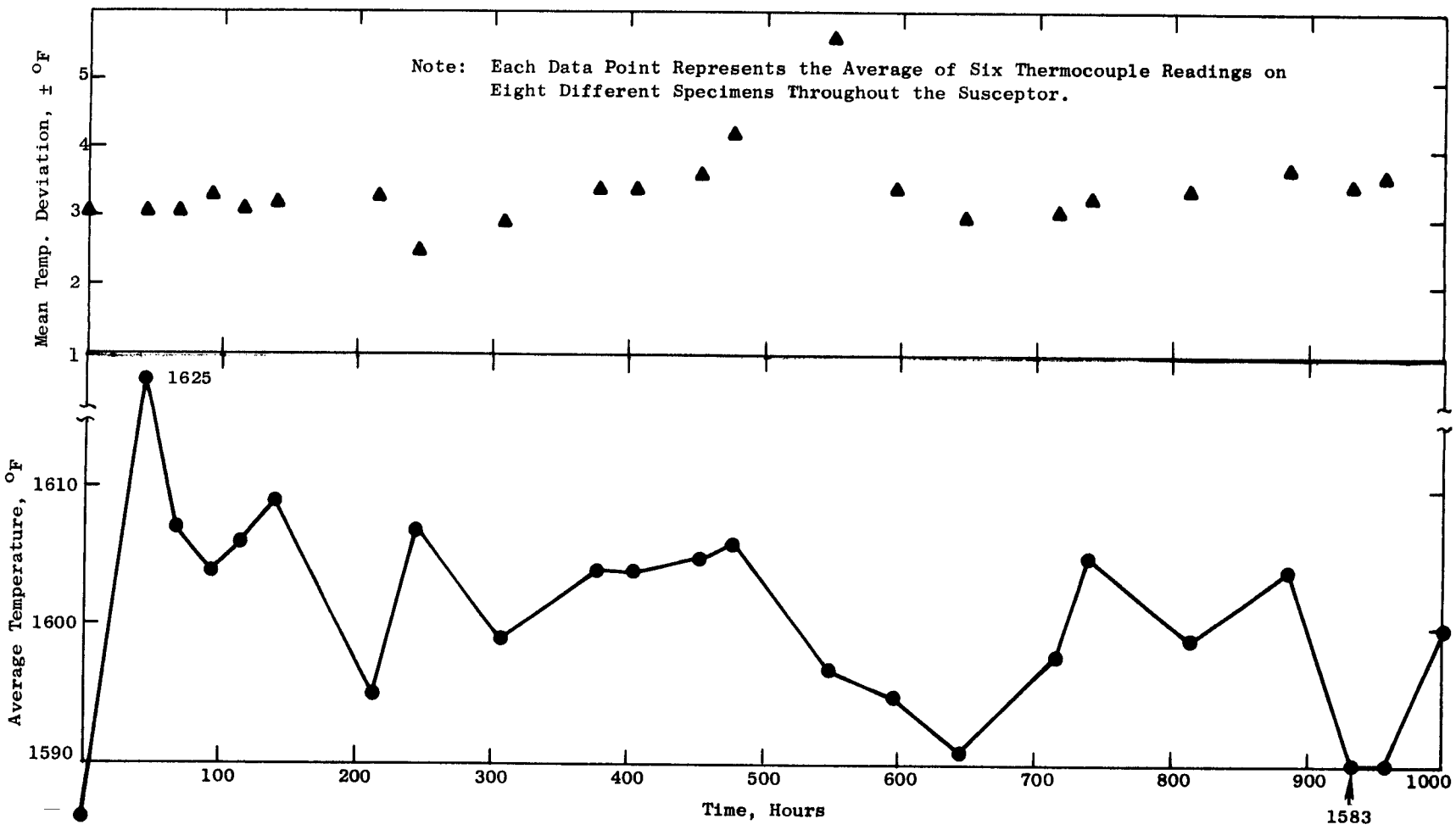

Figure 23. Average Temperature for Dimensional Stability Test No. 3, 1600°F Test.

TABLE XII. DIMENSIONAL AND WEIGHT CHANGES OF SPECIMENS EXPOSED TO VACUUM FOR 1,000 HOURS AT 800°F

(Dimensional Stability Test Run No. 2)

Specimen Identity		Specimen Length, Inches		Dimensional Change	Dimensional Change	Specimen Width, Inches		Dimensional Change	Dimensional Change	Specimen Height, Inches		Dimensional Change	Dimensional Change	Specimen Weight in Grams		Weight Change
Material	MCN No.	Before Test	After Test	Inches x 10^{-3}	Percent	Before Test	After Test	Inches x 10^{-3}	Percent	Before Test	After Test	Inches x 10^{-3}	Percent	Before Test	After Test	Milligrams
Carboloy Grade 999	1035-B-5	1.00180	1.00188	+0.08	+0.008	0.90279	0.90288	+0.09	+0.010	0.80297	0.80292	-0.05	-0.006	175.0852	175.0846	-0.6
	1035-B-6	0.99818	0.99828	+0.10	+0.010	0.90249	0.90256	+0.07	+0.008	0.79823	0.79808	-0.15	-0.019	173.3451	173.3440	-1.1
Carboloy Grade 907	1036-B-5	1.00191	1.00203	+0.12	+0.012	0.90153	0.90162	+0.09	+0.010	0.80203	0.80212	+0.09	+0.011	180.5344	180.5340	-0.4
	1036-B-6	1.00276	1.00282	+0.06	+0.006	0.90176	0.90181	+0.05	+0.006	0.80193	0.80196	+0.03	+0.004	180.7482	180.7481	-0.1
Mo-TZM	1037-B-5	1.00253	1.00262	+0.09	+0.009	0.90227	0.90236	+0.09	+0.010	0.80158	0.80165	+0.07	+0.009	120.7059	120.7060	+0.1
	1037-B-6	1.00080	1.00089	+0.09	+0.009	0.90252	0.90260	+0.08	+0.009	0.80248	0.80255	+0.07	+0.009	120.6718	120.6717	-0.1
Tungsten	1038-B-5	1.00277	1.00184	-0.93	-0.093	0.90185	0.90196	+0.11	+0.012	0.80190	0.80193	+0.03	+0.004	228.4907	228.4916	+0.9
	1038-B-6	1.00209	1.00215	+0.06	+0.006	0.90244	0.90249	+0.05	+0.006	0.80250	0.80251	+0.01	+0.001	228.8780	228.8784	+0.4
Lucalox	1039-B-5	1.00229	1.00221	-0.08	-0.008	0.90160	0.90165	+0.05	+0.006	0.80223	0.80224	+0.01	+0.001	47.1141	47.1146	+0.5
	1039-B-6	1.00275	1.00281	+0.06	+0.006	0.90242	0.90248	+0.06	+0.007	0.80280	0.80284	+0.04	+0.005	47.2995	47.2994	-0.1
Zircoa 1027	1040-B-5	1.00257	1.00275	+0.18	+0.018	0.90249	0.90276	+0.27	+0.030	0.80134	0.80156	+0.22	+0.027	67.9000	67.9000	0.0
	1040-B-6	1.00263	1.00289	+0.26	+0.026	0.90294	0.90325	+0.31	+0.034	0.80042	0.80070	+0.28	+0.035	67.8297	67.8298	+0.1
K601	1041-B-5	1.00274	1.00274	0.00	0.000	0.90216	0.90218	+0.02	+0.002	0.79909	0.79894	-0.15	-0.019	186.6720	186.6722	+0.2
	1041-B-6	1.00271	1.00273	+0.02	+0.002	0.90234	0.90232	-0.02	-0.002	0.80273	0.80258	-0.15	-0.019	187.7321	187.7325	+0.4
TiC	1042-B-5	1.00282	1.00283	+0.01	+0.001	0.90195	0.90202	+0.07	+0.008	0.80257	0.80250	-0.07	-0.009	58.8124	58.8126	+0.2
	1042-B-6	1.00267	1.00275	+0.08	+0.008	0.90195	0.90202	+0.07	+0.008	0.80168	0.80161	-0.07	-0.009	58.7186	58.7187	+0.1
TiC+5%W	1043-B-1	1.00124	1.00125	+0.01	+0.001	0.90150	0.90149	-0.01	-0.001	0.80184	0.80169	-0.15	-0.019	60.4085	60.4087	+0.2
	1043-B-2	1.00121	1.00122	+0.01	+0.001	0.90158	0.90159	+0.01	+0.001	0.80179	0.80164	-0.15	-0.019	60.4870	60.4870	0.0
TiC+10%Mo	1044-B-1	1.00148	1.00149	+0.01	+0.001	0.90257	0.90258	+0.01	+0.001	0.80157	0.80142	-0.15	-0.019	63.7023	63.7024	+0.1
	1044-B-2	0.99848	0.99849	+0.01	+0.001	0.90243	0.90243	0.00	0.000	0.80191	0.80177	-0.14	-0.017	63.4312	63.4314	+0.2
TiC+10%Cb	1045-B-5	1.00259	1.00258	-0.01	-0.001	0.90220	0.90219	-0.01	-0.001	0.80259	0.80238	-0.21	-0.026	61.5982	61.5983	+0.1
	1045-B-6	1.00283	1.00284	+0.01	+0.001	0.90253	0.90252	-0.01	-0.001	0.80272	0.80254	-0.18	-0.022	62.0182	62.0190	+0.8
Grade 7178	1046-B-5	1.00215	1.002'1	+0.06	+0.006	0.90275	0.90280	+0.05	+0.006	0.80215	0.80214	-0.01	-0.001	170.5691	170.5743 170.5740	+5.2 +4.9
	1046-B6	1.00198	1.00210	+0.12	+0.012	0.89903	0.89910	+0.07	+0.008	0.80240	0.80248	+0.08	+0.010	169.8649	169.8650	+0.1
TiB_2	1048-B-5	1.00311	1.00311	0.00	0.000	0.89733	0.89722	-0.11	-0.012	0.80061	0.80047	-0.14	-0.017	50.0839	50.0838	-0.1
	1048-B-6	1.00300	1.00298	-0.02	-0.002	0.89637	0.89637	0.00	0.000	0.80149	0.80134	-0.15	-0.019	50.2078	50.2077	-0.1

TABLE XIII. DIMENSIONAL AND WEIGHT CHANGES OF SPECIMENS EXPOSED TO VACUUM FOR 1,000 HOURS AT 1200° AND 1600°F

(Dimensional Stability Test Run No. 3)

Test Temp. °F	Specimen Identity: Material	Specimen Identity: MCN No.	Specimen Length, Inches: Before Test	Specimen Length, Inches: After Test	Dimensional Change Inches x 10^{-3}	Dimensional Change Percent	Specimen Width, Inches: Before Test	Specimen Width, Inches: After Test	Dimensional Change Inches x 10^{-3}	Dimensional Change Percent	Specimen Height, Inches: Before Test	Specimen Height, Inches: After Test	Dimensional Change Inches x 10^{-3}	Dimensional Change Percent	Specimen Weight in Grams: Before Test	Specimen Weight in Grams: After Test	Weight Change Milligrams
1200	TiC+5%W	1043-B-3	1.00130	1.00131	+0.01	+0.001	0.90164	0.90144	-0.20	-0.022	0.80110	0.80111	+0.01	+0.001	60.5112	60.5111	-0.1
				1.00130*	0.00	0.000		0.90158*	-0.06	-0.007		0.80110*	0.00	0.000			
		1043-B-4	1.00122	1.00122	0.00	0.000	0.90156	0.90135	-0.21	-0.023	0.80112	0.80113	+0.01	+0.001	60.3592	60.3592	0.0
				1.00122*	0.00	0.000		0.90150*	-0.06	-0.007		0.80113*	+0.01	+0.001			
1200	TiC+10%Mo	1044-B-3	1.00043	1.00041	-0.02	-0.002	0.90250	0.90228	-0.22	-0.024	0.80160	0.80160	0.00	0.000	63.5186	63.5185	-0.1
				1.00042*	-0.01	-0.001		0.90249*	-0.01	-0.001		0.80158*	-0.02	-0.002			
		1044-B-4	1.00203	1.00202	-0.01	-0.001	0.90086	0.90065	-0.21	-0.023	0.80151	0.80151	0.00	0.000	62.2589	62.2586	-0.3
				1.00203*	0.00	0.000		0.90087*	+0.01	+0.001		0.80150*	-0.01	-0.001			
1200	Star J	1047-B-3	1.00248	1.00242	-0.06	-0.006	0.90258	0.90232	-0.26	-0.028	0.80235	0.80233	-0.02	-0.002	103.7304	103.7298	-0.6
				1.00253*	+0.05	+0.005		0.90252*	-0.06	-0.007		0.80235*	0.00	0.000			
		1047-B-4	1.00260	1.00251	-0.09	-0.009	0.90263	0.90230	-0.33	-0.037	0.80239	0.80225	-0.14	-0.017	103.7480	103.7477	-0.3
				1.00252*	-0.08	-0.008		0.90250*	-0.13	-0.014		0.80226*	-0.13	-0.016			
1200	TiB_2	1048-B-3	1.00315	1.00319	+0.04	+0.004	0.89736	0.89717	-0.19	-0.021	0.80142	0.80144	-0.02	-0.002	50.1971	50.1964	-0.7
				1.00315*	0.00	0.000		0.89736*	0.00	0.000		0.80141	-0.01	-0.001			
		1048-B-4	1.00029	1.00032	+0.03	+0.003	0.90136	0.90122	-0.14	-0.016	0.79932	0.79928	-0.04	-0.005	48.9202	48.9194	-0.8
				1.00030*	+0.01	+0.001		0.90140*	+0.04	+0.004		0.79925*	-0.07	-0.009			
1600	TiC+5%W	1043-B-5	1.00122	1.00118	-0.04	-0.004	0.90159	0.90136	-0.23	-0.026	0.80182	0.80181	-0.01	-0.001	60.5090	60.5081	-0.9
				1.00117*	-0.05	-0.005		0.90150*	-0.09	-0.010		0.80182*	0.00	0.000			
		1043-B-6	1.00121	1.00118	-0.03	-0.003	0.90154	0.90131	-0.23	-0.026	0.80189	0.80187	-0.02	-0.002	60.4412	60.4403	-0.9
				1.00117*	-0.04	-0.004		0.90144	-0.10	-0.011		0.80186	-0.03	-0.004			
1600	TiC+10%Mo	1044-B-5	1.00149	1.00146	-0.03	-0.003	0.90260	0.90238	-0.22	-0.024	0.80196	0.80192	-0.04	-0.005	63.7270	63.7254	-1.6
				1.00147*	-0.02	-0.002		0.90258*	-0.02	-0.002		0.80191*	-0.05	-0.006			
		1044-B-6	1.00144	1.00140	-0.04	-0.004	0.90261	0.90239	-0.22	-0.024	0.80190	0.80210	+0.20	+0.025	63.7211	63.7197	-1.4
				1.00142*	-0.02	-0.002		0.90260*	-0.01	-0.001		0.80190*	0.00	0.000			
1600	Star J	1047-B-1	1.00255	1.00309	+0.54	+0.054	0.90259	0.90308	+0.49	+0.049	0.80239	0.80291	+0.52	+0.065	103.7763	103.7709	-5.4
		1047-B-2	1.00266	1.00320	+0.54	+0.054	0.90259	0.90313	+0.54	+0.060	0.80237	0.80302	+0.65	+0.081	103.8761	103.8707	-5.4
1600	TiB_2	1048-B-1	1.00334	1.00350	+0.16	+0.016	0.89798	0.89778	-0.20	-0.022	0.80049	0.80053	+0.04	+0.005	50.1466	50.1448	-1.8
				1.00344*	0.00	0.000		0.89795*	-0.03	-0.003		0.80054*	+0.05	+0.006			
		1048-B-2	1.00308	1.00286	-0.22	-0.022	0.89881	0.89862	-0.19	-0.021	0.80223	0.80225	+0.02	+0.002	50.2786	50.2768	-1.8
				1.00286*	-0.22	-0.022		0.89880*	-0.01	-0.001		0.80221*	-0.02	-0.002			
1600	Carboloy Grade 999	1035-B-7	1.00205	1.00215	+0.10	+0.010	0.89802	0.89791	-0.11	-0.012	0.80826	0.79835	-9.91	-1.230	179.0776	179.0752	-2.4
				1.00213*	+0.08	+0.008		0.89807*	+0.05	+0.006		0.79834*	-9.92	-1.230			
1600	Zircoa 1027	1040-B-7	1.00249	1.00670	+4.11	+0.411	0.90275	0.90643	+3.68	+0.408	0.80173	0.80570	+3.97	+0.495	68.1000	68.0988	-1.2

* Specimen Remeasured

Specimen MCN-1046-B-5, Grade 7178, shows an unusually large weight change. Although the specimen was reweighed to confirm the post-test weight, there is no apparent reason for this high value. It is believed that the pre-test weight value is in error as substantiated by the fact that the duplicate specimen tested at 800°F and the specimens tested at 1200° and 1600°F indicate negligible weight changes.

Of the four remaining materials tested in the dimensional stability test run No. 3 at 1200° and 1600°F, the Star J specimens tested at 1600°F were the only specimens to show any significant change in dimensions, i.e., about 0.5×10^{-3} inch or approximately 0.06%. The high dimensional change in the height dimension of the Carboloy Grade 999 specimen, MCN-1035-B-7, is attributed to an incorrect pre-test measurement. Discounting this high value, the Carboloy Grade 999 specimen, MCN-1035-B-7, along with the Zircoa 1027 specimen, MCN-1040-B-7, confirmed the results of duplicate specimens tested in dimensional stability test No. 1 (see Quarterly Progress Report No. 6[6], Table XIII).

Three pieces of 0.060-inch thick Cb-1Zr alloy sheet (MCN-418-2) which were placed on the top of three of the top specimen boxes in the susceptors and exposed to the test temperatures for the duration of the 1,000-hour tests to evaluate the quality of the test environments, were removed and stored for future evaluation if required.

Thermal Expansion

The mean coefficient of thermal expansion as a function of temperature was determined on duplicate specimens of the following seven materials:

Material	MCN
K601	1041-C-1 and -2
TiC	1042-C-1 and -2
TiC+5%W	1043-C-1 and -2
TiC+10%Mo	1044-C-1 and -2
TiC+10%Cb	1045-C-1 and -2
Star J	1047-C-1 and -2
TiB_2	1048-C-1 and -2

These tests mark the completion of the test program to establish the thermal expansion characteristics of the 14 candidate bearing materials. Data for the other seven materials were reported previously[6].

The testing was performed under purified helium utilizing techniques summarized in Quarterly Progress Report No. 6[6]. A description of the facility is reported in Progress Report No. 5[4]. Periodic check tests of the Pyros 56 standard continued to be conducted at random intervals during the testing to document the continuing reproducibility and accuracy of the Chevenard instrument. These data

are presented in Table XIV and Figure 24. The thermal expansion data for the seven candidate bearing materials are presented in Tables XV through XXI and Figures 25 through 31.

As indicated previously, the duplicate tests show excellent reproducibility in the heating and cooling curves. None of the seven materials revealed any evidence of instability over the temperature range investigated, i.e., room temperature to 1600°F. Also, micrometer measurements of the over-all length of each specimen before and after testing showed no permanent change in length for any of the seven materials.

Table XXII presents a summary of the mean coefficient of thermal expansion an inch/inch/°F at 400°, 800°, 1200° and 1600°F for each of the 14 candidate materials. Data for Cb-1Zr, T-111 and Type 316 SS are included for comparison.

Hot Hardness

One surface of each hot hardness specimen was given a metallographic polish utilizing polishing techniques supplied by the vendor of each material.

The initial run in the test program was performed on an unalloyed tungsten specimen which also was selected for the control sample to be used throughout the test series. Room temperature hardness readings were taken on both a Kentron instrument and the hot hardness tester using a Vickers diamond pyramid under a 100-gram load and a fifteen second holding period. The specimen, MCN-1038-D-1, was heated at a rate of approximately 10°F/minute and hardness impressions were made at about 100°F intervals. However, when the specimen had reached 900°F, the solenoid which operates the loading mechanism failed, resulting in loss of control of the load/unload cycle of the indenter. The test was terminated and the defective solenoid was repaired. The partial data generated in this initial test are presented in Table XXIII and Figure 32.

A second test was carried out on the same specimen, MCN-1038-D-1, with the impressions being placed in an untested area of the polished surface. Again, difficulty with the loading/unloading mechanism was encountered, this time at 1200°F, and the test was stopped. The data realized in the second test run are presented in Table XXIV and Figure 33.

Subsequently, the solenoid was replaced, the loading system was inspected to ensure that linkages were in proper working order and a third test was conducted successfully, through the entire test cycle, i.e., room temperature to 1600°F to room temperature. The data are shown in Table XXV and Figure 34. The spread in hardness between the heating and cooling curves is probably due to differences in the bulk hardness from the edge to the center of the specimen resulting from inhomogeniety in the amount of strain hardening imparted to the tungsten rod during processing. Recovery is not expected to play a dominate role in the softening of the specimen since the original tungsten rod was stress-relieved for one hour at 2000°F.

TABLE XIV. CALIBRATION TESTS OF THE CHEVENARD DILATOMETER USING A PYROS 56 STANDARD

Test No. 7[1]
Date: 10-17-64

Test Temp. °F	Mean Coefficient of Thermal Expansion in/in/°F x 10^{-6}			
	Heating[2,3]	Cooling[2,3]	Average	Std. Calib.[4]
77-392	7.58	7.58	7.58	7.57
77-572	7.69	7.69	7.69	7.79
77-752	8.01	8.01	8.01	8.08
77-932	8.29	8.29	8.29	8.36
77-1112	8.52	8.52	8.52	8.62
77-1292	8.79	8.79	8.79	8.89
77-1472	9.05	9.05	9.05	9.12
77-1562	9.17	9.17	9.17	9.24
77-1607	9.19	9.19	9.19	--
77-1652	--	--	--	9.36

Test No. 8
Date: 10-24-64

Test Temp. °F	Mean Coefficient of Thermal Expansion in/in/°F x 10^{-6}			
	Heating[2,3]	Cooling[2,3]	Average	Std. Calib.[4]
77-392	7.50	7.50	7.50	7.57
77-572	7.75	7.75	7.75	7.79
77-752	7.94	7.94	7.94	8.08
77-932	8.29	8.29	8.29	8.36
77-1112	8.57	8.57	8.57	8.62
77-1292	8.77	8.77	8.77	8.89
77-1472	9.03	9.03	9.03	9.12
77-1562	9.17	9.17	9.17	9.24
77-1607	9.18	9.18	9.18	--
77-1652	--	--	--	9.36

TABLE XIV. (Cont'd)

Test No. 9
Date: 12-16-64

Test Temp. °F	Mean Coefficient of Thermal Expansion in/in/°F x 10^{-6}			
	Heating (2,3)	Cooling (2,3)	Average	Std. Calib. (4)
77-392	7.50	7.50	7.50	7.57
77-572	7.75	7.75	7.75	7.79
77-752	8.05	8.05	8.05	8.08
77-932	8.32	8.32	8.32	8.36
77-1112	8.62	8.57	8.60	8.62
77-1292	8.81	8.77	8.79	8.89
77-1472	9.09	9.01	9.05	9.12
77-1562	9.24	9.17	9.21	9.24
77-1607	9.23	9.21	9.22	--
77-1652	--	--	--	9.36

(1) Calibration Test No. 1 to 6 Reported in Quarterly Progress Report No. 6.

(2) Heating and Cooling Rate 575°F/Hour.

(3) Test Environment, High-Purity Helium.

(4) Pyros 56 Data Supplied with Chevenard Dilatometer Manual "Instructions for Assembly and Operation of Chevenard Mechanical Dilatometer," R. Y. Ferner Co., Inc., Malden, Massachusetts.

TABLE XV. THERMAL EXPANSION DATA FOR K601

(Nominal Composition: 84.5%W-10%Ta-5.5%C)

Specimen No.: MCN-1041-C-1
Date: 10-1-64

Test Temp. °F	Mean Coefficient of Thermal Expansion in/in/°F x 10^{-6}		
	Heating(1,2)	Cooling(1,2)	Average
77-392	2.25	2.25	2.25
77-572	2.33	2.33	2.33
77-752	2.41	2.41	2.41
77-932	2.49	2.49	2.49
77-1112	2.54	2.54	2.54
77-1292	2.57	2.57	2.57
77-1472	2.64	2.64	2.64
77-1562	2.67	2.67	2.67
77-1607	2.68	2.68	2.68

Initial Over-all Length - 2.5592 Inches.
Final Over-all Length - 2.5592 Inches.

Specimen No.: MCN 1041-C-2
Date: 10-2-64

Test Temp. °F	Mean Coefficient of Thermal Expansion in/in/°F x 10^{-6}		
	Heating(1,2)	Cooling(1,2)	Average
77-392	2.25	2.25	2.25
77-572	2.33	2.33	2.33
77-752	2.41	2.41	2.41
77-932	2.49	2.49	2.49
77-1112	2.54	2.54	2.54
77-1292	2.57	2.57	2.57
77-1472	2.64	2.64	2.64
77-1562	2.66	2.66	2.66
77-1607	2.68	2.68	2.68

Initial Over-all Length - 2.5590 Inches.
Final Over-all Length - 2.5590 Inches.

---

(1) Heating and Cooling Rate, 575°F/Hour.

(2) Test Environment, High-Purity Helium.

TABLE XVI. THERMAL EXPANSION FOR TiC

(Nominal Composition: 94% TiC)

Specimen No.: MCN-1042-C-1
Date: 10-15-64

Test Temp. °F	Mean Coefficient of Thermal Expansion in/in/°F x 10^{-6}		
	Heating(1,2)	Cooling(1,2)	Average
77-392	3.33	3.33	3.33
77-572	3.50	3.50	3.50
77-752	3.70	3.70	3.70
77-932	3.87	3.87	3.87
77-1112	3.98	3.98	3.98
77-1292	4.04	4.04	4.04
77-1472	4.11	4.11	4.11
77-1562	4.14	4.14	4.14
77-1607	4.17	4.14	4.14

Initial Over-all Length - 2.5592 Inches.
Final Over-all Length - 2.5592 Inches.

Specimen No.: MCN-1042-C-2
Date: 10-16-64

Test Temp. °F	Mean Coefficient of Thermal Expansion in/in/°F x 10^{-6}		
	Heating(1,2)	Cooling(1,2)	Average
77-392	3.33	3.33	3.33
77-572	3.50	3.50	3.50
77-752	3.66	3.66	3.66
77-932	3.81	3.81	3.81
77-1112	3.90	3.90	3.90
77-1292	3.97	3.97	3.97
77-1472	4.03	4.03	4.03
77-1562	4.11	4.11	4.11
77-1607	4.12	4.12	4.12

Initial Over-all Length - 2.5590 Inches.
Final Over-all Length - 2.5590 Inches.

---

(1) Heating and Cooling Rate, 575°F/Hour.

(2) Test Environment, High-Purity Helium.

TABLE XVII. THERMAL EXPANSION DATA FOR TiC+5%W

Specimen No.: MCN-1043-D-1
Date: 10-20-64

Test Temp. °F	Mean Coefficient of Thermal Expansion in/in/°F x 10^{-6} Heating(1,2)	Cooling(1,2)	Average
77.392	3.42	3.42	3.42
77.572	3.55	3.55	3.55
77-752	3.58	3.58	3.58
77-932	3.78	3.78	3.78
77-1112	3.88	3.88	3.88
77-1292	3.97	3.97	3.97
77-1472	4.03	4.03	4.03
77-1562	4.07	4.07	4.07
77-1607	4.12	4.12	4.12

Initial Over-all Length - 2.5593 Inches
Final Over-all Length - 2.5593 Inches

Specimen No.: MCN-1043-D-2
Date: 10-21-64

Test Temp. °F	Mean Coefficient of Thermal Expansion in/in/°F x 10^{-6} Heating(1,2)	Cooling(1,2)	Average
77-392	3.42	3.33	3.38
77-572	3.66	3.50	3.58
77-752	3.66	3.70	3.68
77-932	3.84	3.78	3.81
77-1112	3.85	3.90	3.88
77-1292	3.93	4.00	3.97
77-1472	4.00	4.05	4.03
77-1562	4.04	4.11	4.08
77-1607	4.08	4.15	4.12

Initial Over-all Length - 2.5595 Inches
Final Over-all Length - 2.5595 Inches

---

(1) Heating and Cooling Rate, 575°F/Hour.

(2) Test Environment, High-Purity Helium.

TABLE XVIII. THERMAL EXPANSION DATA FOR TiC+10%Mo

Specimen No.: MCN-1044-C-1
Date: 10-22-64

Test Temp. °F	Mean Coefficient of Thermal Expansion in/in/°F x 10^{-6}		
	Heating(1,2)	Cooling(1,2)	Average
77-392	3.42	3.42	3.42
77-572	3.50	3.50	3.50
77-752	3.58	3.58	3.58
77-932	3.71	3.71	3.71
77-1112	3.83	3.83	3.83
77-1292	3.89	3.89	3.89
77-1472	3.98	3.98	3.98
77-1562	4.04	4.04	4.04
77-1607	4.05	4.05	4.05

Initial Over-all Length - 2.5597 Inches
Final Over-all Length - 2.5597 Inches

Specimen No.: MCN-1044-C-2
Date: 10-23-65

Test Temp. °F	Mean Coefficient of Thermal Expansion in/in/°F x 10^{-6}		
	Heating(1,2)	Cooling(1,2)	Average
77-392	3.42	3.42	3.42
77-572	3.50	3.50	3.50
77-752	3.58	3.58	3.58
77-932	3.75	3.71	3.73
77-1112	3.85	3.80	3.83
77-1292	3.91	3.89	3.90
77-1472	3.98	3.98	3.98
77-1562	4.04	4.00	4.02
77-1607	4.06	4.05	4.06

Initial Over-all Length - 2.5597 Inches
Final Over-all Length - 2.5597 Inches

---

(1) Heating and Cooling Rate, 575°F/Hour.

(2) Test Environment, High-Purity Helium.

TABLE XIX. THERMAL EXPANSION DATA FOR TiC+10%Cb

Specimen No.: MCN 1045-C-1
Date: 10-29-64

Test Temp. °F	Mean Coefficient of Thermal Expansion in/in/°F x 10^{-6} Heating(1,2)	Cooling(1,2)	Average
77-392	3.42	3.42	3.42
77-572	3.55	3.55	3.55
77-752	3.66	3.66	3.66
77-932	3.78	3.78	3.78
77-1112	3.83	3.83	3.83
77-1292	3.89	3.89	3.89
77-1472	3.98	3.98	3.98
77-1562	4.00	4.00	4.00
77-1607	4.01	4.01	4.01

Initial Over-all Length - 2.5595 Inches.
Final Over-all Length - 2.5595 Inches.

Specimen No.: MCN-1045-C-2
Date: 12-14-65

Test Temp. °F	Mean Coefficient of Thermal Expansion in/in/°F x 10^{-6} Heating(1,2)	Cooling(1,2)	Average
77-392	3.42	3.42	3.42
77-572	3.55	3.55	3.55
77-752	3.66	3.66	3.66
77-932	3.78	3.78	3.78
77-1112	3.83	3.83	3.83
77-1292	3.89	3.89	3.89
77-1472	3.98	3.98	3.98
77-1562	4.00	4.00	4.00
77-1607	4.01	4.01	4.01

Initial Over-all Length - 2.5590 Inches.
Final Over-all Length - 2.5590 Inches.

---

(1) Heating and Cooling Rate, 575°F/Hour.

(2) Test Environment, High-Purity Helium.

TABLE XX. THERMAL EXPANSION DATA FOR STAR J

(Nominal Composition: 17%W-32%Cr-2.5%Ni-3%Fe-2.5%C-Bal. Co)

Specimen No.: MCN-1047-C-1
Date: 12-15-64

Test Temp. °F	Mean Coefficient of Thermal Expansion in/in/°F x 10^{-6} Heating(1,2)	Cooling(1,2)	Average
77-392	6.33	6.33	6.33
77-572	6.53	6.53	6.53
77-752	6.73	6.73	6.73
77-932	6.97	6.97	6.97
77-1112	7.20	7.20	7.20
77-1292	7.43	7.43	7.43
77-1472	7.69	7.69	7.69
77-1562	7.75	7.75	7.75
77-1607	7.82	7.82	7.82

Initial Over-all Length - 2.5592 Inches.
Final Over-all Length - 2.5592 Inches.

Specimen No.: MCN-1047-C-2
Date: 12-17-64

Test Temp. °F	Mean Coefficient of Thermal Expansion in/in/°F x 10^{-6} Heating(1,2)	Cooling(1,2)	Average
77-392	6.33	6.33	6.33
77-572	6.53	6.53	6.53
77-752	6.73	6.73	6.73
77-932	6.97	6.97	6.97
77-1112	7.20	7.20	7.20
77-1292	7.43	7.43	7.43
77-1472	7.69	7.69	7.69
77-1562	7.75	7.75	7.75
77-1607	7.82	7.82	7.82

Initial Over-all Length - 2.5590 Inches.
Final Over-all Length - 2.5590 Inches.

---

(1) Heating and Cooling Rate, 575°F/Hour.

(2) Test Environment, High-Purity Helium.

TABLE XXI. THERMAL EXPANSION DATA FOR TiB_2

(Nominal Composition: 98% TiB_2)

Specimen No.: MCN-1048-C-1
Date: 10-27-64

Test Temp. °F	Mean Coefficient of Thermal Expansion in/in/°F x 10^{-6}		
	Heating(1,2)	Cooling(1,2)	Average
77-392	2.92	2.92	2.92
77-572	3.08	3.08	3.08
77-752	3.27	3.27	3.27
77-932	3.41	3.41	3.41
77-1112	3.55	3.55	3.55
77-1292	3.65	3.65	3.65
77-1472	3.73	3.73	3.73
77-1562	3.79	3.79	3.79
77-1607	3.82	3.82	3.82

Initial Over-all Length - 2.5580 Inches.
Final Over-all Length - 2.5580 Inches.

Specimen No.: MCN-1048-C-2
Date: 10-28-64

Test Temp. °F	Mean Coefficient of Thermal Expansion in/in/°F x 10^{-6}		
	Heating(1,2)	Cooling(1,2)	Average
77-392	2.92	2.92	2.92
77-572	3.08	3.08	3.08
77-752	3.27	3.27	3.27
77-932	3.41	3.41	3.41
77-1112	3.55	3.55	3.55
77-1292	3.65	3.65	3.65
77-1472	3.73	3.73	3.73
77-1562	3.79	3.79	3.79
77-1607	3.82	3.82	3.82

Initial Over-all Length - 2.5580 Inches.
Final Over-all Length - 2.5580 Inches.

---

(1) Heating and Cooling Rate, 575°F/Hour.

(2) Test Environment, High-Purity Helium.

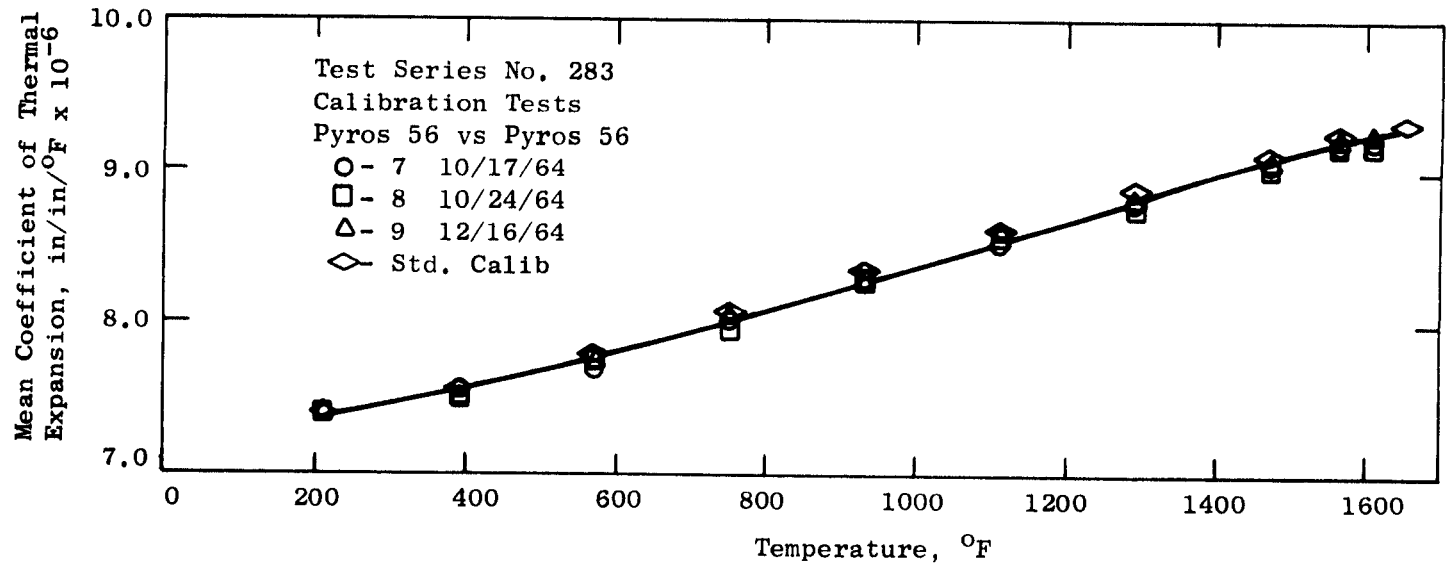

Figure 24. Mean Coefficient of Thermal Expansion of Pyros 56 Standard as a Function of Temperature

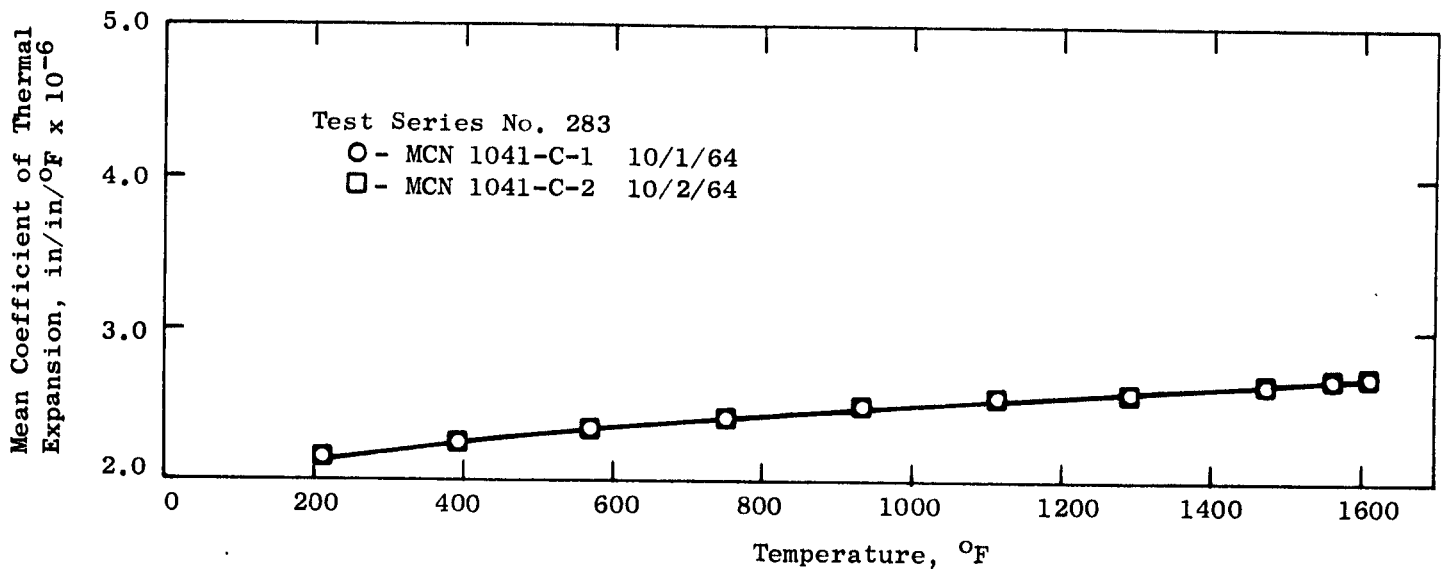

Figure 25. Mean Coefficient of Thermal Expansion of K-601 as a Function of Temperature

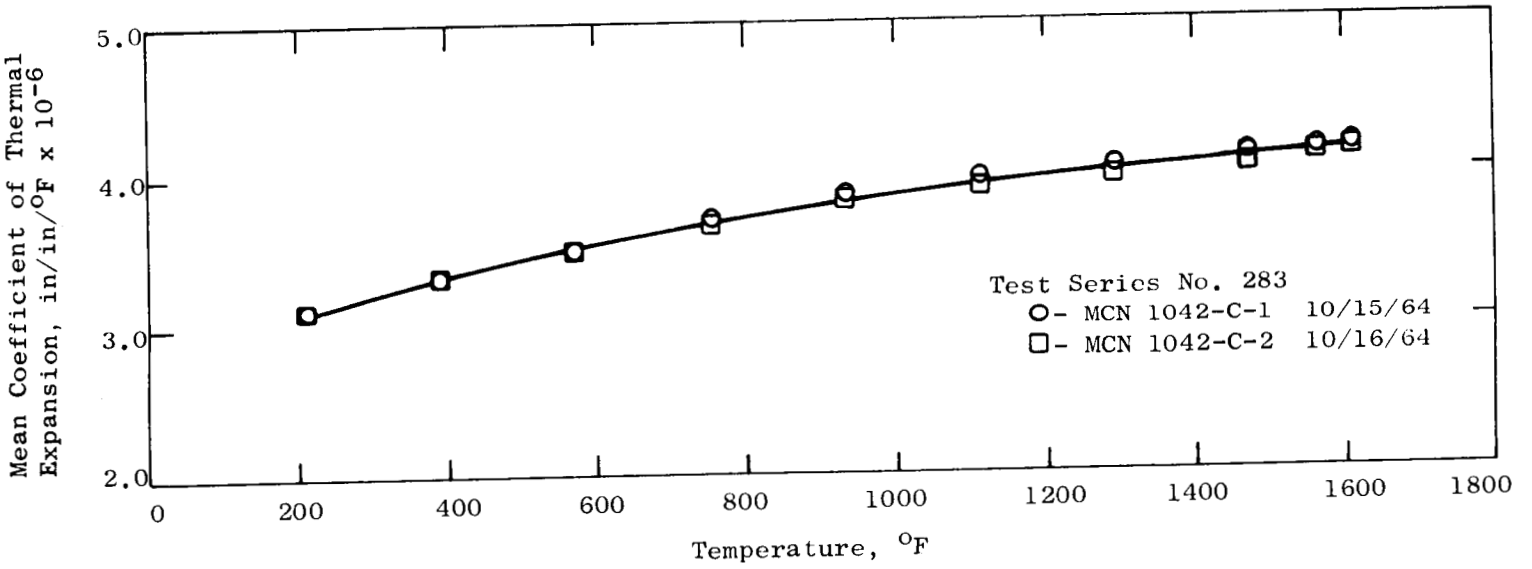

Figure 26. Mean Coefficient of Thermal Expansion of TiC as a Function of Temperature

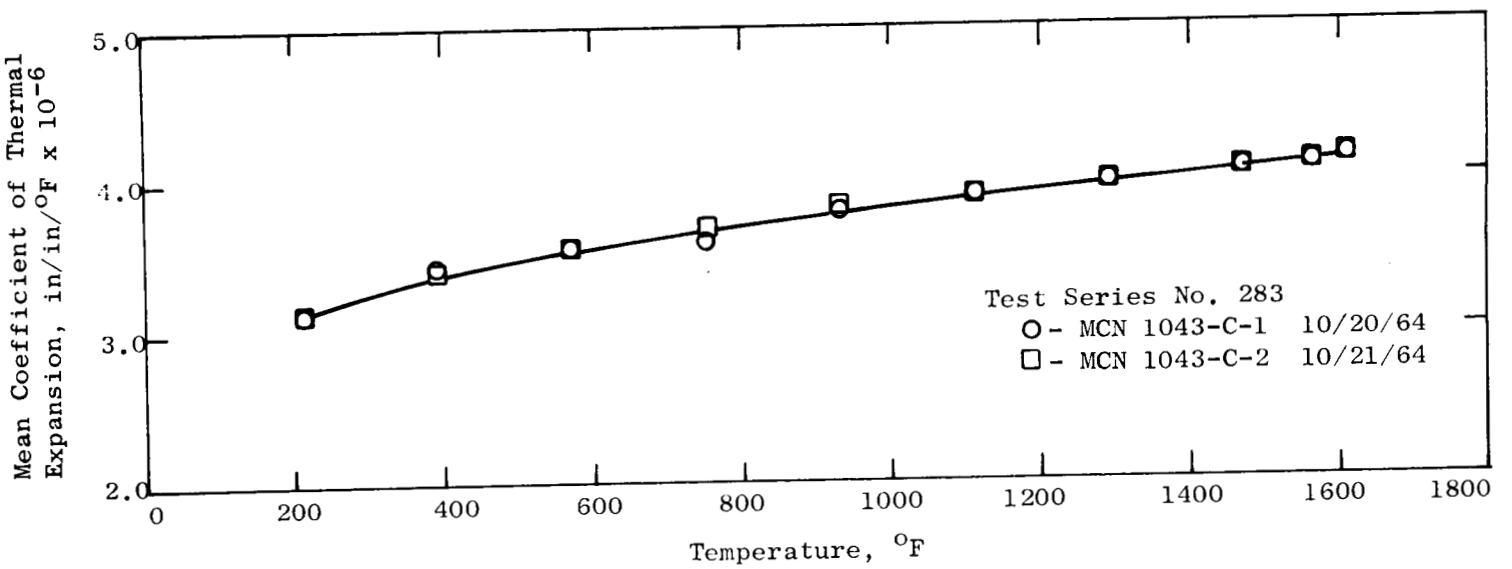

Figure 27. Mean Coefficient of Thermal Expansion of TiC+5%W as a Function of Temperature.

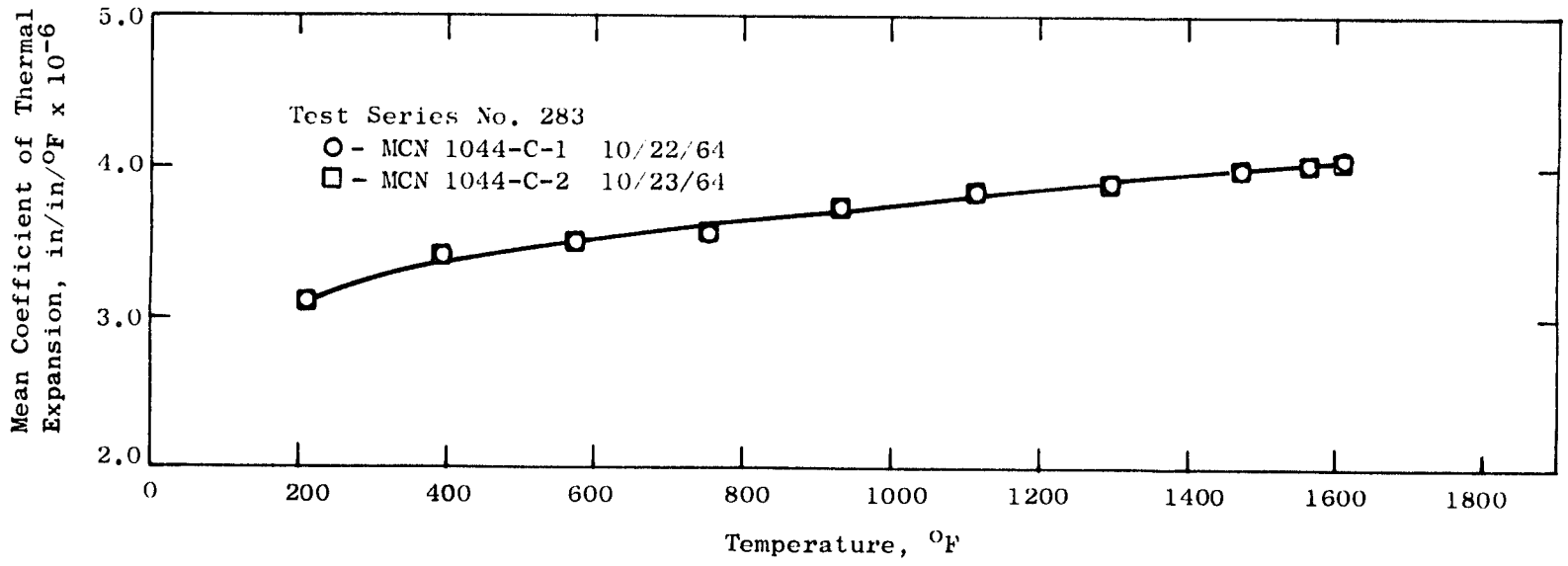

Figure 28. Mean Coefficient of Thermal Expansion of TiC+10%Mo as a Function of Temperature.

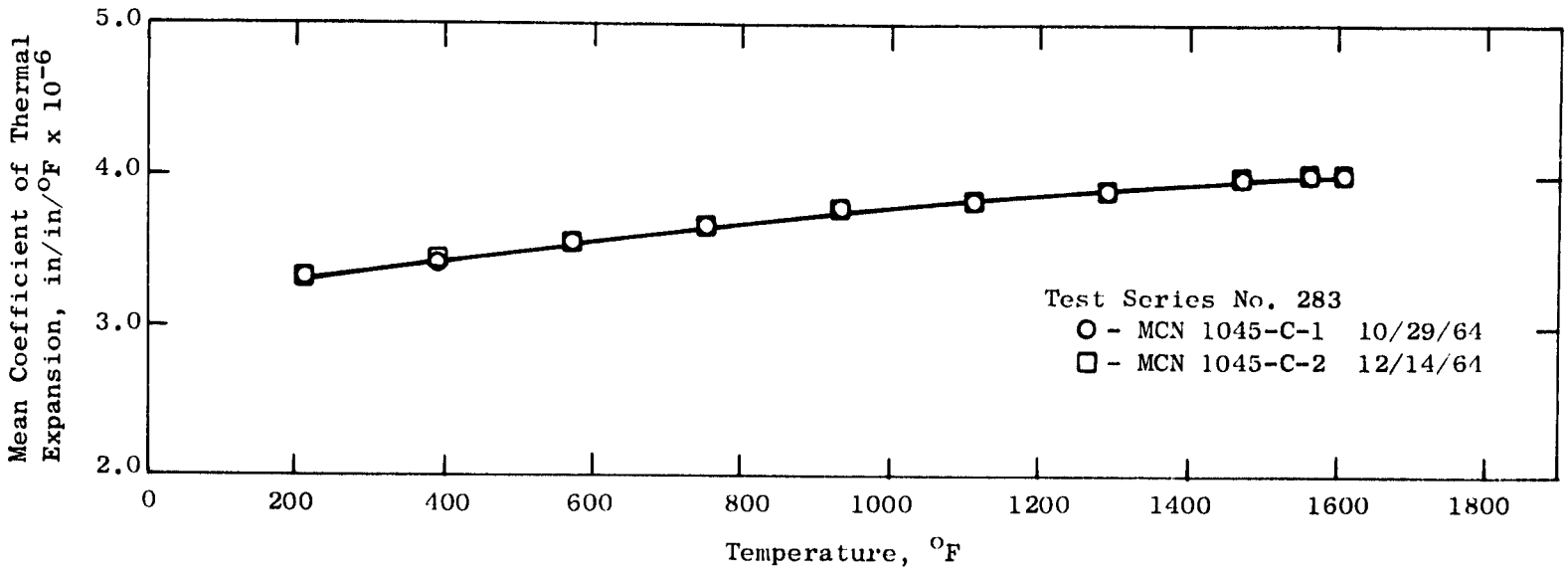

Figure 29. Mean Coefficient of Thermal Expansion of TiC+10%Cb as a Function of Temperature.

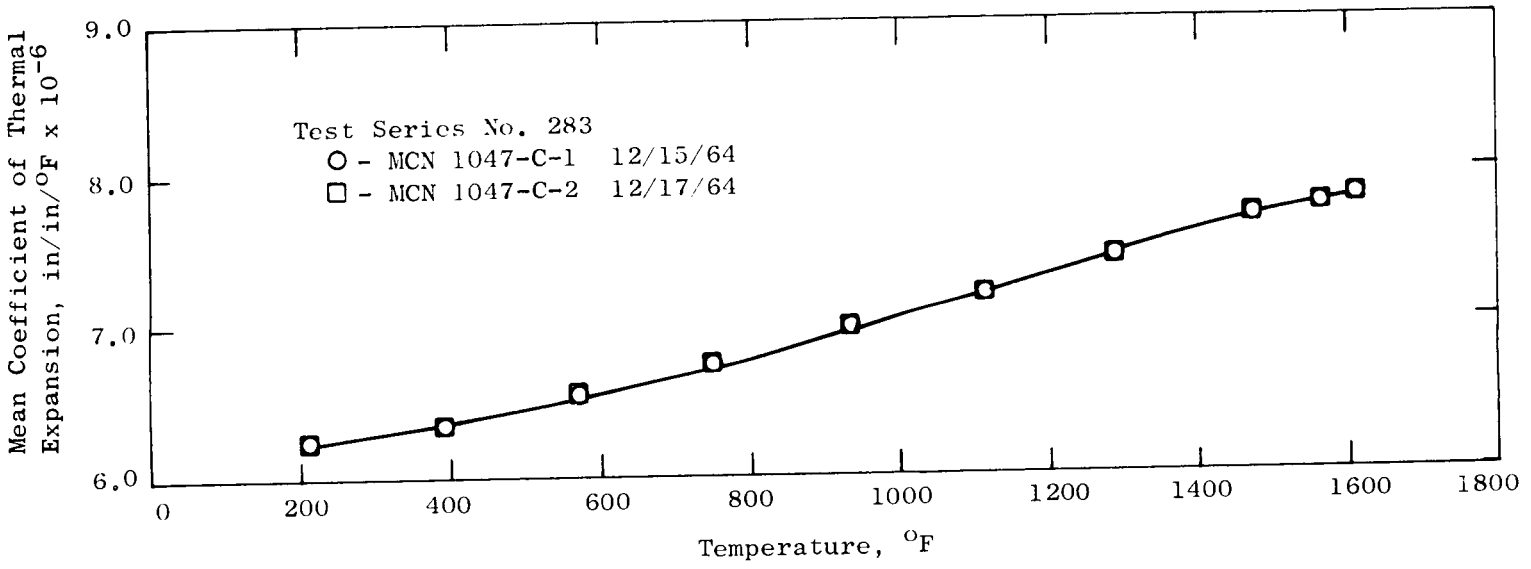

Figure 30. Mean Coefficient of Thermal Expansion of Star J as a Function of Temperature.

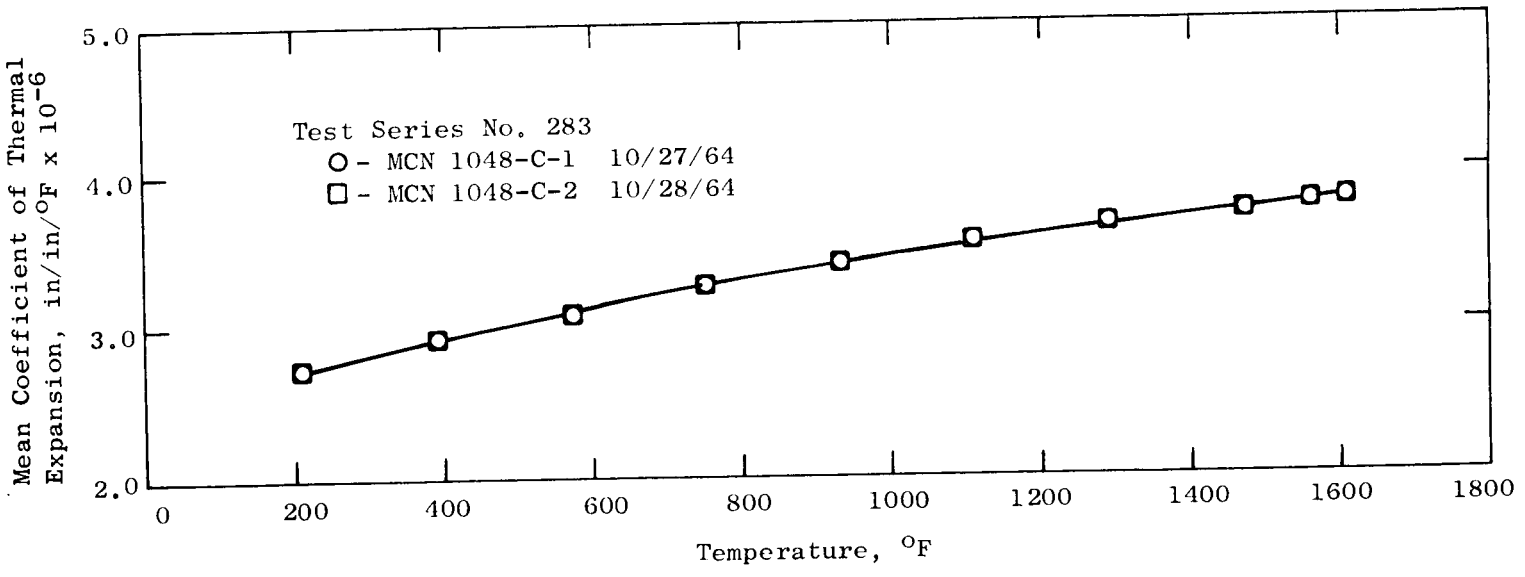

Figure 31. Mean Coefficient of Thermal Expansion of TiB_2 as a Function of Temperature

TABLE XXII. SUMMARY OF THERMAL EXPANSION DATA OF THE CANDIDATE BEARING MATERIALS

Material	Mean Coefficient of Thermal Expansion in/in/°F x 10^{-6}			
	77°-400°F	77°-800°F	77°-1200°F	77°-1600°F
1. Carboloy 999	2.30	2.42	2.58	2.72
2. Carboloy 907	2.65	2.82	2.97	3.11
3. Mo-TZM	2.60	2.92	2.98	3.04
4. Tungsten	2.25	2.32	2.37	2.41
5. Lucalox	3.37	3.81	4.12	4.33
6. Zircoa 1027	4.70	4.88	4.91	5.15
7. K601	2.25	2.45	2.55	2.70
8. TiC	3.35	3.70	4.00	4.15
9. TiC+5%W	3.40	3.70	3.90	4.10
10. TiC+10%Mo	3.40	3.65	3.85	4.05
11. TiC+10%Cb	3.43	3.70	3.90	4.00
12. Grade 7178	2.30	2.52	2.62	2.72
13. Star J	6.35	6.75	7.30	7.80
14. TiB_2	2.95	3.30	3.60	3.80
15. T-111 (1)	3.0	3.4	3.7	3.9
16. Columbium (2)	4.0	4.1	4.2	4.3
17. Cb-1Zr (3)	3.9	4.2	4.4	4.4
18. Type 316 SS (4)	8.90	9.75	10.35	10.55

(1) The Engineering Properties of Tantalum and Tantalum Alloys, DMIC Report No. 189, Sept. 13, 1963.

(2) The Engineering Properties of Columbium and Columbium Alloys, DMIC Report No. 189, Sept. 13, 1963.

(3) C. R. Fisher and P. Y. Achener, "Alkali Metals Evaluation Program", Aerojet-General-Nucleonics AGN-8131, Qtly Progress Report Oct. 1 - Dec. 31, 1964, Contract AT(04-3)-368, Jan. 1965.

(4) Aerospace Structural Metals Handbook, Vol I Ferrous Alloys, March 6, 1963, Syracuse Univ. Press.

TABLE XXIII. HOT HARDNESS DATA FOR UNALLOYED ARC CAST TUNGSTEN

Specimen Identity - MCN-1038-D-1

Specimen Condition - Stress-Relieved 2000°F/1 Hour

Test Number - 1

Date - December 1, 1964

Indenter - 136° Diamond Pyramid (Vickers)

Load - 100 Grams

Holding Time - 15 Seconds

Time Minutes	Vacuum Torr	Temp. °F	Hardness Kg/mm^2
--	--	RT	420 (1)
0	--	RT	381 (2)
4	4.5×10^{-6}	131	421
12	7.0×10^{-6}	200	330
23	1.5×10^{-5}	300	323
34	2.5×10^{-5}	406	236
50	2.4×10^{-5}	541	214
55	2.4×10^{-5}	608	245
66	2.0×10^{-5}	700	187
77	1.5×10^{-5}	806	176
90	1.5×10^{-5}	912	176
Indenter Inoperative - Test Terminated			
--	--	RT	408 (3)

---

(1) Room Temperature Hardness of the Specimen on a Kentron Tester Using a Vickers Diamond Pyramid, a 100-Gram Load and 15-Second Hold:

Maximum 438 Kg/mm^2

Minimum 413 Kg/mm^2

Average 420 Kg/mm^2

TABLE XXIII. (Cont'd)

(2) Room Temperature Hardness of the Specimen on the Hot Hardness Tester Using a Vickers Diamond Pyramid, a 100-Gram Load and 15-Second Hold:

Maximum	431 Kg/mm^2
Minimum	353 Kg/mm^2
Average	381 Kg/mm^2

(3) Room Temperature Hardness of the Specimen, After Test, on a Kentron Tester Using a Vickers Diamond Pyramid, a 100-Gram Load and a 15-Second Hold.

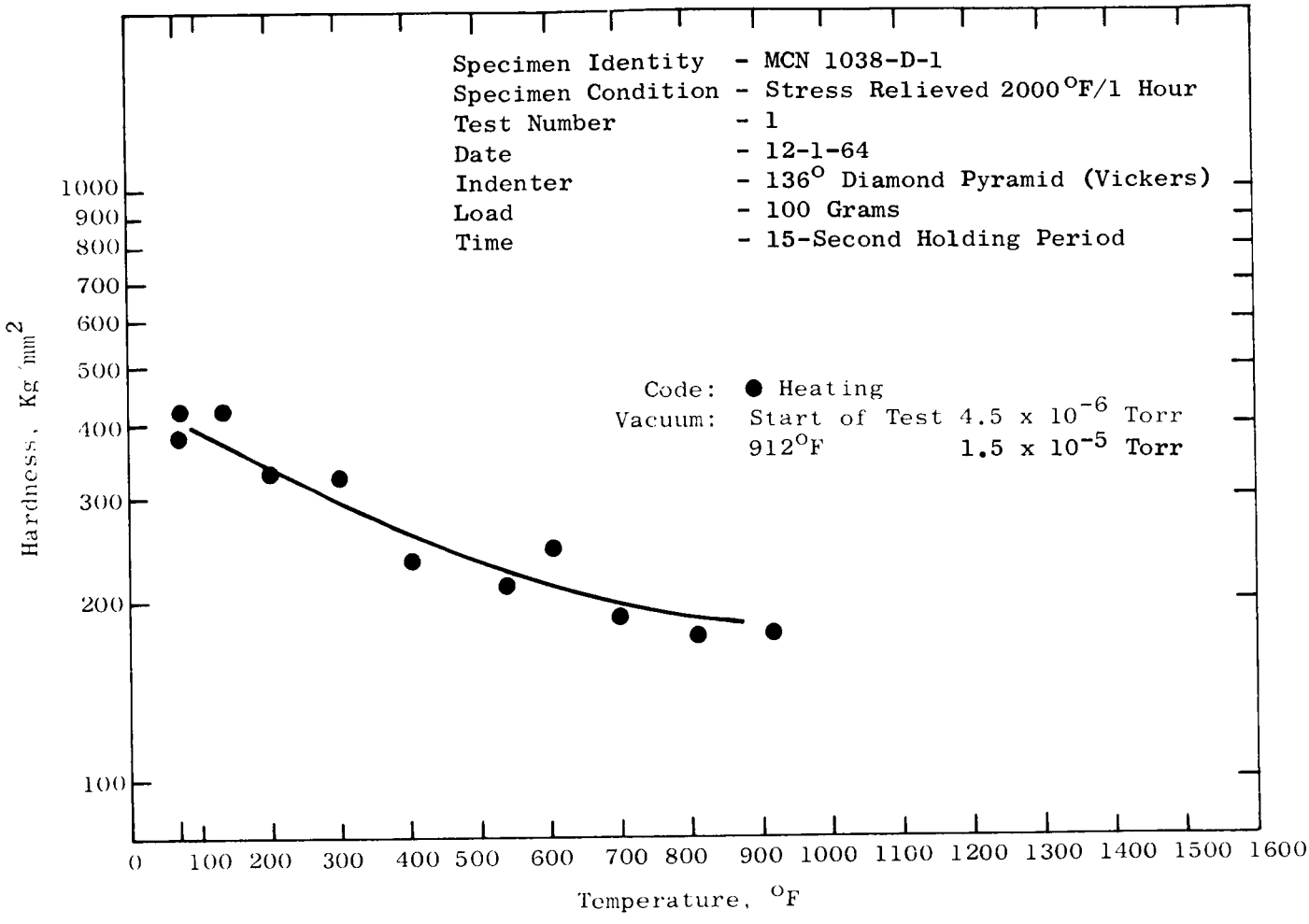

Figure 32. Hot Hardness of Unalloyed Arc Cast Tungsten as a Function of Temperature.

TABLE XXIV. HOT HARDNESS DATA FOR UNALLOYED ARC CAST TUNGSTEN

Specimen Identity - MCN-1038-D-1

Specimen Condition - Stress-Relieved 2000°F/1 Hour

Test Number - 2

Date - December 4, 1964

Indenter - 136° Diamond Pyramid (Vickers)

Load - 100 Grams

Holding Time - 15 Seconds

Time Minutes	Vacuum Torr	Temp. °F	Hardness Kg/mm^2
--	--	RT	401 (1)
0	--	RT	385 (2)
5	7.2×10^{-6}	100	304
16	1.2×10^{-5}	200	334
28	1.2×10^{-5}	304	366
45	4.4×10^{-5}	509	214
57	3.5×10^{-5}	612	181
68	2.5×10^{-5}	705	196
77	2.5×10^{-5}	800	189
94	2.2×10^{-5}	961	167
100	2.0×10^{-5}	1008	157
110	2.0×10^{-5}	1118	159
120	2.0×10^{-5}	1210	167
Indenter Inoperative - Test Terminated			
--	--	RT	390 (3)

---

(1) Room Temperature Hardness of the Specimen on a Kentron Tester Using a Vickers Diamond Pyramid, a 100-Gram Load and a 15-Second Hold:

Maximum	408 Kg/mm^2
Minimum	394 Kg/mm^2
Average	401 Kg/mm^2

TABLE XXIV. (Cont'd)

(2) Room Temperature Hardness of the Specimen on the Hot Hardness Tester Using a Vickers Diamond Pyramid, a 100-Gram Load and a 15-Second Hold:

	361 Kg/mm^2
	391 Kg/mm^2
	401 Kg/mm^2
	387 Kg/mm^2
Average	385 Kg/mm^2

(3) Room Temperature Hardness of the Specimen, After Test, on the Hot Hardness Tester Using a Vickers Diamond Pyramid, a 100-Gram Load and a 15-Second Hold:

	401 Kg/mm^2
	382 Kg/mm^2
	378 Kg/mm^2
	406 Kg/mm^2
	382 Kg/mm^2
Average	390 Kg/mm^2

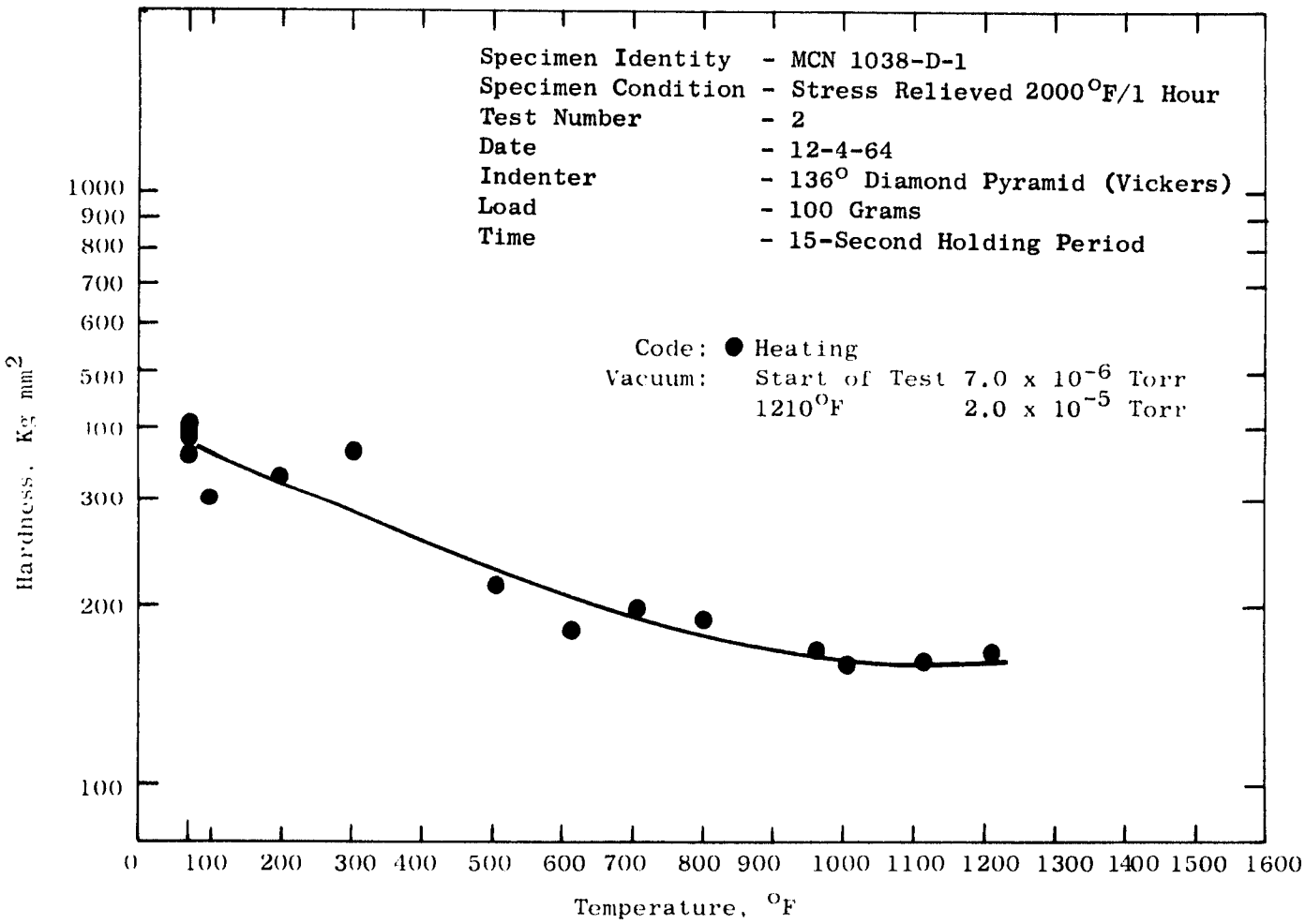

Figure 33. Hot Hardness of Unalloyed Arc Cast Tungsten as a Function of Temperature.

TABLE XXV. HOT HARDNESS DATA FOR UNALLOYED TUNGSTEN

Specimen Identity - MCN-1038-D-1

Specimen Condition - Stress-Relieved 2000°F/1 Hour

Test Number - 3

Date - December 9, 1964

Indenter - 136° Diamond Pyramid (Vickers)

Load - 100 Grams

Holding Time - 15 Seconds

Time Minutes	Vacuum Torr	Temp. °F	Hardness Kg/mm^2
0	1×10^{-6}	RT	412 (1)
7	2.8×10^{-6}	100	369
17	1.2×10^{-5}	196	387
26	5.5×10^{-5}	300	349
33	1.2×10^{-4}	406	289
41	2.0×10^{-4}	519	261
50	1.6×10^{-4}	608	192
107	3.2×10^{-5}	910	176
119	3.5×10^{-5}	1022	160
125	3.2×10^{-5}	1100	148
138	3.0×10^{-5}	1204	146
162	3.2×10^{-5}	1507	132
168	3.2×10^{-5}	1600	129
	Power Off		
215	2.0×10^{-5}	1517	149
235	1.2×10^{-5}	1417	146
248	9.0×10^{-6}	1204	140
266	5.0×10^{-6}	1000	134
296	5×10^{-6}	700	138
346	3×10^{-6}	476	178
360	3×10^{-6}	431	170
380	2×10^{-6}	317	230
420	2×10^{-6}	294	236
-	--	RT	418 (2)

TABLE XXV. (Cont'd)

(1) Room Temperature Hardness of the Specimen on the Hot Hardness Tester Using a Vickers Diamond Pyramid, a 100-Gram Load and a 15-Second Hold:

	431 Kg/mm^2
	421 Kg/mm^2
	415 Kg/mm^2
	415 Kg/mm^2
	415 Kg/mm^2
	415 Kg/mm^2
	369 Kg/mm^2
Average	412 Kg/mm^2

(2) Room Temperature Hardness of the Specimen, After the Test Cycle, on a Kentron Tester Using a Vickers Diamond Pyramid, a 100-Gram Load and a 15-Second Hold.

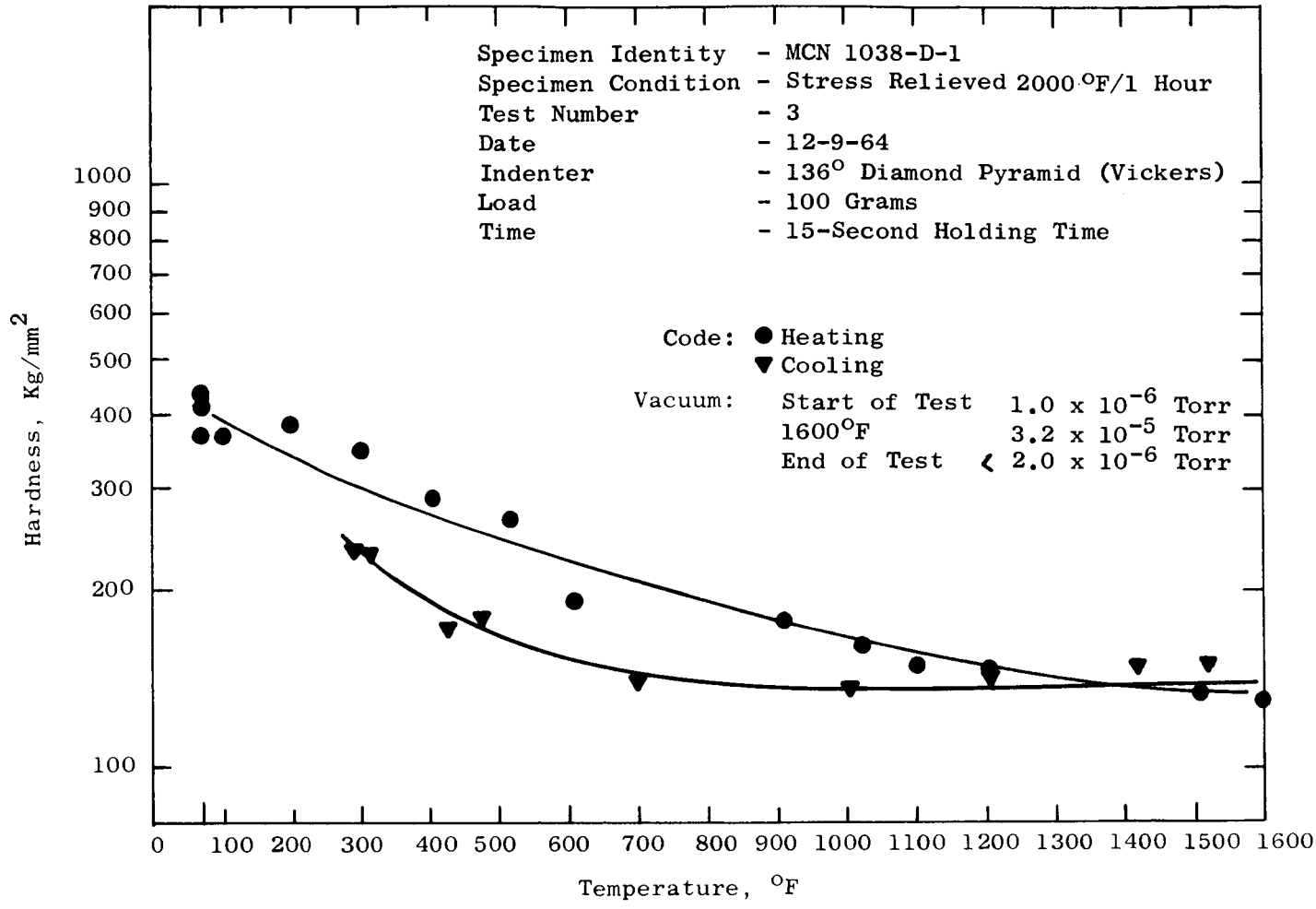

Figure 34. Hot Hardness of Unalloyed Arc Cast Tungsten as a Function of Temperature.

In order to utilize the specimen as a reference standard, the specimen was given a recrystallization anneal for two hours at 2200°F in a vacuum of 1×10^{-6} torr to remove any hardness gradients due to varying amounts of lattice strain. Prior to the anneal, the specimen was cleaned in alcohol and wrapped in tantalum foil. Subsequently, a hardness traverse was made across the surface of the specimen using the type of indenter, load and loading rate employed in the hot hardness tests. The resultant data indicated the hardness from the edge to the center of the specimen to be reasonably uniform with the hardness ranging from 378 to 444 Kg/mm^2 (an average value of 429 Kg/mm^2 for 17 readings). Early in the next report interim, the specimen will be subjected to the test cycle in the hot hardness tester to evaluate the effect of the annealing treatment on the heating and cooling hardness curves of the tungsten.

During the interim, testing of the other candidate materials also was initiated. Tests were completed on a specimen of each of the 14 candidate materials. The data for 10 of the materials are presented in Tables XXVI through XXXV and Figures 35 through 44.

A comparison of the hardness data obtained for TiC on this program with the data obtained on an undefined lot of TiC at the General Electric Research Laboratory show good agreement, Table XXXVI. Also, note the existence of two hardness curves for Star J material denoting the difference in hardness for the matrix and the carbide phase.

There is some scatter in the hardness values for most of the materials tested, especially so in the case of Grade 7178. An examination of the hardness impressions in the Grade 7178 specimen revealed an unusual amount of porosity. Although many of the hardness impressions were positioned in areas of apparent high density, the possibility of voids beneath the impression may have contributed to the wide spread in hardness values for this material.

Several factors contributed to the general spread in data points. The most important is the fact that the operator cannot pre-select sound areas in the specimen for the placement of each impression. Once the specimen is committed to the test cycle, the specimen is advanced and the impressions are made automatically. Therefore, if areas of surface imperfections, i.e., porosity or poor surface preparation, lie in the parth of the indentations, considerable scatter in the hardness values result. A second factor is the result of the selection of the 100-gram load used in the test to obtain comparative data for the 14 materials (a decision had been made to employ the same load, load rate and holding time for each materials). The 100-gram load was selected on the basis of prior experience in testing hard materials. The problem is to avoid cracking that might occur in making the impressions in hard materials and still obtain an impression of measurable dimensions. However, in many of the materials tested in this program, the resultant impressions were of such a small magnitude that considerable difficulty was encountered in obtaining an accurate dimensional measurement. Since the length of the diagonals is a square function in the calculation of the hardness value, a small error in the measurement of the diagonals results in a considerable variation in the hardness number.

Some hardness readings were lost on several of the specimens because of a malfunction of the specimen positioner. The specimen either tended to tilt up indicating that it had advanced, and then fell back to the original position resulting in several impressions being superimposed over one another; or, the specimen would resist the forward movement of the positioner and then skid a greater distance than intended. The latter case resulted in confusion in correlating the impressions during the post-test optical measurements with the assumed location recorded on the test cycle log. Additional testing is planned to rectify some of the problem areas discussed above.

The hot hardness cycle also was completed on specimens of Lucalox, TiB_2 and TiC+10%Mo. However, difficulty was encountered in reading the impressions on these specimens because of the translucency of the Lucalox, the dull-brown matte finish of the TiB_2 and the flat, grey lusterless appearance of the TiC+10%Mo. New optical lighting techniques will be necessary to sharply define the impressions in these materials.

TABLE XXVI. HOT HARDNESS DATA FOR Mo-TZM ALLOY

Specimen Identity - MCN-1037-D-1

Specimen Condition - Stress-Relieved 2250°F/1/2 Hour

Test Number - 1

Date - December 10, 1964

Indenter - 136° Diamond Pyramid (Vickers)

Load - 100 Grams

Holding Time - 15 Seconds

Time Minutes	Vacuum Torr	Temp. °F	Hardness Kg/mm^2
0	--	RT	306 (1)
5	1.2×10^{-5}	100	307
14	2.8×10^{-5}	194	295
23	5.8×10^{-5}	305	238
31	9.8×10^{-5}	407	243
45	1.4×10^{-4}	507	243
59	6.0×10^{-5}	594	238
73	4.2×10^{-5}	716	226
83	4.2×10^{-5}	814	234
92	4.3×10^{-5}	908	226
99	4.0×10^{-5}	1005	222
109	3.0×10^{-5}	1111	218
119	2.8×10^{-5}	1209	210
130	2.4×10^{-5}	1375	226
147	3.0×10^{-5}	1492	222
162	3.8×10^{-5}	1599	203
	Power Off		
207	1.2×10^{-5}	1401	203
210	1.0×10^{-5}	1044	196
-	--	RT	333 (2)
-	--	RT	293 (3)

---

(1) Room Temperature Hardness of the Specimen on the Hot Hardness Tester Using a Vickers Diamond Pyramid, a 100-Gram Load and a 15-Second Hold:

TABLE XXVI. (Cont'd)

	301 Kg/mm^2
	307 Kg/mm^2
	314 Kg/mm^2
	301 Kg/mm^2
Average	306 Kg/mm^2

(2) Room Temperature Hardness of the Specimen, After the Test Cycle, on the Hot Hardness Tester Using a Vickers Diamond Pyramid, a 100-Gram Load and a 15-Second Hold:

	366 Kg/mm^2
	289 Kg/mm^2
	349 Kg/mm^2
	327 Kg/mm^2
Average	333 Kg/mm^2

(3) Room Temperature Hardness of the Specimen, After the Test Cycle, on the Kentron Tester Using a Vickers Diamond Pyramid, a 100-Gram Load and a 15-Second Hold.

TABLE XXVII. HOT HARDNESS DATA FOR TiC

Specimen Identity - MCN-1042-D-1

Test Number - 1

Date - December 11, 1964

Indenter - 136° Diamond Pyramid (Vickers)

Load - 100 Gram

Holding Time - 15 Seconds

Time Minutes	Vacuum Torr	Temp. °F	Hardness Kg/mm^2
--	--	RT	2150(1)
0	--	RT	2253(2)
6	9.0×10^{-6}	120	1813
14	2.0×10^{-5}	209	1965
22	3.8×10^{-5}	306	2176
30	8.2×10^{-5}	384	1964
36	1.2×10^{-4}	515	1964
47	1.2×10^{-4}	608	1768
62	3.4×10^{-5}	701	1607
76	2.9×10^{-5}	827	1607
91	2.8×10^{-5}	927	1132
104	2.0×10^{-5}	1015	1048
123	1.7×10^{-5}	1168	813
134	1.8×10^{-5}	1375	737
158	1.8×10^{-5}	1500	670
173	--	1606	546
	Power Off		
184	--	1392	786
202	--	939	1230
242	6.0×10^{-6}	641	1529
268	5.0×10^{-6}	545	1607
--	--	RT	2042(3)
--	--	RT	2120(4)

TABLE XXVII. (Cont'd)

(1) Room Temperature Hardness of the Specimen on a Kentron Tester Using a Vickers Diamond Pyramid, a 100-Gram Load and a 15-Second Hold:

	2210 Kg/mm^2
	2120 Kg/mm^2
	2120 Kg/mm^2
Average	2150 Kg/mm^2

(2) Room Temperature Hardness of the Specimen on the Hot Hardness Tester Using a Vickers Diamond Pyramid, a 100-Gram Load and a 15-Second Hold:

	1768 Kg/mm^2
	1768 Kg/mm^2
	2816 Kg/mm^2
	2595 Kg/mm^2
	2319 Kg/mm^2
Average	2253 Kg/mm^2

(3) Room Temperature Hardness of the Specimen After the Test Cycle on the Hot Hardness Tester Using a Vickers Diamond Pyramid, a 100-Gram Load and a 15-Second Hold:

	1964 Kg/mm^2
	1964 Kg/mm^2
	2176 Kg/mm^2
	2065 Kg/mm^2
Average	2042 Kg/mm^2

(4) Room Temperature Hardness of the Specimen After the Test Cycle on a Kentron Tester Using a Vickers Diamond Pyramid, a 100-Gram Load and a 15-Second Hold.

TABLE XXVIII. HOT HARDNESS DATA FOR CARBOLOY 999

Specimen Identity - MCN-1035-D-1

Test No. - 1

Date - 12-17-64

Indenter - 136° Diamond Pyramid (Vickers)

Load - 100 Grams

Holding Time - 15 Seconds

Time Minutes	Vacuum Torr	Temp. °F	Hardness Kg/mm^2
--	--	RT	1766(1)
0	8×10^{-4}	RT	1809(2)
4	6×10^{-5}	106	1684
13	3×10^{-5}	200	1645
22	4.5×10^{-5}	314	1458
29	8.5×10^{-5}	401	1132
42	9.8×10^{-5}	507	1529
49	--	590	1458
69	--	720	1367
84	3.8×10^{-5}	819	1109
93	4×10^{-5}	917	1109
106	3.4×10^{-5}	1032	1088
118	2.8×10^{-5}	1120	1088
131	1.8×10^{-5}	1199	1068
141	1.8×10^{-5}	1400	1025
154	1.8×10^{-5}	1500	989
163	2.2×10^{-5}	1600	1003
	Power Off		
176	8×10^{-6}	1169	969
186	6.5×10^{-6}	979	1310
215	4.6×10^{-6}	722	--(3)
249	3.6×10^{-6}	557	--
316	2.8×10^{-6}	384	--
342	2.5×10^{-6}	341	--
--	--	RT	1735(4)

TABLE XXVIII. (Cont'd)

(1) Room Temperature Hardness of the Specimen on a Kentron Tester Using a Vickers Diamond Pyramid, a 100-Gram Load and a 15-Second Hold.

	1710 Kg/mm^2
	1810 Kg/mm^2
	1780 Kg/mm^2
Average	1766 Kg/mm^2

(2) Room Temperature Hardness of the Specimen on the Hot Hardness Tester Using a Vickers Diamond Pyramid, a 100-Gram Load and a 15-Second Hold.

	2006 Kg/mm^2
	1861 Kg/mm^2
	1684 Kg/mm^2
	1813 Kg/mm^2
	1964 Kg/mm^2
	1684 Kg/mm^2
	1725 Kg/mm^2
Average	1809 Kg/mm^2

(3) Equipment Malfunction.

(4) Room Temperature Hardness of the Specimen After the Test Cycle on the Hot Hardness Tester Using a Vickers Diamond Pyramid, a 100-Gram Load and a 15-Second Hold.

	2065 Kg/mm^2
	1684 Kg/mm^2
	1458 Kg/mm^2
Average	1735 Kg/mm^2

TABLE XXIX. HOT HARDNESS DATA FOR CARBOLOY 907

Specimen Identity - MCN-1036-D-1

Test Number - 1

Date - 12-22-64

Indenter - 136° Diamond Pyramid (Vickers)

Load - 100 Grams

Holding Time - 15 Seconds

Time Minutes	Vacuum Torr	Temp. °F	Hardness Kg/mm^2
--	--	RT	1190(1)
0	7.5×10^{-6}	RT	1365(2)
4	9×10^{-6}	108	1496
13	2×10^{-5}	209	1643
24	5.5×10^{-5}	324	1643
32	9×10^{-5}	431	1254
40	9.6×10^{-5}	523	1309
50	6.5×10^{-5}	604	1203
56	2.8×10^{-5}	700	1110
83	1.8×10^{-5}	821	1027
97	1.5×10^{-5}	897	813
102	1.5×10^{-5}	992	813
118	--	1143	902
127	1.2×10^{-5}	1209	902
140	1×10^{-5}	1400	936
159	1×10^{-5}	1500	841
173	1.5×10^{-5}	1590	670
178	2×10^{-5}	1600	650
	Power Off		
188	8×10^{-6}	1367	1007
--	6×10^{-6}	983	1228
204	6×10^{-6}	567	1337
--	6×10^{-6}	367	1769
306	2×10^{-6}	323	1531
--	--	RT	1598(3)

TABLE XXIX. (Cont'd)

(1) Room Temperature Hardness of the Specimen on a Kentron Tester Using a Vickers Diamond Pyramid, a 100-Gram Load and a 15-Second Hold.

	1210 Kg/mm^2
	1150 Kg/mm^2
	1210 Kg/mm^2
Average	1190 Kg/mm^2

(2) Room Temperature Hardness of the Specimen on the Hot Hardness Tester Using a Vickers Diamond Pyramid, a 100-Gram Load and a 15-Second Hold.

	1398 Kg/mm^2
	1132 Kg/mm^2
	1337 Kg/mm^2
	1337 Kg/mm^2
	1604 Kg/mm^2
Average	1365 Kg/mm^2

(3) Room Temperature Hardness of the Specimen, After the Test Cycle, on the Hot Hardness Tester Using a Vickers Diamond Pyramid, a 100-Gram Load and a 15-Second Hold.

	1769 Kg/mm^2
	1462 Kg/mm^2
	1567 Kg/mm^2
Average	1598 Kg/mm^2

TABLE XXX. HOT HARDNESS DATA FOR GRADE 7178

Specimen Identity - MCN-1046-D-1

Test Number - 1

Date - 12-23-64

Indenter - 136° Diamond Pyramid (Vickers)

Load - 100 Grams

Holding Time - 15 Seconds

Time Minutes	Vacuum Torr	Temp. °F	Hardness Kg/mm^2
--	--	RT	2240(1)
0	--	RT	2488(2)
4	6.5×10^{-6}	117	2522
12	2×10^{-5}	206	1496
22	5×10^{-5}	336	1684
35	9.5×10^{-5}	450	2184
46	8×10^{-5}	567	2067
50	6×10^{-5}	600	--
69	3×10^{-5}	733	2184
77	3×10^{-5}	801	2378
91	2×10^{-5}	941	1861
100	2×10^{-5}	1017	1814
107	1.5×10^{-5}	1100	1814
117	1.5×10^{-5}	1211	1960
126	1.5×10^{-5}	1407	1684
143	1.5×10^{-5}	1500	1643
154	2×10^{-5}	1607	1398
158	2×10^{-5}	1615	1155
	Power Off		
161	7×10^{-6}	1350	1462
181	5×10^{-6}	941	1337
235	3×10^{-6}	589	1726
--	3×10^{-6}	397	2184

(1) Room Temperature Hardness of the Specimen on a Kentron Tester Using a Vickers Diamond Pyramid, a 100-Gram Load and a 15-Second Hold.

TABLE XXX. (Cont'd)

	2240 Kg/mm^2
	2240 Kg/mm^2
	2240 Kg/mm^2
	2240 Kg/mm^2
	2240 Kg/mm^2
Average	2240 Kg/mm^2

(2) Room Temperature Hardness of the Specimen on the Hot Hardness Tester Using a Vickers Diamond Pyramid, a 100-Gram Load and a 15-Second Hold.

	2378 Kg/mm^2
	2184 Kg/mm^2
	3144 Kg/mm^2
	2246 Kg/mm^2
Average	2488 Kg/mm^2

TABLE XXXI. HOT HARDNESS DATA FOR ZIRCOA 1027

Specimen Identity - MCN-1040-D-1

Test Number - 1

Date - 12-31-64

Indenter - 136° Diamond Pyramid (Vickers)

Load - 100 Grams

Holding Time - 15 Seconds

Time Minutes	Vacuum Torr	Temp. °F	Hardness Kg/mm^2
0	9×10^{-6}	RT	1226(1)
6	1×10^{-5}	119	1370
16	2×10^{-5}	200	1160
26	5×10^{-5}	323	1180
35	9×10^{-5}	443	1050
41	1.2×10^{-4}	513	1160
62	6×10^{-5}	651	1010
69	4×10^{-5}	708	815
82	3×10^{-5}	803	860
92	3×10^{-5}	908	815
100	3×10^{-5}	1004	615
113	2×10^{-5}	1143	620
125	2×10^{-5}	1350	603
132	1.5×10^{-5}	1400	490
148	1.5×10^{-5}	1500	480
167	2×10^{-5}	1600	459
170	2×10^{-5}	1606 (Power Off)	430
180	9.8×10^{-6}	1358	430
195	7.5×10^{-6}	981	480
210	6×10^{-6}	832	702
--	---	RT	1255(2)

(1) Room Temperature Hardness of the Specimen on the Hot Hardness Tester Using a Vickers Diamond Pyramid, a 100-Gram Load and a 15-Second Hold.

	1260 Kg/mm^2
	1530 Kg/mm^2
	1700 Kg/mm^2
	1130 Kg/mm^2
	1010 Kg/mm^2
Average	1226 Kg/mm^2

TABLE XXXI. (Cont'd)

(2) Hot Hardness of the Specimen, After the Test Cycle, on the Hot Hardness Tester Using a Vickers Diamond Pyramid, a 100-Gram Load and a 15-Second Hold.

	1260 Kg/mm^2
	1460 Kg/mm^2
	1230 Kg/mm^2
	1230 Kg/mm^2
	1200 Kg/mm^2
	1200 Kg/mm^2
	1180 Kg/mm^2
	1280 Kg/mm^2
Average	1255 Kg/mm^2

TABLE XXXII. HOT HARDNESS DATA FOR STAR J

Specimen Identity - MCN-1047-D-1

Test Number - 1

Date - 12-28-64

Indenter - 136° Diamond Pyramid (Vickers)

Load - 100 Grams

Holding Time - 15 Seconds

Time Minutes	Vacuum Torr	Temp. °F	Hardness Kg/mm^2
--	--	RT	765(1)
--	--	RT	1750(2)
0	8×10^{-6}	RT	803(3)
4	10×10^{-6}	117	815
12	1.6×10^{-5}	200	803
23	5.2×10^{-5}	330	815
30	9×10^{-5}	406	600
44	9×10^{-5}	515	672
56	8×10^{-5}	626	504
67	6×10^{-5}	726	488
79	3.5×10^{-5}	838	880
90	3×10^{-5}	917	504
97	3×10^{-5}	1006	525
110	2.5×10^{-5}	1150	535
115	2×10^{-5}	1227	545
127	2×10^{-5}	1442	463
135	1.8×10^{-5}	1500	485
165	1.5×10^{-5}	1600	623
168	1.5×10^{-5}	1600 (Power Off)	552
177	9×10^{-6}	1384	455
197	6×10^{-6}	937	1150
210	5×10^{-6}	821	558
227	4×10^{-6}	697	765
243	3×10^{-6}	604	515
--	--	RT	816(4)
--	--	RT	682(5)
--	--	RT	1340(6)

TABLE XXXII. (Cont'd)

(1) Room Temperature Hardness of the Matrix of the Specimen on a Kentron Tester, Using a Vickers Diamond Pyramid, a 100-Gram Load and a 15-Second Holding Period.

	816 Kg/mm^2
	689 Kg/mm^2
	790 Kg/mm^2
Average	765 Kg/mm^2

(2) Room Temperature Hardness of the Second Phase of the Specimen Using a Kentron Tester, a Vickers Diamond Pyramid, a 100-Gram Load and a 15-Second Hold.

	1810 Kg/mm^2
	1560 Kg/mm^2
	1880 Kg/mm^2
Average	1750 Kg/mm^2

(3) Room Temperature Hardness of the Specimen (Matrix) on the Hot Hardness Tester Using a Vickers Diamond Pyramid, a 100-Gram Load and a 15-Second Hold.

	690 Kg/mm^2
	912 Kg/mm^2
	769 Kg/mm^2
	785 Kg/mm^2
	859 Kg/mm^2
Average	803 Kg/mm^2

(4) Room Temperature Hardness of the Specimen (Matrix), After the Test Cycle, on the Hot Hardness Tester Using a Vickers Diamond Pyramid, a 100-Gram Load and a 15-Second Hold.

	885 Kg/mm^2
	748 Kg/mm^2
Average	816 Kg/mm^2

(5) Room Temperature Hardness of the Matrix of the Specimen, After the Test Cycle, on a Kentron Tester Using a Vickers Diamond Pyramid, a 100-Gram Load and a 15-Second Hold.

	580 Kg/mm^2
	785 Kg/mm^2
Average	682 Kg/mm^2

TABLE XXXII. (Cont'd)

(6) Room Temperature Hardness of the Second Phase of the Specimen, After the Test Cycle, on a Kentron Tester Using a Vickers Diamond Pyramid, á 100-Gram Load and a 15-Second Hold.

1340 Kg/mm^2

TABLE XXXIII. HOT HARDNESS DATA FOR K601

Specimen Identity - MCN-1041-D-2

Test Number - 1

Date - 1-4-65

Indenter - 136° Diamond Pyramid (Vickers)

Load - 100 Grams

Holding Time - 15 Seconds

Time Minutes	Vacuum Torr	Temp. °F	Hardness Kg/mm^2
--	--	RT	1860(1)
0	8×10^{-6}	RT	2225(2)
5	1×10^{-5}	114	1460
15	2×10^{-5}	200	1820
25	5×10^{-5}	314	2320
37	9×10^{-5}	443	1720
43	9.5×10^{-5}	497	1500
58	8×10^{-5}	618	1820
69	6×10^{-5}	704	1640
82	4×10^{-5}	814	1820
92	3×10^{-5}	915	1560
119	1.5×10^{-5}	1124 (Manual Lift)	1310
160	1×10^{-5}	1375	1230
167	1×10^{-5}	1500	1130
183	1.5×10^{-5}	1600	1090
185	1.5×10^{-5}	1600	1070
190	1.5×10^{-5}	1647 (Power Off)	1090
195	1×10^{-5}	1484	1130
200	8×10^{-6}	1200	770
212	6×10^{-6}	994	785
238	2×10^{-5}	744	1760
260	3×10^{-5}	624	2110
265	3×10^{-6}	598	1980
268	3×10^{-6}	585	1820
300	3×10^{-6}	476	1860
338	2.5×10^{-6}	386	1680
--	--	75	2186(3)

TABLE XXXIII. (Cont'd)

(1) Room Temperature Hardness of the Specimen on a Kentron Tester Using a Vickers Diamond Pyramid, a 100-Gram Load and a 15-Second Hold.

	1860 Kg/mm^2
	1860 Kg/mm^2
	1860 Kg/mm^2
	1860 Kg/mm^2
	1860 Kg/mm^2
Average	1860 Kg/mm^2

(2) Room Temperature Hardness of the Specimen on the Hot Hardness Tester Using a Vickers Diamond Pyramid, a 100-Gram Load and a 15-Second Hold.

	1910 Kg/mm^2
	2440 Kg/mm^2
	2110 Kg/mm^2
	2440 Kg/mm^2
Average	2225 Kg/mm^2

(3) Room Temperature Hardness of the Specimen, After the Test Cycle, on the Hot Hardness Tester Using a Vickers Diamond Pyramid, a 100-Gram Load and a 15-Second Hold.

	2440 Kg/mm^2
	2320 Kg/mm^2
	1785 Kg/mm^2
	2200 Kg/mm^2
Average	2186 Kg/mm^2

TABLE XXXIV. HOT HARDNESS DATA FOR TiC+5%W

Specimen Identity - MCN-1043-D-2

Test Number - 1

Date - 1-5-65

Indenter - 136° Diamond Pyramid (Vickers)

Load - 100 Grams

Holding Time - 15 Seconds

Time Minutes	Vacuum Torr	Temp. °F	Hardness Kg/mm^2
0	9×10^{-6}	RT	2450(1)
7	1×10^{-5}	103	2590
25	4×10^{-5}	219	2240
32	10×10^{-5}	427	2120
36	2×10^{-4}	495	1680
53	9×10^{-5}	610	1900
67	4×10^{-5}	712	1470
77	3.5×10^{-5}	829	1160
101	1.9×10^{-5}	1035	910
115	1.5×10^{-5}	1176	770
120	1.5×10^{-5}	1221	770
140	1.5×10^{-5}	1475	702
148	1.5×10^{-5}	1500	682
158	2×10^{-5}	1600	651
161	2×10^{-5}	1600	579
163	2×10^{-5}	1600 (Power Off)	598
172	1×10^{-5}	1392	955
--	--	RT	2008(2)

TABLE XXXIV. (Cont'd)

(1) Room Temperature Hardness of the Specimen on the Hot Hardness Tester Using a Vickers Diamond Pyramid, a 100-Gram Load and a 15-Second Hold.

	3140 Kg/mm^2
	2860 Kg/mm^2
	2670 Kg/mm^2
	1680 Kg/mm^2
	1900 Kg/mm^2
Average	2450 Kg/mm^2

(2) Room Temperature Hardness of the Specimen, After the Test Cycle, on the Hot Hardness Tester Using a Vickers Diamond Pyramid, a 100-Gram Load and a 15-Second Hold.

	1860 Kg/mm^2
	2020 Kg/mm^2
	1980 Kg/mm^2
	2200 Kg/mm^2
	1980 Kg/mm^2
Average	2008 Kg/mm^2

TABLE XXXV. HOT HARDNESS DATA FOR TiC+10%Cb

Specimen Identity - MCN-1045-D-1

Test Number - 1

Date - 1-6-65

Indenter - 136° Diamond Pyramid (Vickers)

Load - 100 Grams

Holding Time - 15 Seconds

Time Minutes	Vacuum Torr	Temp. °F	Hardness Kg/mm^2
0	9×10^{-6}	RT	2206(1)
4	1×10^{-5}	107	2250
18	3×10^{-5}	245	1840
23	4.5×10^{-5}	307	2100
32	9×10^{-5}	416	2250
40	1.5×10^{-4}	505	1810
55	7×10^{-5}	598	1500
69	4×10^{-5}	709	1680
77	3×10^{-5}	805	1230
88	2.5×10^{-5}	915	1280
96	2×10^{-5}	1017	1060
105	2×10^{-5}	1113	1010
117	1×10^{-5}	1219	905
132	1.2×10^{-5}	1400	785
152	1.2×10^{-5}	1500	775
164	1.5×10^{-5}	1600	750
--	--	1606	690
--	--	--	642
172	--	1615	650
175	--	1623	711
178	1.5×10^{-5}	1623 (Power Off)	660
186	1×10^{-5}	1400	775
190	9.5×10^{-6}	1300	870
195	8×10^{-6}	1087	885
216	5×10^{-6}	835	1260
240	4×10^{-6}	657	1390
263	3.5×10^{-6}	567	1770
300	3×10^{-6}	441	1970
--	--	RT	2530(2)

TABLE XXXV. (Cont'd)

(1) Room Temperature Hardness of the Specimen on the Hot Hardness Tester Using a Vickers Diamond Pyramid, a 100-Gram Load and a 15-Second Hold.

	2530 Kg/mm^2
	2240 Kg/mm^2
	2120 Kg/mm^2
	2070 Kg/mm^2
	2070 Kg/mm^2
Average	2206 Kg/mm^2

(2) Room Temperature Hardness, After the Test Cycle, on the Hot Hardness Tester Using a Vickers Diamond Pyramid, a 100-Gram Load and a 15-Second Hold.

	2530 Kg/mm^2
	2530 Kg/mm^2
Average	2530 Kg/mm^2

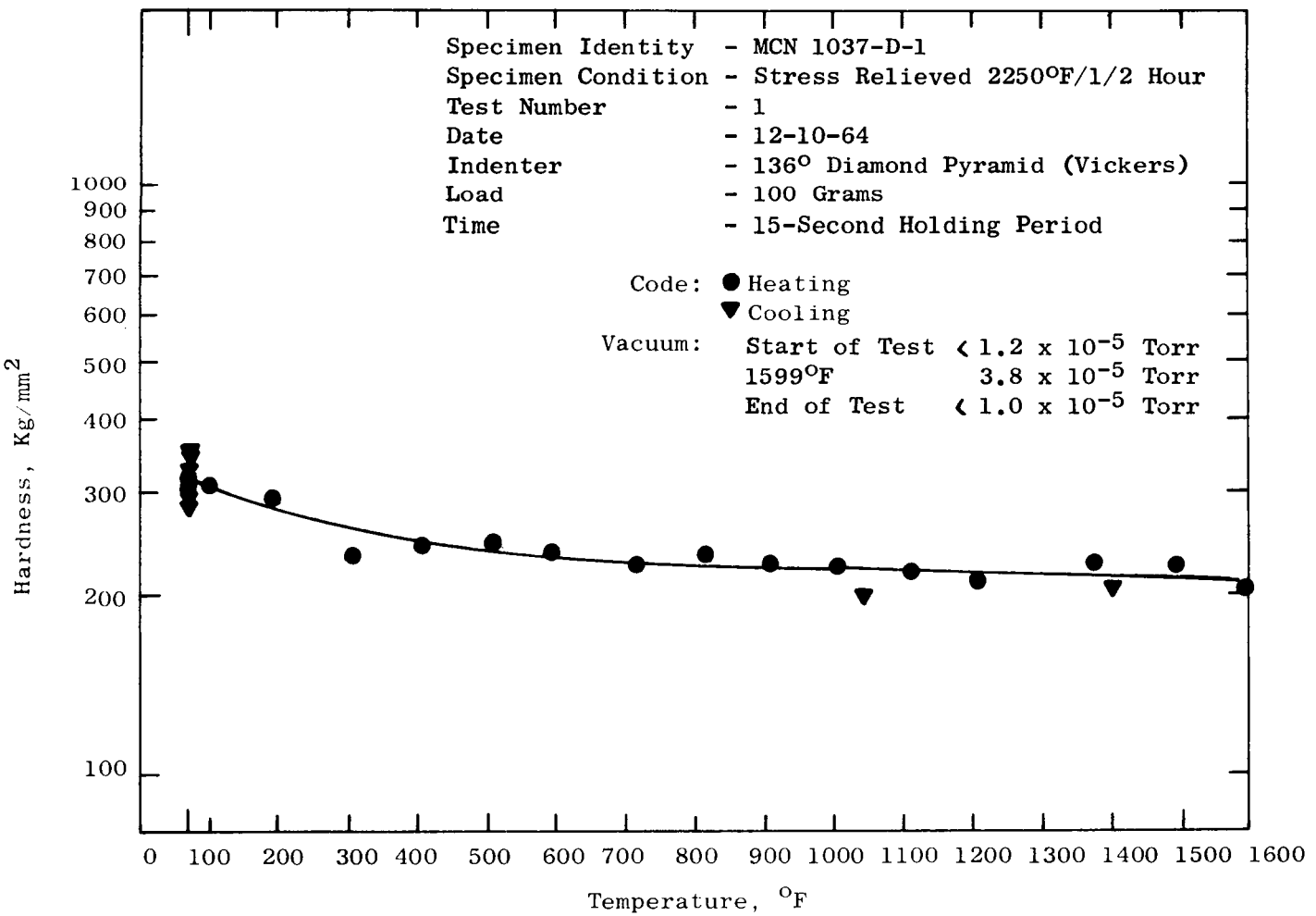

Figure 35. Hot Hardness of Mo-TZM Alloy as a Function of Temperature.

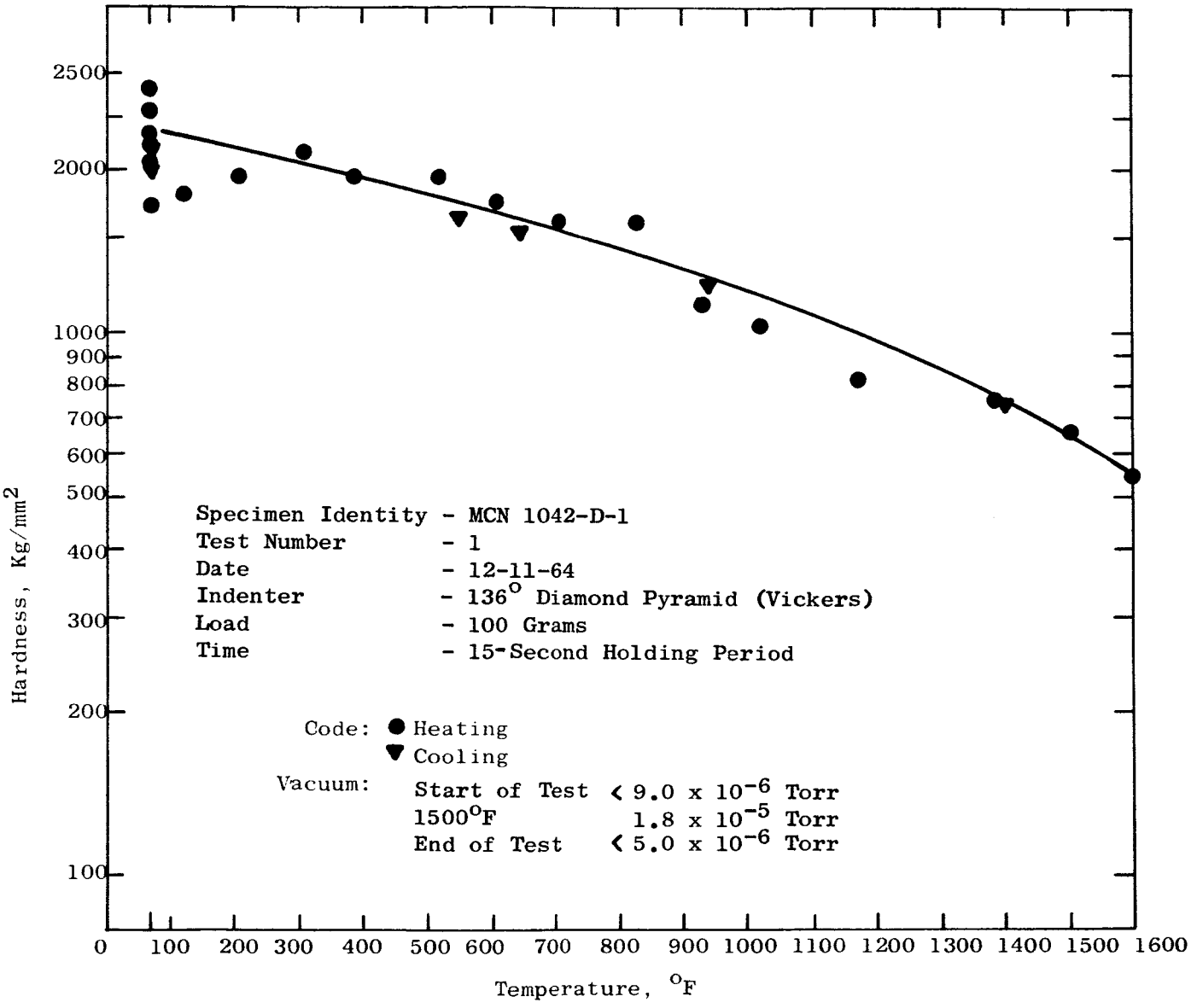

Figure 36. Hot Hardness of TiC as a Function of Temperature.

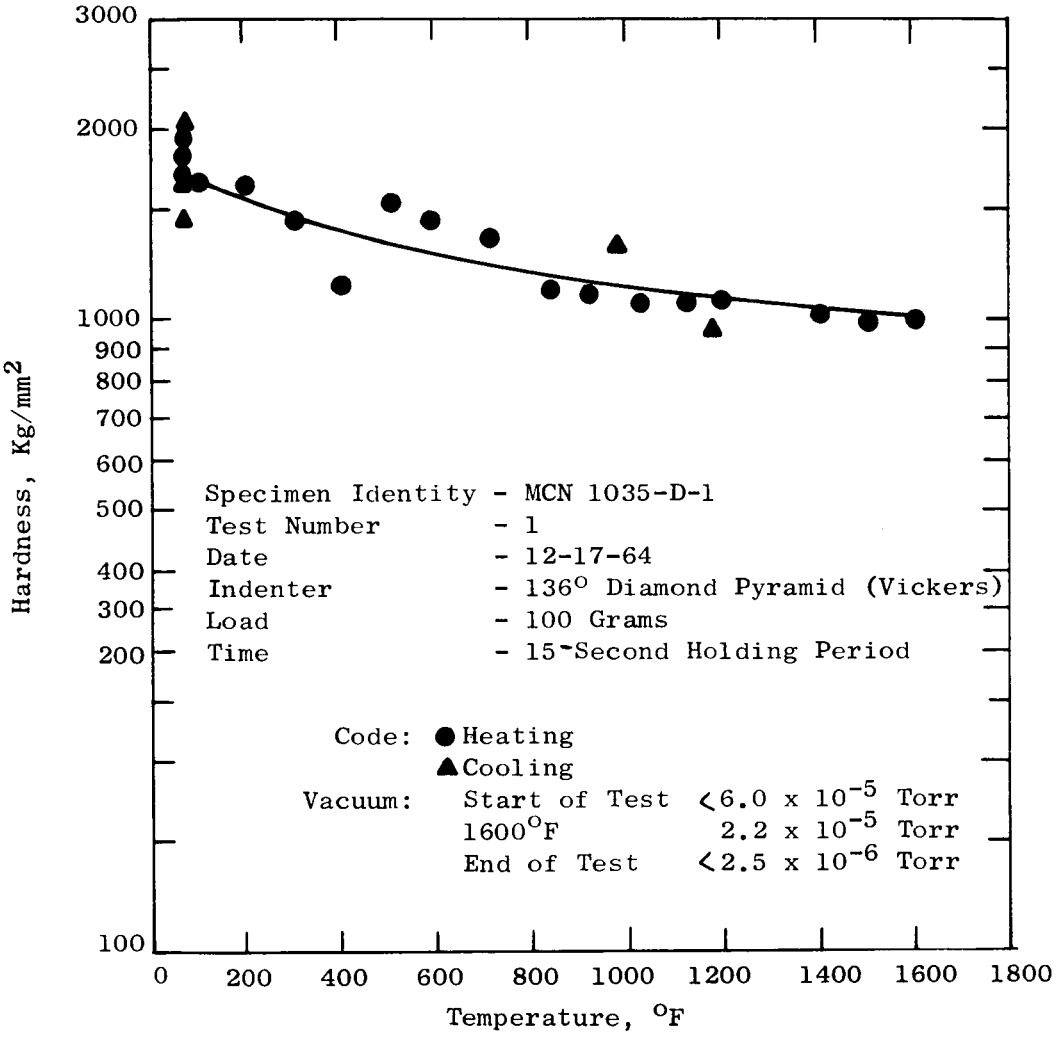

Figure 37. Hot Hardness of Carboloy 999 as a Function of Temperature.

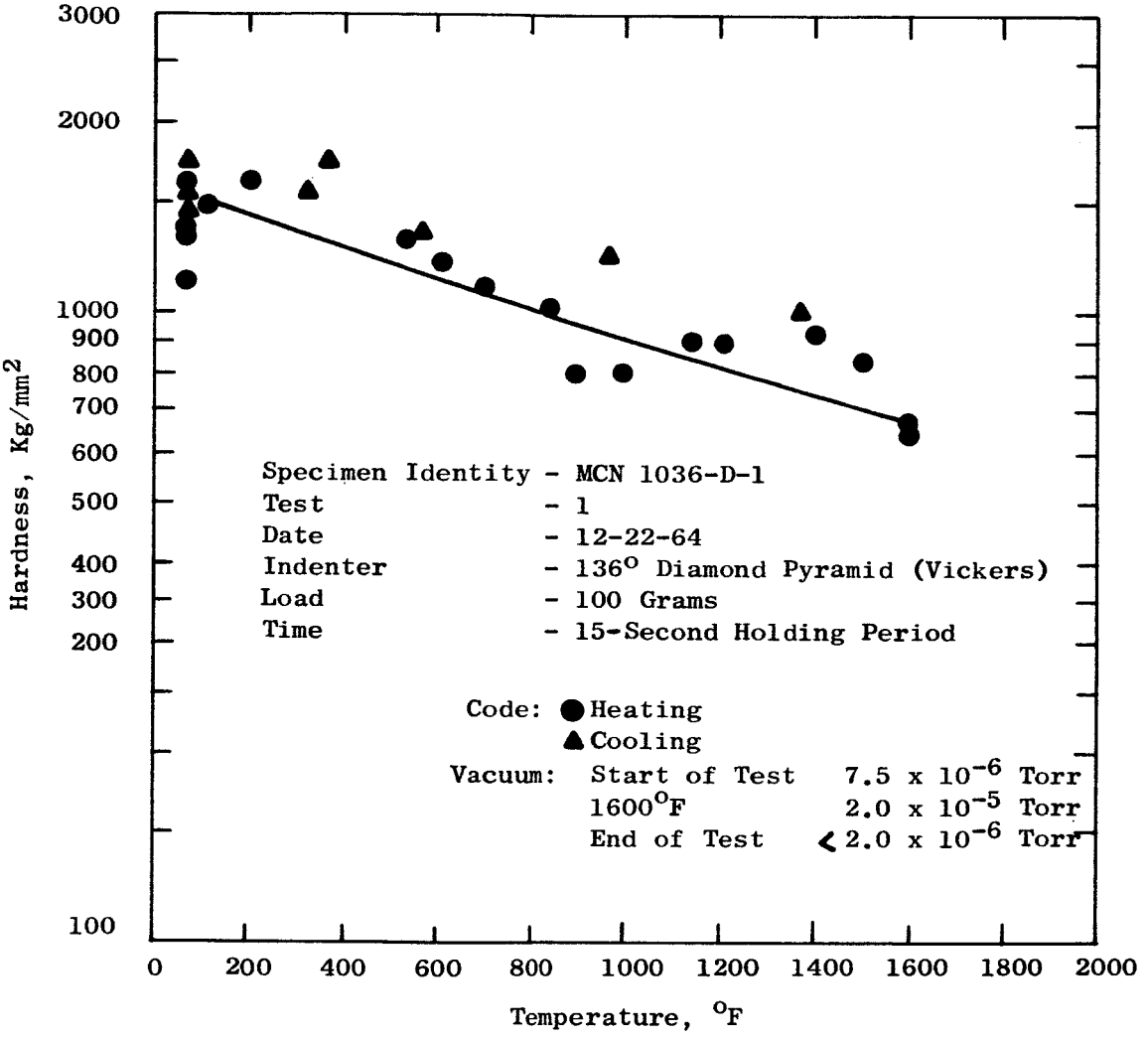

Figure 38. Hot Hardness of Carboloy 907 as a Function of Temperature.

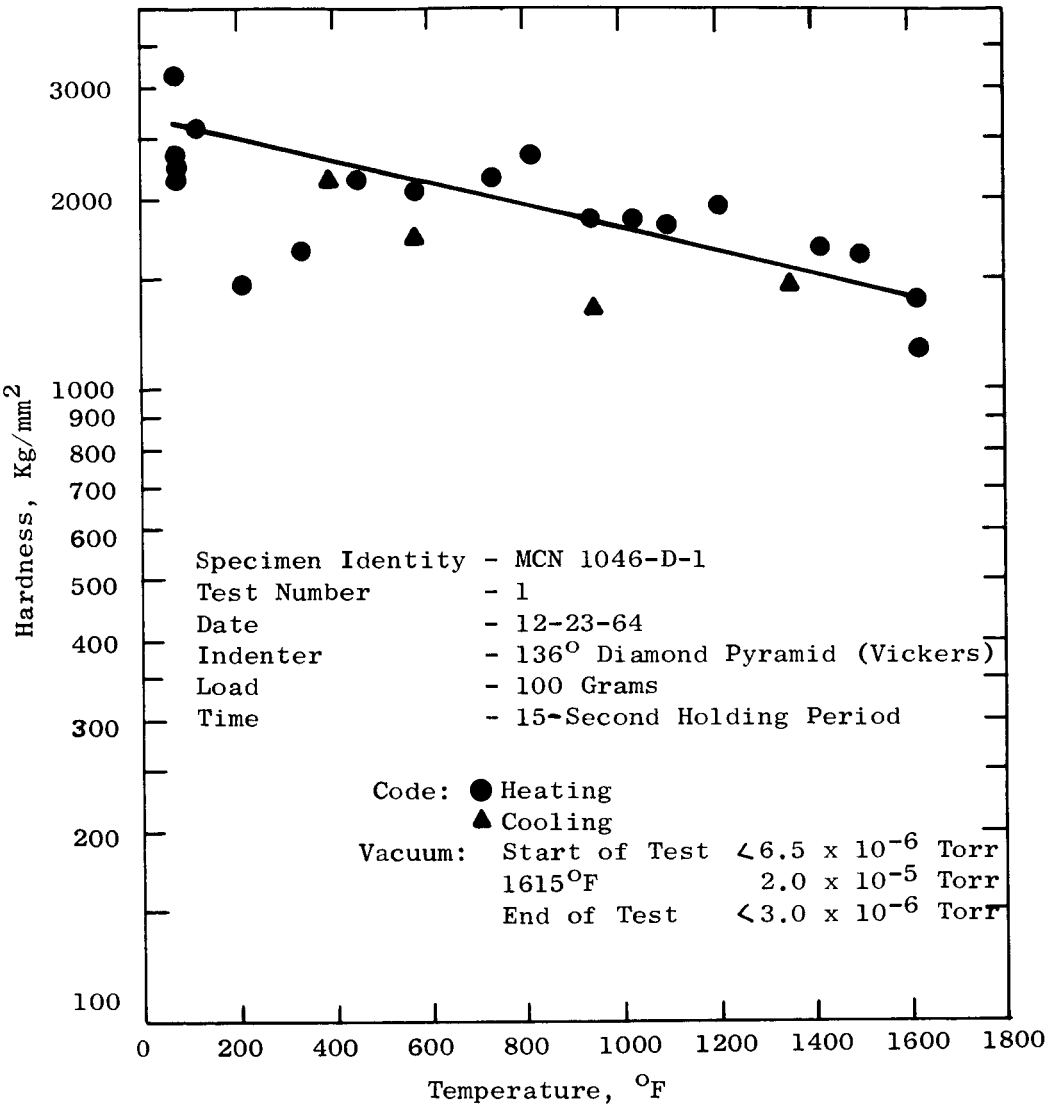

Figure 39. Hot Hardness of Grade 7178 as a Function of Temperature.

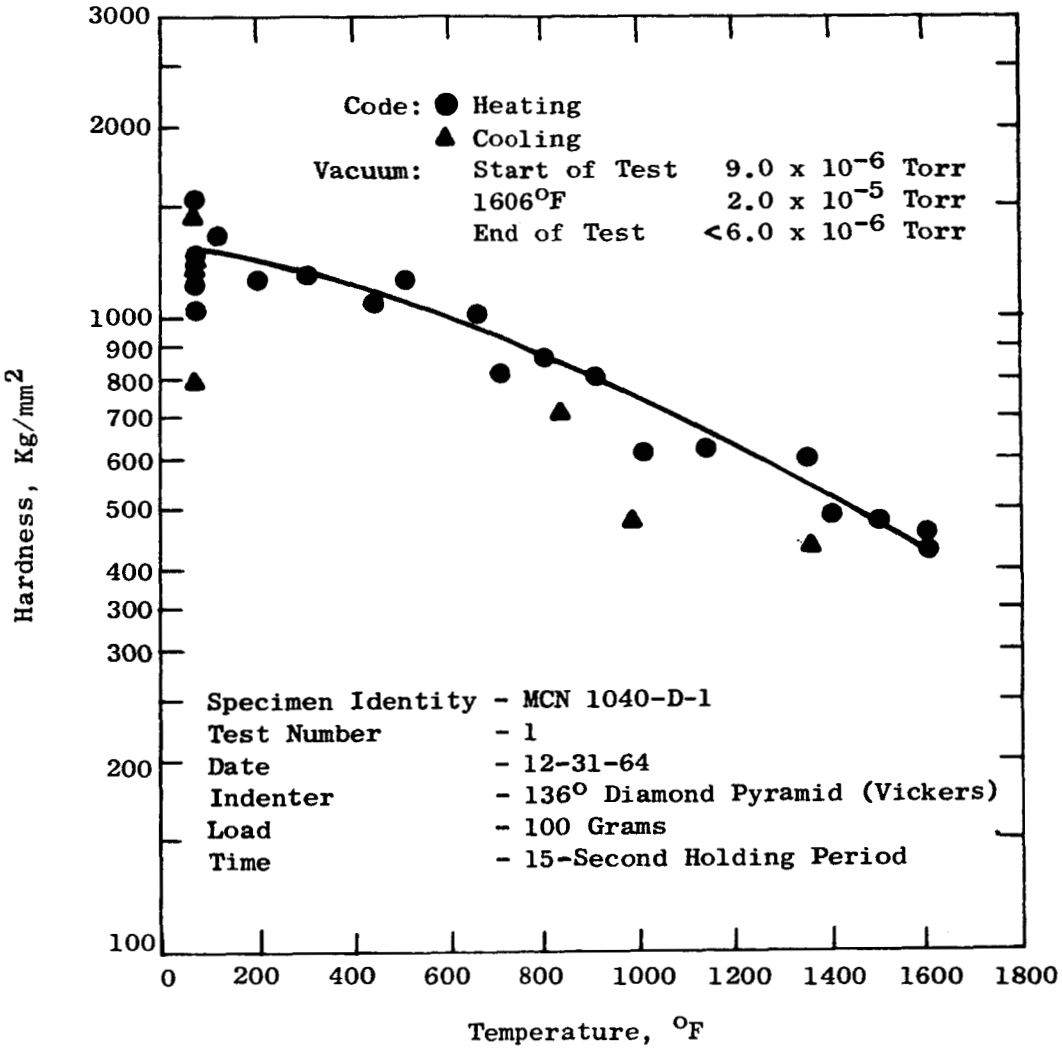

Figure 40. Hot Hardness of Zircoa 1027 as a Function of Temperature.

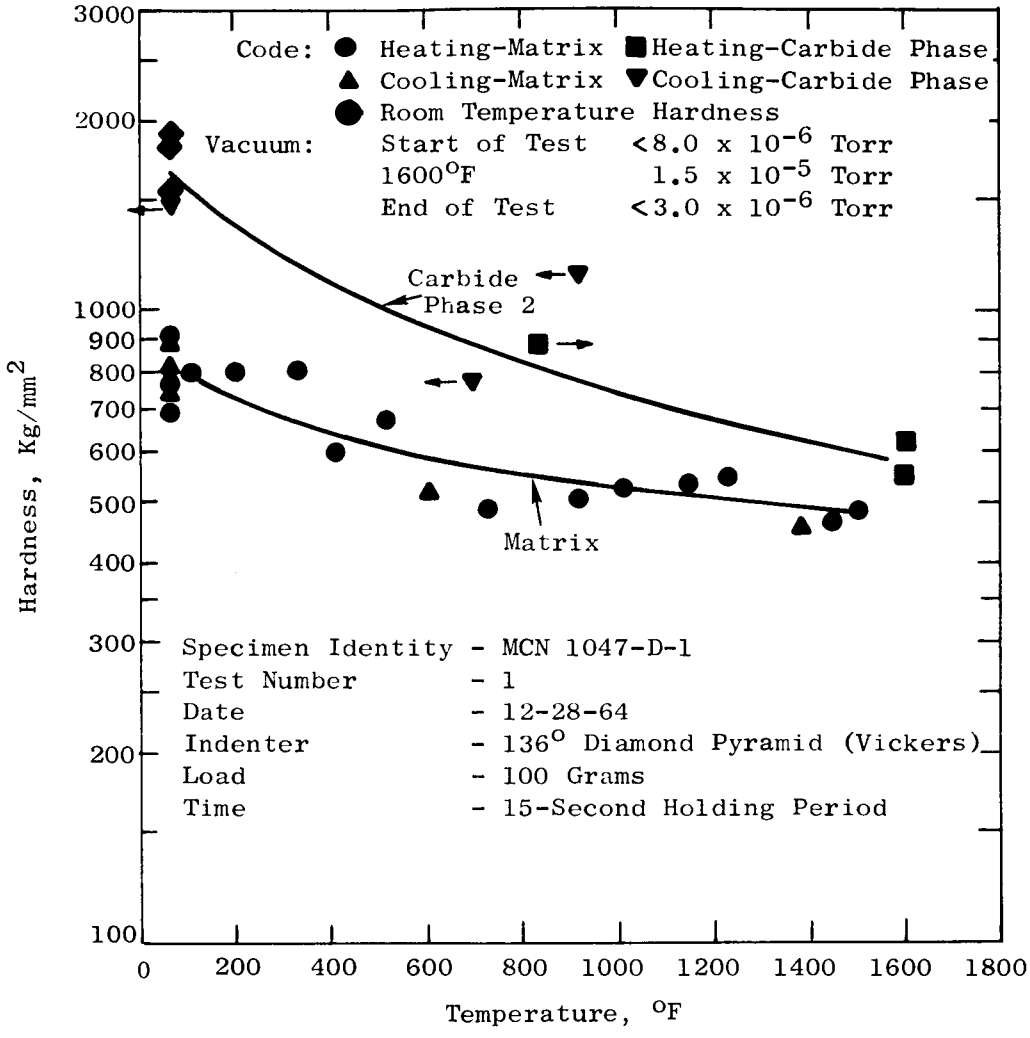

Figure 41. Hot Hardness of Star J as a Function of Temperature

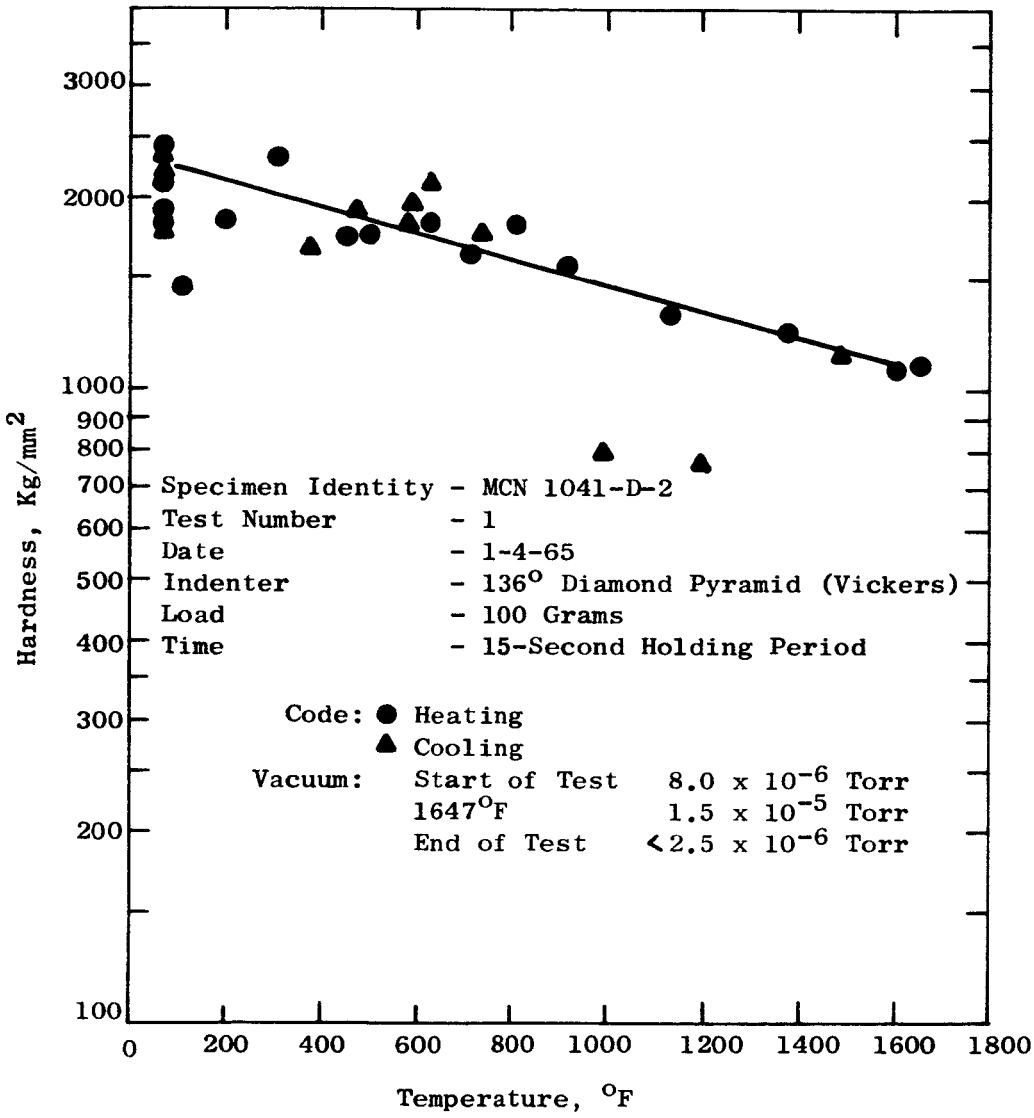

Figure 42. Hot Hardness of K-601 as a Function of Temperature.

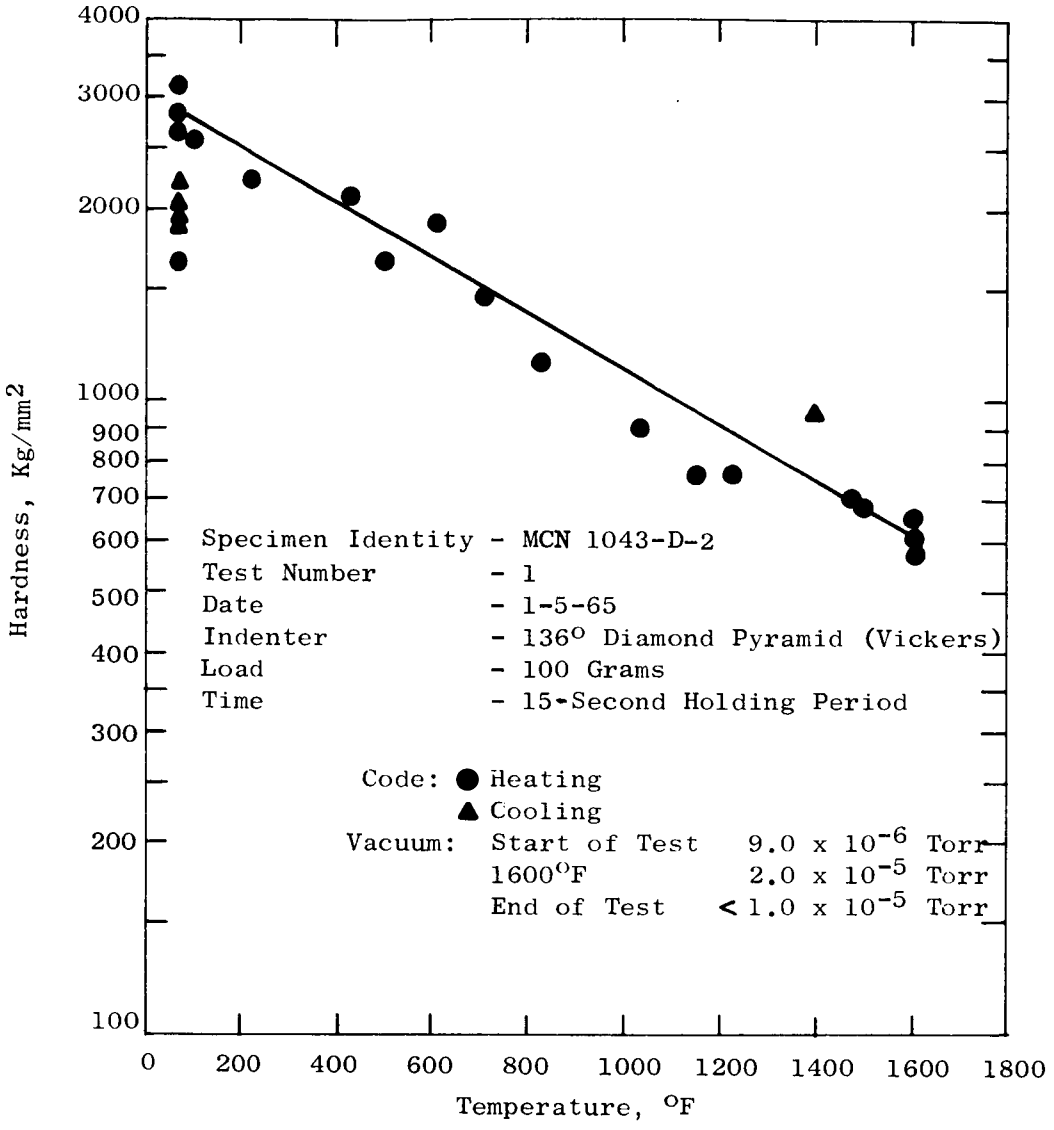

Figure 43. Hot Hardness of TiC+5%W as a Function of Temperature.

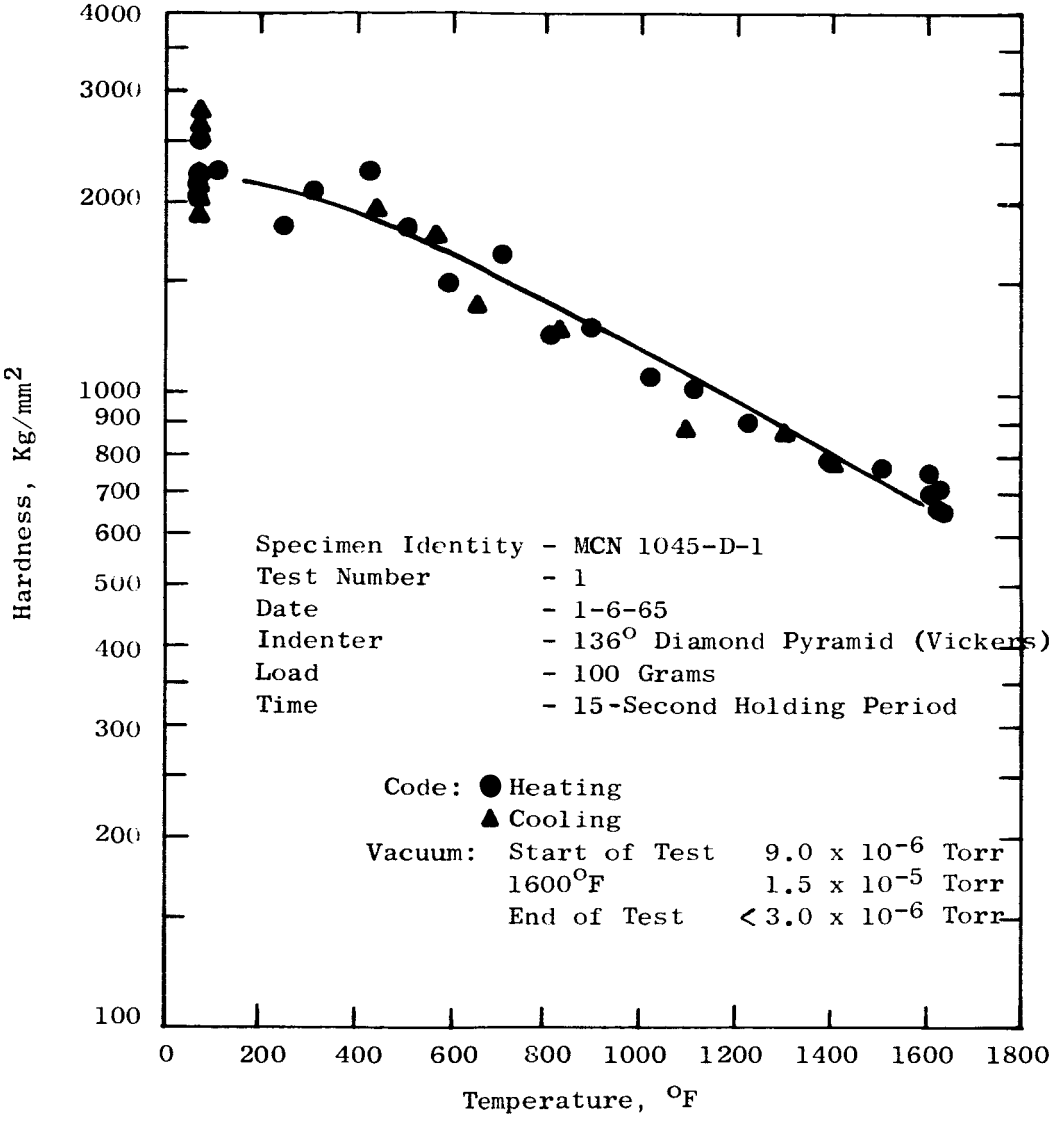

Figure 44. Hot Hardness of TiC+10%Cb as a Function of Temperature.

TABLE XXXVI. COMPARISON OF HOT HARDNESS DATA FOR TiC

Temp., °F	Hardness, Kg/mm^2 TiC(1)	TiC(2)
RT	2253	3100
200	2100	2500
400	1950	1900
600	1700	1600
800	1400	1200
1000	1200	950
1200	980	750
1400	760	650
1600	550	500

(1) This Program.

(2) Previous Work, General Electric Research Laboratory[7].

VI. FUTURE PLANS

The summary which follows enumerates the steps to be pursued during the succeeding quarter to implement this study.

1. The candidate bearing couples will be selected and procurement of the friction and wear test specimens will be initiated.

2. Evaluation of the corrosion test specimens which were exposed to potassium for 1,000 hours at 1600°F will continue and evaluation of those specimens tested at 1200° and 800°F will be initiated.

3. The hot hardness test program will be completed; the compression test program will continue.

4. The checkout of the high vacuum friction and wear tester will be completed.

5. The liquid potassium friction and wear tester will be installed and checkout tests initiated.

6. The build-up of the wetting facility will be initiated.

REFERENCES

[1] "Materials for Potassium Lubricated Journal Bearings," Qtr. Prog. Rept. 1, Ctr. NAS 3-2534 (July 22, 1963), SPPS, MSD, General Electric Company; Rept. NASA-CR-54006.

[2] DeMoney, F. W., "Static and Dynamic Creep-Rupture Properties of B50R207 and B50R311 Alloys," General Electric Company, Contract No. X241982-2, University of Minnesota, June 15, 1954.

[3] "Materials for Potassium Lubricated Journal Bearings," Qtr. Prog. Rept. 4, Ctr. NAS 3-2534 (April 22, 1964), SPPS, MSD, General Electric Company; Rept. NASA-CR-54113.

[4] "Materials for Potassium Lubricated Journal Bearings," Qtr. Prog. Rept. 5, Ctr. NAS 3-2534 (July 22, 1964), SPPS, MSD, General Electric Company; Rept. NASA-CR-54169.

[5] Basham, S. J., Lagedrost, J. F., Kissle, J. W., Rieder, W. G., Glaeser, W. A. and Allen, C. M., "Development of a Long-Life Contact Seal for a High-Speed Rotating Shaft in Liquid-Metal Dynamic Power Systems," October 15, 1964, Battelle Memorial Institute.

[6] "Materials for Potassium Lubricated Journal Bearings," Qtr. Prog. Rept. 6, Ctr. NAS 3-2534 (October 22, 1964), SPPS, MSD, General Electric Company; Rept. NASA-CR-54264.

[7] Westbrook, J. H., "An Improved Microhardness Tester for High Temperature Use," ASTM Bulletin No. 246, May, 1960.

DISTRIBUTION LIST
QUARTERLY PROGRESS REPORTS

Contract NAS 3-2534

NASA
Washington, D.C. 20546
Attn: James J. Lynch (RNP)

NASA
Washington, D.C. 20546
Attn: George C. Deutsch (RR)

NASA
Scientific & Technical Information
Facility
Box 5700
Bethesda, Maryland 20014
Attn: NASA Representative 2 + Repro

NASA
Ames Research Center
Moffet Field, California 94035
Attn: Librarian

NASA
Goddard Space Flight Center
Greenbelt, Maryland 20771
Attn: Librarian

NASA
Langley Research Center
Hampton, Virginia 23365
Attn: Librarian

NASA
Lewis Research Center
21000 Brookpark Road
Cleveland, Ohio 44135
Attn: Librarian

NASA
Lewis Research Center
21000 Brookpark Road
Cleveland, Ohio 44135
Attn: Report Control Office, MS 5-5

NASA
Lewis Research Center
21000 Brookpark Road
Cleveland, Ohio 44135
Attn: Dr. Bernard Lubarsky (SPSD)

NASA
Lewis Research Center
21000 Brookpark Road
Cleveland, Ohio 44135
Attn: Roger Mather (NPTB) (500-309)

NASA
Lewis Research Center
21000 Brookpark Road
Cleveland, Ohio 44135
Attn: G. M. Ault

NASA
Lewis Research Center
21000 Brookpark Road
Cleveland, Ohio 44135
Attn: J. P. Joyce (NPTB)

NASA
Lewis Research Center
21000 Brookpark Road
Cleveland, Ohio 44135
Attn: R. L. Davies (NPTB)

NASA
Lewis Research Center
21000 Brookpark Road
Cleveland, Ohio 44135
Attn: J. E. Dilley (SPSPS)

NASA
Lewis Research Center
21000 Brookpark Road
Cleveland, Ohio 44135
Attn: John Weber
Technology Utilization Office

NASA
Lewis Research Center
21000 Brookpark Road
Cleveland, Ohio 44135
Attn: Thomas Strom

NASA
Lewis Research Center
21000 Brookpark Road
Cleveland, Ohio 44135
Attn: T. A. Moss (NPTB)

NASA
Lewis Research Center
21000 Brookpark Road
Cleveland, Ohio 44135
Attn: Dr. Louis Rosenblum (MSD)

NASA
Manned Spacecraft Center
Houston, Texas 77001
Attn: Librarian

NASA
George C. Marshall Space Flight Center
Huntsville, Alabama 38512
Attn: Librarian

NASA
Jet Propulsion Laboratory
4800 Oak Grove Drive
Pasadena, California 99103
Attn: Librarian

NASA
Western Operations Office
150 Pico Boulevard
Santa Monica, California 90400
Attn: John Keeler

National Bureau of Standards
Washington, D. C. 20225
Attn: Librarian

Flight Vehicle Power Branch
Air Force Aero Propulsion Laboratory
Wright Patterson AFB, Ohio
Attn: Charles Armbruster ASRPP-10

Flight Vehicle Power Branch
Air Force Aero Propulsion Laboratory
Wright Patterson AFB, Ohio
Attn: T. Cooper (MAMP)

Flight Vehicle Power Branch
Air Force Aero Propulsion Laboratory
Wright Patterson AFB, Ohio
Attn: Librarian

Flight Vehicle Power Branch
Air Force Aero Propulsion Laboratory
Wright Patterson AFB, Ohio
Attn: John L. Morris

Army Ordnance Frankford Arsenal
Bridesburg Station
Philadelphia, Pennsylvania 19137
Attn: Librarian

Bureau of Ships
Department of the Navy
Washington, D. C. 20225
Attn: Librarian

Bureau of Weapons
Research & Engineering
Material Division
Washington, D. C. 20225
Attn: Librarian

U. S. Atomic Energy Commission
Technical Reports Library
Washington, D. C. 20545
Attn: J. M. O'Leary 2

U. S. Atomic Energy Commission
P. O. Box 1102
Middletown, Connecticut 06458
Attn: H. Pennington
Canel Project Office

U. S. Atomic Energy Commission
Germantown, Maryland 20767
Attn: Col. E. L. Douthett
SNAP 50/SPUR Project Office

U. S. Atomic Energy Commission
Germantown, Maryland 20767
Attn: H. Rochen
SNAP 50/SPUR Project Office

U. S. Atomic Energy Commission
Germantwon, Maryland 20767
Attn: Socrates Christopher

U. S. Atomic Energy Commission
Germantown, Maryland 20767
Attn: Major Gordon Dicker
SNAP 50/SPUR Project Office

U. S. Atomic Energy Commission
Technical Information Service Extension
P. O. Box 62
Oak Ridge, Tennessee 37831 3

U. S. Atomic Energy Commission
Washington, D. C. 20545
Attn: M. J. Whitman

Argonne National Laboratory
9700 South Cross Avenue
Argonne, Illinois 60440
Attn: Librarian

Brookhaven National Laboratory
Upton, Long Island, New York 11973
Attn: Librarian

Oak Ridge National Laboratory
Oak Ridge, Tennessee 37831
Attn: W. O. Harms

Oak Ridge National Laboratory
Oak Ridge, Tennessee 37831
Attn: Dr. A. J. Miller

Oak Ridge National Laboratory
Oak Ridge, Tennessee 37831
Attn: Librarian

Office of Naval Research
Power Division
Washington, D. C. 20225
Attn: Librarian

U. S. Naval Research Laboratory
Washington, D. C. 20225
Attn: Librarian

Advanced Technology Laboratories
Division of American Standard
369 Whisman Road
Mountain View, California 94040-2
Attn: Librarian

Aerojet General Corporation
P. O. Box 296
Azusa, California 91702
Attn: Librarian

Aerojet General Nucleonics
P. O. Box 77
San Ramon, California 94583
Attn: Librarian

AiResearch Manufacturing Company
Sky Harbor Airport
402 South 36th Street
Phoenix, Arizona 85000
Attn: Librarian

AiResearch Manufacturing Company
Sky Harbor Airport
402 South 36th Street
Phoenix, Arizona 85000
Attn: E. A. Kovacevich

AiResearch Manufacturing Company
9851-9951 Sepulveda Boulevard
Los Angeles, California 90045
Attn: Librarian

IIT Research Institute
10 W. 35th Street
Chicago, Illinois 60616
Attn: Librarian

Atomics International
8900 DeSoto Avenue
Canoga Park, California 91303
Attn: Librarian

Avco
Research and Advanced Development
Department
201 Lowell Street
Wilmington, Massachusetts 01800
Attn: Librarian

Babcock and Wilcox Company
Research Center
Alliance, Ohio 44601-2
Attn: Librarian

Battelle Memorial Institute
505 King Avenue
Columbus, Ohio 43200
Attn: C. M. Allen

Battelle Memorial Institute
505 King Avenue
Columbus, Ohio 43200
Attn: Librarian

The Bendix Corporation
Research Laboratories Div.
Southfield, Detroit, Mich. 48200
Attn: Librarian

The Boeing Company
Seattle, Washington 98100
Attn: Librarian

Climax Molybdenum Co., of Michigan
Detroit, Michigan 48200
Attn: Librarian

Carborundum Company
Niagara Falls, New York 14300
Attn: Librarian

Chance Vought Aircraft, Inc.
P. O. Box 5907
Dallas 22, Texas 75222
Attn: Librarian

Clevite Corporation
Mechanical Research Division
540 East 105th Street
Cleveland, Ohio 44108
Attn: Mr. N. C. Beerli
Project Administrator

Convair Astronautics
5001 Kerrny Villa Road
San Diego, California 92111
Attn: Librarian

Crucible Steel Co. of America
Pittsburgh, Pennsylvania 15200
Attn: Librarian

Curtiss-Wright Corporation
Research Division
Quehanna, Pennsylvania
Attn: Librarian

E. I. duPont de Nemours and Co., Inc.
Wilmington, Delaware 19898
Attn: Librarian

Electro-Optical Systems, Inc.
Advanced Power Systems Division
Pasadena, California 91100
Attn: Librarian

Fansteel Metallurgical, Corp.
North Chicago, Illinois 60600
Attn: Librarian

Firth Sterling, Incorporated
McKeesport, Pennsylvania
Attn: Librarian

Aeronutronic Div. of Philco Corp.
Ford Road
Newport Beach, California
Attn: Ferne M. Black/HDL
Acquisitions Librarian

General Atomic
John Jay Hopkins Laboratory
P. O. Box 608
San Diego, California 92112
Attn: Librarian

General Electric Company
Atomic Power Equipment Div.
P. O. Box 1131
San Jose, California

General Electric Company
Missile and Space Vehicle Dept.
3198 Chestnut Street
Philadelphia, Pennsylvania 19104
Attn: Librarian

General Electric Company
Vallecitos
Vallecitos Atomic Lab.
Pleasanton, California 94566
Attn: Librarian

General Dynamics/Fort Worth
P. O. Box 748
Fort Worth, Texas 76100
Attn: Librarian

General Motors Corporation
Allison Division
Indianapolis, Indiana 46206
Attn: Librarian

Hamilton Standard
Div. of United Aircraft Corp.
Windsor Locks, Connecticut
Attn: Librarian

Hughs Aircraft Company
Engineering Division
Culver City, California 90230-2
Attn: Librarian

Kennametal, Incorporated
Latrobe, Pennsylvania
Attn: Librarian

Latrobe Steel Company
Latrobe, Pennsylvania
Attn: Librarian

Lockheed Missiles and Space Division
Lockheed Aircraft Corporation
Sunnyvale, California
Attn: Librarian

Marquardt Aircraft Company
P. O. Box 2013
Van Nuys, California
Attn: Librarian

The Martin Company
Baltimore, Maryland 21203
Attn: Librarian

The Martin Company
Nuclear Division
P. O. Box 5042
Baltimore, Maryland 21220
Attn: Librarian

Martin Marietta Corporation
Metals Technology Laboratory
Wheeling, Illinois

Massachusetts Institute of Technology
Cambridge, Massachusetts 02139
Attn: Librarian

Materials Research and Development
Manlabs, Inc.
21 Erie Street
Cambridge, Massachusetts 02139

Materials Research Corporation
Orangeburg, New York
Attn: Librarian

McDonnell Aircraft
St. Louis, Missouri 63100
Attn: Librarian

MSA Research Corporation
Callery, Pennsylvania 16024
Attn: Librarian

North American Aviation
Los Angeles Division
Los Angeles, California 90009
Attn: Librarian

Norton Company
Worcester, Massachusetts 01600
Attn: Librarian

Pratt & Whitney Aircraft
400 Main Street
East Hartford, Connecticut 06108
Attn: Librarian

Pratt & Whitney Aircraft
CANEL
P. O. Box 611
Middletown, Connecticut 06458
Attn: Librarian

Pratt & Whitney Aircraft Corporation
Division of United Aircraft
CANEL
P. O. Box 611
Middletown, Connecticut 06458
Attn: Glen Wood

Republic Aviation Corp.
Farmingdale, Long Island, New York
Attn: Librarian

Rocketdyne
Canoga Park, California 91303
Attn: Librarian

Sintercast Div. of Chromalloy Corp.
West Nyack, New York
Attn: Librarian

S K F Industries, Inc.
Philadelphia, Pennsylvania 19100
Attn: Librarian

Solar
2200 Pacific Highway
San Diego, California 92112
Attn: Librarian

Southwest Research Institute
8500 Culebra Road
San Antonio, Texas 78206
Attn: Librarian

Superior Tube Company
Norristown, Pennsylvania
Attn: Mr. A Bound

Sylvania Electrics Products, Inc.
Chem. & Metallurgical
Towanda, Pennsylvania
Attn: Librarian

Oak Ridge National Laboratory
Oak Ridge, Tennessee
Attn: W. H. Cook

Thompson Ramo Wooldridge, Inc.
Caldwell Res Center
23555 Euclid Avenue
Cleveland, Ohio 44117
Attn: Librarian

Thompson Ramo Wooldridge, Inc.
Caldwell Res Center
23555 Euclid Avenue
Cleveland, Ohio 44117
Attn: G. J. Guarnieri

Thompson Ramo Wooldridge, Inc.
New Devices Laboratories
7209 Platt Avenue
Cleveland, Ohio 44104
Attn: Librarian

The Timken Roller Bearing Co.
Canton, Ohio 44706
Attn: Librarian

Union Carbide Metals
Niagara Falls, New York 14300
Attn: Librarian

Union Carbide Corp., Stellite Division
Kokomo, Indiana
Attn: Librarian

Union Carbide Nuclear Company
P. O. Box X
Oak Ridge, Tennessee 37831
Attn: X-10 Laboratory
Records Department 2

United Nuclear Corporation
5 New Street
White Plains, New York 10600-5
Attn: Librarian

United Nuclear Corporation
5 New Street
White Plains, New York 10600-5
Attn: Mr. Albert Weinstein
Senior Engineer

Universal Cyclops Steel Corp.
Refractomet Division
Bridgeville, Pennsylvania
Attn: C. P. Mueller

University of Michigan
Department of Chemical & Metallurgical Engineering
Ann Arbor, Michigan 48103
Attn: Librarian

Vanadium Alloys Steel Company
Latrobe, Pennsylvania
Attn: Librarian

Vought Astronautics
P.O. Box 5907
Dallas, Texas 75222
Attn: Librarian

Wah Chang Corporation
Albany, Oregon
Attn: Librarian

Westinghouse Electric Corporation
Astonuclear Laboratory
P.O. Box 10864
Pittsburgh, Pennsylvania 15236
Attn: Librarian

Westinghouse Electric Corp.
Materials Mfg. Division
RD#2 Box 25
Blairsville, Pennsylvania
Attn: Librarian

Westinghouse Electric Corp.
Materials Mfg. Division
RD#2 Box 25
Blairsville, Pennsylvania
Attn: F. L. Orrell

Mr. Rudolph Rust - MS 138-214
Jet Propulsion Laboratory
4800 Oak Grove Drive
Pasadena, California 91103

Mr. W. H. Podolny
United Aircraft Corporation
Pratt & Whitney Division
400 W. Main Street
Hartford 8, Connecticut

Zirconium Corporation of America
Solon, Ohio
Attn: Librarian

Wyman-Gordon Company
North Grafton, Massachusetts
Attn: Librarian

Westinghouse Electric Corporation
Astronuclear Laboratory
P.O. Box 10864
Pittsburgh 36, Pennsylvania
Attn: R. T. Begley

Union Carbide Corporation
Parma Research Center
P.O. Box 6115
Cleveland, Ohio 44101
Attn: Technical Information Service

Westinghouse Electric Corporation
Research & Development Center
Pittsburgh, Pennsylvania 15235
Attn: E. S. Bober

E. I. DuPont de Nemours & Co., Inc.
Wilmington, Delaware 19858
Attn: E. M. Mahla

Westinghouse Electric Corporation
Aerospace Electrical Division
Lima, Ohio
Attn: R. W. Briggs

Eitel McCullough, Incorporated
301 Industrial Way
San Carlos, California
Attn: Leonard Reed

Mechanical Technology, Inc.
968 Albany-Shaker Road
Latham, New York
Attn: Mr. Eli B. Arwas

Varian Associates
Vacuum Products Division
611 Hansen Way
Palo Alto, California
Attn: J. Shields

Ultek Corporation
920 Commercial Street
Palo Alto, California
Attn: Librarian